Aus der Chirurgischen Klinik (Zentrum) der Universität Heidelberg

Zentrumssprecher: Prof. Dr. med. Matthias Karck

Klinik für Allgemein-, Viszeral- und Transplantationschirurgie

(Ärztlicher Direktor: Prof. Dr. Dr. h.c. Markus W. Büchler)

Tumour biomarkers that identify molecular subtypes and best responders to chemotherapy in patients with pancreatic ductal adenocarcinoma

Inauguraldissertation

zur Erlangung des Doctor scientiarum humanarum (Dr. sc. hum)

an der

Medizinischen Fakultät Heidelberg

der Ruprecht-Karls-Universität Heidelberg

vorgelegt von

Xu Zhou

aus

Inner Mongolia Autonomous Regions

Volksrepublik China

2022

Dekan: Herr Prof. Dr. Hans-Georg Kräusslich

Doktorvater: Herr PD. Dr. Franco Fortunato

Dedicated to my family

CONTENTS

CONTENTS

LIST OF ABBREVIATIONS

Abbreviation	Full Name
5F-dUMP	5-Fluoro-uridine-5'-monophosphate
5-FU	5-fluorouracil
5F-UTP	5-Fluoro-uridine-5'-triphosphate
ADEX	Aberrantly differentiated endocrine exocrine
ADM	Acinar-to-ductal metaplasia
APC	7-ethyl-10[4-N-(5-aminopentanoicacid)-1-piperidino] carbonyloxy-camptothecin
ASR	Age-standardized rate
CAF	Cancer-associated fibroblast
CK5/17/19/81(KRT5/17/19/81)	Cytokeratin 5/17/19/81
COMPASS	Cardiovascular Outcomes for People Using Anticoagulation Strategies
CP	Chronic pancreatitis
CT	Computed tomography
CTX	Chemotherapy
CYP3A4/5/7	Cytochrome P450 Family 3 Subfamily A Member 4/5/7
DAPI	4′, 6-Diamidino -2- phenylindole dihydrochloride
DC	Dendritic cell
DCIS	Ductal carcinoma in situ
dCTP	Deoxycytidine triphosphate
dFdCTP	Difluorodeoxycytidine triphosphate
dH_2O	Distilled water
DKFZ	German Cancer Research Centre
DNA	Deoxyribonucleic acid
DPBS	Dulbecco's phosphate-buffered saline
EGFR	Epidermal growth factor receptor
EMT	Epithelial-to-mesenchymal transition
ENT	Equilibrative nucleoside transporters
EPZ	European Pancreas Centre
ESPAC	European Study Group for Pancreatic Cancer
FA	Folinic acid
FAMMM	Family atypical multiple-mole melanoma syndrome
FFPE	Formalin-fixed, paraffin-embedded
FOLFIRINOX, FFX	Drug combination of folinic acid, 5-FU, irinotecan and oxaliplatin
GATA6	GATA Binding Protein 6
GEM	Gemcitabine
GWA	Genome-wide association
H&E	Hematoxylin & eosin
HCC	Hepatocellular carcinoma
HDI	Human Development Index
hENT1	Human equilibrative nucleoside transporter 1
HMEC	Normal mammary epithelial cells

HNF1/4A	Hepatocyte nuclear factor 1/4 homeobox A
IBC	Invasive breast cancer
IF	Immunofluorescence
IgG	Immunoglobulin G
IPMN	Intraductal papillary mucinous neoplasm
LCM	Laser capture microdissection
LIT	Lymphocyte immunization therapy
MDCT	Multidetector computed tomography
MODY	maturity-onset diabetes of the young
MOS	Median overall survival
MRI	Magnetic resonance imaging
mTORC2	Mammalian target of rapamycin complex 2
NBMPR	Nitrobenzylthioinosine
NCT	National Centre for Tumour Diseases Heidelberg
NCT	National Centre for Tumour Diseases Heidelberg
NPC	7-ethyl-10[4-amino-1-piperidino] carbonyloxy-camptothecin
NT	Nucleoside transporter
OS	Overall survival
PanIN	Pancreatic intraepithelial neoplasia
PCA	Principal component analysis
PDAC	Pancreatic ductal adenocarcinoma
PDO	Patient-derived organoid
PNET	Pancreatic neuroendocrine tumour
PXR	Pregnane X receptor
QM-PDA	Quasi-mesenchymal pancreatic ductal adenocarcinoma
RNA	Ribonucleic acid
RNA-seq	RNA sequencing
ROI	Region of interest
ROS	Reactive oxygen species
RT	Room temperature
S100A2	S100 calcium-binding protein A2
SLC29A1	Solute Carrier Family 29 Member 1
SN-38	7-ethyl-10-hydroxy-camptothecin
SNP	Single nucleotide polymorphisms
TCGA	The Cancer Genome Atlas
TME	Tumour microenvironment
TSs	Treatment Signatures
TTR	Time to relapse
UMP	Uridine monophosphate

1. INTRODUCTION

Pancreatic ductal adenocarcinoma is an intractable malignant disease with slowly increasing incidence and a closely paralleled mortality. The high mortality can be mostly attributed to the difficulty of diagnosis and generally poor response to therapy. Most patients remain asymptomatic and are not diagnosed until the disease is advanced. Less than 20% of patients are eligible for upfront surgical resection and adjuvant chemotherapy, which is the only treatment for cure, but a considerable number of them will end up with recurrence. Thirty percent of patients with locally advanced disease require neoadjuvant therapy for restaging and possible surgery, while 50% of patients have metastasis with little chance of survival beyond several months with any type of therapy (Kleeff et al. 2007; Russo et al. 2016; Sultana et al. 2008). Therefore the major clinical objectives now are to optimize chemotherapeutic regimen selection based on predictive response markers including transcriptomic molecular subtyping and transcriptomic treatment specific signatures, and personal precision treatment using advances currently being made involving pathogenic single gene aberrations and structural and clustered genomic aberrations (Consortium 2020; Springfeld et al. 2019; Tiriac et al. 2018).

1.1 Epidemiology

The International Agency for Research on Cancer estimated that in 2018 there were 458,918 new cases of pancreatic cancer, with roughly the same number of deaths (432,242) (Bray et al. 2018). Both incidence and mortality are slightly higher in males than in females (incidence 243,033 vs 215,885; mortality 226,910 vs 205,332). Pancreatic cancer has become the fourth leading cause of cancer-related death in the United States and the European Union, and the seventh in the whole world (Maisonneuve 2019). The estimated new cases in the United States in 2021 was 60,430, along with the lowest overall survival (10%) (Siegel et al. 2021). Geographically, the

age-standardized rate (ASR) incidence was both higher in Europe (7.7 per 100,000 people) and North America (7.6 per 100,000 people) with an equivalent ASR mortality (7.2 in Europe and 6.5 in North America) than elsewhere in the world (Bird et al. 2017). The lowest ASR incidence and mortality were in Africa (both 2.2) (Rawla et al. 2019). Globally, pancreatic cancer occurs slightly more frequently in urban areas than in rural areas and the death rate is higher in black people than in white people. However, geographic and ethnic variations are influenced by diagnostic capacity and access to care. The incidence rates are 3- to 4-fold higher in high Human Development Index (HDI) countries, while underdiagnosis in Africa, India and Southeast Asia may cause bias to relatively low incidence (Wong et al. 2017).

Despite testing many new treatments, the 5-year survival rate of pancreatic cancer remains the lowest among all the cancers (Neoptolemos et al. 2018). This poor prognosis is correlated with late diagnosis, resistance or tolerance to chemo(radio)-therapy, a high rate of recurrence, specific collections of molecular alterations and the complex microenvironment of pancreatic cancer (Jones et al. 2008).

Given that the incidence and mortality rates of pancreatic cancer tend to be stable compared with the other declining cancers, it is projected to be the second leading cause of cancer death by 2030 (Rahib et al. 2014).

1.2 Risk Factors

Increasing age is one of the dominant risk factors for pancreatic cancer. People before 50 years of age are seldomly diagnosed with PDAC. The incidence of PDAC in people between 50 to 64 years of age was 11.5 per 100,000 people, which then rose to peak at 36.3 per 100,000 people between 65 to 79 years (Global Cancer Observatory: https://gco.iarc.fr/today/home). A hereditary background is also a determinant risk factor. It is estimated that around 10% of the pancreatic cancer cases have a family history due to a multitude of different gene mutations rather than a small handful of pathogenic variants (Klein 2021). There are several germline mutations associated with familial pancreatic cancer syndromes including BRCA2 mutations in hereditary

breast and ovarian cancer (HBOC) (Lax 2017), CDKN2A mutations in the family atypical multiple-mole melanoma syndrome (FAMMM) (Cremin et al. 2018), LKB1/STK11 mutations in Peutz-Jeghers syndrome (Guldberg et al. 1999), and TP53 mutations in Li-Fraumeni syndrome (Amadou et al. 2018; DaVee et al. 2018; Klein 2021). Some common variations like specific single nucleotide polymorphisms (SNPs) in the non-O blood group of the ABO gene also cause a modest risk (Risch et al. 2013; Rizzato et al. 2013). Cigarette smoking is another firmly associated factor responsible for around 14% of the pancreatic cancer cases (Korc et al. 2017). Smokers have a 2- to 3-fold higher risk of developing pancreatic cancer (Yadav and Lowenfels 2013). However, long-term cessation (more than 10 years) of tobacco smoking has been shown to reduce the risk of developing pancreatic cancer by around 30% (Thompson et al. 1999). Chronic pancreatitis due to inherited PRSS1 and/or CFTR mutations or other pancreatitis associated inherited gene variants, and excess alcohol consumption also predisposes to pancreatic cancer (Greenhalf et al. 2020). As well as increasing the risk of chronic pancreatitis, heavy alcohol consumption is directly positively correlated with the development of pancreatic cancer (Go et al. 2005; Tramacere et al. 2010). Finally, lack for physical exercise, body mass index, new diabetes mellitus, and diet also contribute to the risk of pancreatic cancer (Mario et al. 2018).

1.3 Histopathology

Pancreatic neoplasms are classified by cellular lineage which could best represent their histopathological characters. Exocrine pancreatic neoplasms are the most common types, consisting of serous neoplasms, mucinous neoplasms, intraductal neoplasms, intraepithelial neoplasms and acinar cell neoplasms. Pancreatic ductal adenocarcinoma (PDAC) takes up the vast majority (95%) of exocrine pancreatic neoplasms. PDAC is an invasive, mucin-producing neoplasm with an abundant stromal desmoplastic reaction and haphazard gland arrangement (Hruban 2009). It can be divided into well, moderately, and poorly differentiated grades. Pancreatic cancer arises from microscopic distinctive morphological and genetic precursor lesions characterized as

pancreatic intraepithelial neoplasia (PanIN), intraductal papillary mucinous neoplasms (IPMNs) and mucinous cystic neoplasms (Kleeff et al. 2016).

The classification of pancreatic cancer types contributes to the clinical prognosis evaluation. Endocrine pancreatic tumours have a better prognosis than exocrine cancers. Pancreatic neuroendocrine tumours (PNETs), have high 5-year overall survival rates of over 50% compared to 10% for PDAC (Ellison et al. 2014; Siegel et al. 2021). Once established all PDACs are highly invasive irrespective of their morphological phenotype and are generally treated in the same way (Kleeff et al. 2016; Neoptolemos et al. 2018; Springfeld et al. 2019). A deeper understanding of the molecular programming of pancreatic cancers will help to develop more effective targeted therapies.

1.4 Gene Mutations and Molecular Subtyping

KRAS mutations dominate the gene aberration pattern in pancreatic adenocarcinoma, as it occurs in over 90% of the tumours, followed by mutations and other genetic alterations of TP53 (66%), SMAD4 (22%) and CDKN2A (19%) (The Cancer Genome Atlas (TCGA) database: http://www.cbioportal.org.). Other pathogenic gene aberrations occur with a 5-10% prevalence, such as those of KDM6A, BCORL1, RBM10, MLL3, ARID1A, and TGFBR2 (Collisson et al. 2019). Unlike some well-studied gene aberrations which frequently influence the clinical treatment in other cancer types, for example, the HER2 gene in breast cancer (Ahmed et al. 2015), BCR-ABL in chronic myelogenous leukaemia (Prejzner 2002), and EGFR in non-small cell lung cancer (Aoki et al. 2018), less than 5% of gene alterations affect clinical treatment options in PDAC. These include BRCA1/2 germline and somatic mutations, high microsatellite instability, the $KRAS^{G12C}$ mutation, and NTRK, NRGG1 and other fusions (Mosele et al. 2020).

The development of the next-generation RNA sequencing (RNA-seq), offers a new opportunity to understand how tumours might respond to various treatments based on transcriptomic taxonomy first described in PDAC by Collisson and colleagues in 2011

(Collisson et al. 2011). They classified PDAC into three molecular subtypes: classical, quasi-mesenchymal and exocrine-like subtypes. The classical subtype, with a relatively better prognosis, was more sensitive to erlotinib, while the quasi-mesenchymal subtype, associated with higher tumour grade and a poorer prognosis, was sensitive to gemcitabine-based treatment. Being concerned that the variable stromal reaction observed in pancreatic tumours may affect the quality and reproducibility of molecular subtyping, Moffitt and colleagues employed a virtual microdissection technique of PDAC tumours called non-negative matrix factorization (NMF) for profiling (Moffitt et al. 2015). In this way, they identified two epithelial cell-based subtypes called classical and basal-like, and two stromal cell-based subtypes called normal and activated (Moffitt et al. 2015). Other approaches include classifying 21 distinct mutational signatures based on somatic whole genome next-generation sequencing (NGS) (Alexandrov et al. 2013), and differential genome-wide DNA methylation patterns (Nones et al. 2014).

Waddell and colleagues classified PDACs into four subtypes based on patterns of variation in chromosomal structure termed stable, locally rearranged, scattered and unstable, the latter responsive to platinum therapy and BRCA1/2 germline carriers also sensitive to both platinum and PARP inhibitors (Waddell et al. 2015).

In 2016, Bailey and colleagues performed an mRNA hybridization analysis on known pancreatic cancer pathological subtypes including colloid, adenosquamous, PDAC associated with IPMN, acinar cell carcinoma and other rare variants (Bailey et al. 2016). They defined four transcriptomic subtypes: squamous, pancreatic progenitor, immunogenic and aberrantly differentiated endocrine exocrine (ADEX). The three transcriptomic subtype classification systems described by Collison et al (2011), Moffit et al (2015) and Bailey et al (2016) turned out to have overlapping features. For instance, the quasi-mesenchymal subtype, the basal-like subtype and the squamous subtype are well aligned with a relatively poor prognosis in clinical data. The exocrine subtype and the ADEX subtype were reckoned as the same type. In addition, the basal-like subtypes were found to be associated with mutations in genes involved in

chromatin modification including DNA methylation and acetylation. Tumours of this subtype lost their endodermal identity through methylation of some genes such as HNF4A and GATA6, which are important for the diverse differentiation destinies of pancreatic cells. This finding gives us a hint that transcriptomic changes may be able to separate different subtypes with different therapy efficacy and prognosis (Brunton et al. 2020).

In 2018, Puleo et al. subdivided the canonical dichotomized classical and basal classification into pure classical, immune classical, desmoplastic, pure basal-like and stroma activated subtypes (Puleo et al. 2018), with additional features based on tumour differentiation and stromal activation state. Laser capture microdissection (LCM) was introduced to enrich tumour samples for pancreatic cancer epithelial cells. Maurer et al. recruited 60 pairs of matched tumour and stroma samples by LCM, and clarified the epithelial/stroma identities of the existing subtypes, giving a clearer understanding of the former molecular gene signatures built from bulk tissue (Maurer et al. 2019). In 2020, Chan-Seng-Yue et al. also performed LCM to purify 248 PDAC samples with further whole-transcriptome sequencing, accompanied by single-cell RNA sequencing on 13 resected and 2 metastatic tumour samples (Chan-Seng-Yue et al. 2020). This study subdivided the Moffitt classification into classical A, B, basal-like A, B and hybrid subtypes. The study found that classical and basal clusters coexisted in 13 of the 15 patient samples that had single-cell RNA sequencing. The basal-like signatures showed correlation with epithelial-to-mesenchymal transition (EMT) gene programs and were enriched for the major imbalance of allelic states of KRAS ($KRAS^{Ma}$), which turned out to be more chemo-resistant.

Multiple attempts at molecular subtyping have been undertaken in PDAC but have yet few to have a significant practical clinical impact. It remains a major challenge to develop approaches to molecular subtyping that will support clinical approaches to better chemotherapy drug selection, drug response monitoring and patient prognosis.

1.5 Diagnosis and Treatment

Early stage-pancreatic cancer lacks specific clinical signs. Almost 70% of pancreatic cancers occur in the head and neck of the gland and result in obstructive jaundice due to intra-pancreatic choledochal (bile duct) invasion. Most other patients show up with indistinct digestive symptoms, such as anorexia, nausea, emesis and abdominal pain. Some patients also have new-onset diabetes. Blood levels of carbohydrate antigen 19-9 (CA19-9) are usually elevated in PDAC and its measurement is useful for prognosis and monitoring response to treatment but it lacks sufficient sensitivity and specificity for early diagnosis (Takaori et al. 2016). Cross axial imaging such as computed tomography (CT) and magnetic resonance imaging (MRI) is the best way to detect pancreatic abnormalities (Lee and Lee 2014; Tempero et al. 2017). It assists in defining the tumour stage as well as determining the treatment strategy by identifying any tumour involvement of adjacent structures such as major blood vessels and the presence of any metastasis (Pietryga and Morgan 2015). Due to the non-specific manifestation of symptoms and lack of accurate biomarkers, primary population screening and early-stage diagnosis is a major challenge for pancreatic cancer research (Greenhalf et al 2020).

Surgery with adjuvant chemotherapy is the only potential cure for pancreatic cancer (Neoptolemos et al. 2018). However, due to non-specific symptoms, limited means of early detection and rapidly progressing disease, most of the patients are diagnosed with locally advanced or metastatic disease (30%-40% with borderline resectable tumour or locally unresectable tumour, and 50%-60% with metastasis). Around 20% of the patients can receive surgery, and surgery alone will usually not benefit long term survival, so it is essential to give adjuvant chemotherapy after resection. Even so, 80% of patients will relapse by five years, necessitating the need to optimize existing therapeutic options for personal precise medicine as well as developing novel treatments.

Before the 1990s, chemotherapy was mainly based on 5-fluorouracil (5-FU), an S-

phase-specific, fluorinated pyrimidine with a similar structure to the pyrimidine bases cytosine and thymine used in DNA synthesis. 5-FU is metabolized intracellularly to its active form 5-fluorodeoxyuridine monophosphate (5F-dUMP) via the de novo pyrimidine pathway, causing cytotoxicity. Its main mechanism of action is to inhibit the enzymatic activity of thymidylate synthase (TS) that methylates deoxyuridine monophosphate (dUMP) to form the pyrimidine nucleotide thymidine monophosphate (dTMP), which is required for DNA replication. Inhibition of TS requires the formation of a ternary complex involving 5F-dUMP, TS, and 5,10-methylene-tetrahydrofolate (5,10-CH_2-FH_4). Folinic acid (leucovorin, FA) is administered along with 5-FU as FA is metabolized to 5,10-CH_2-FH_4. This is because increased intracellular concentrations of 5,10-CH_2-FH_4 enhance the formation and stability of the 5F-dUMP/TS/5,10-CH_2-FH_4 inhibitory ternary complex thereby increasing cytotoxicity (Tsukihara et al. 2016). Secondary mechanisms of cell death involving other 5-FU metabolites involve 5-fluorouridine 5'-triphosphate (FUTP) being incorporated into RNA and 5-fluoro-2′-deoxyuridine 5′-triphosphate (FdUTP) being incorporated into DNA in both cases leading to apoptotic cell death (Derissen et al. 2016).

In 1999, the clinical trial in resectable pancreatic cancer launched by the European Organization for Research and Treatment of Cancer found that the adjuvant chemoradiotherapy group with infusional 5-FU as the radiosensitizer had no survival benefit compared with the observation group (Klinkenbijl et al. 1999). The ESPAC-1 trial showed no survival benefit for adjuvant chemoradiotherapy using an intravenous bolus of 5-FU as the radiosensitizer in resectable PDAC with a 5-year overall survival of 10% for patients with chemoradiotherapy vs 19.6% without (Neoptolemos et al. 2001). However, adjuvant systemic 5-FU chemotherapy with FA showed better survival than no adjuvant chemotherapy with a 5-year overall survival of 21% for patients with chemotherapy and 8% without (Neoptolemos et al. 2004).

In 1997, Burris et al. reported that gemcitabine was more effective than 5-FU in patients with non-resectable pancreatic cancer (1-yeat survival: 18% for gemcitabine

vs 2% for 5-FU; median overall survival: 5.6 months for gemcitabine vs 4.4 months for 5-FU) (Howard A. Burris III 1997). 2′,2′-difluoro-2′-deoxycytidine (dFdC) is an S-phase nucleoside deoxycytidine analogue with multiple modes of action to terminate DNA replication (Shore et al. 2003). Gemcitabine undergoes successive phosphorylation by deoxycytidine kinase to dFdC-monophosphate (dFdCMP), dFdeC-diphosphate (dFdCDP), then to dFdC-triphosphate (dFdCTP). Ribonucleotide reductase, which convertf cytidine diphosphate (CDP) to deoxycytidine diphosphate (dCTP) required for DNA replication, is inhibited by dFdCDP. Two gemcitabine triphosphate nucleotides (dFdCTP) are incorporated into the replicating DNA making the gemcitabine nucleotides less susceptible to exonuclease excision repair resulting in masked termination. Gemcitabine also sustains its own activity by blocking deoxycytidine kinase inhibition by dCTP. Gemcitabine is metabolized to FdUMP by deoxycytidine monophosphate deaminase but is itself inhibited directly by dFdCTP and indirectly inhibited by dFdCDP (Shore et al. 2003).

The ESPAC-3 trial in resectable PDAC compared the effect of gemcitabine adjuvant therapy compared with 5-FU plus FA as in the ESPAC-1 trial (Neoptolemos 2010). The results showed no survival benefit for gemcitabine over 5-FU and FA but with less serious adverse events, establishing gemcitabine as the treatment of choice. Then the ESPAC-4 trial, an adjuvant trial in resectable PDAC, found that combination therapy with gemcitabine and capecitabine (an orally active prodrug of 5-FU) plus FA had a significant survival benefit that pushed 5-year overall survival to 29% with acceptable toxicity compared to 16% for gemcitabine monotherapy (Neoptolemos et al. 2017). Gemcitabine-capecitabine therapy is recommended as a standard therapy for patients with resected pancreatic cancer in clinical practice (Khorana et al. 2017).

The combination of FA, 5-FU, irinotecan and oxaliplatin (FOLFIRINOX) has demonstrated robust activity with improved survival as first-line therapy compared with gemcitabine for both patients with metastatic pancreatic cancer (median overall survival was 11.1 months in the FOLFIRINOX group vs 6.8 months in the gemcitabine group) and resected pancreatic cancer (median disease-free survival was 21.6 months

in the modified-FOLFIRINOX group and 12.8 months in the gemcitabine group) (Conroy et al. 2011; Conroy et al. 2018). This combination therapy has become a widely used treatment modality for PDAC. However, the limitation of this combination is that it can only be used in patients with good cardiovascular and overall performance status (Eastern Cooperative Oncology Group performance status score 0 or 1) aged under 76 years old with metastatic disease or less than 80 years with resectable disease. In 2012, a regimen of gemcitabine and albumin-bound paclitaxel was introduced with improved survival efficacy (1-yeat survival: 35% vs. 22% for gemcitabine alone; median overall survival: 8.5 months vs. 6.7 months for gemcitabine alone) (Von Hoff et al. 2013).

The role of neoadjuvant chemotherapy and/or chemoradiation in patients with borderline resectable, or locally advanced unresectable pancreatic cancer is currently under evaluation (Ferrone et al. 2015; Hackert et al. 2016). For patients with borderline ,the ESPAC5 trial has shown that neoadjuvant chemotherapy improved overall survival compared to upfront surgery (Ghaneh 2020). The Alliance A021501 and ESPAC5 trials both showed that chemoradiation added to neoadjuvant chemotherapy was associated with increased toxicity and reduced survival (Ghaneh 2020; Matthew H. G. Katz 2021). The role of neoadjuvant chemotherapy and/or chemoradiation in patients with the resectable disease is controversial, with no positive randomized controlled trials showing improved survival compared to upfront surgery and adjuvant therapy (Leonhardt et al. 2020; Sohal DPS 2021; Springfeld and Neoptolemos 2022; Versteijne et al. 2020).

1.6 Predictive Response Biomarkers and Molecular Signatures

Therapeutic options for patients with pancreatic cancer are based on the stage of the disease, overall patient performance status and the severity of any comorbidities. Most treatment options include different types of chemotherapy, but drug response and the development of drug resistance show considerable diversity. Thus, there is an urgent

need for personalized and more precise medicine to guide clinical therapeutic decisions. The concept of Treatment Specific Signatures (TSSs) was first mentioned by David Tuverson's group, who developed molecular and therapeutic profiling using patient-derived organoids (PDOs) (Tiriac et al. 2018). Tiriac and colleagues successfully predicted patient clinical outcomes to FOLFIRINOX and gemcitabine/nab-paclitaxel regimens using transcriptomic profiling. However, transcriptomic signal clustering varies according to tumour heterogeneity and cellularity. The signals may also be influenced by the abundant stroma content of the tissue samples. Here we introduce five biomarkers that appear promising in classifying PDAC subtypes, and predicting therapeutic response and/or patient outcome.

GATA6

GATA Binding Protein 6 (GATA6) is a member of a small family of zinc finger transcription factors (GATA1-6) that bind to the (A/T)GATA(A/G) consensus sequence (Maeda et al. 2005). Family members play an important role in the regulation of cellular differentiation and organogenesis during vertebrate development. The GATA6 gene is expressed during early embryogenesis and localizes to endo- and mesodermal derived cells during later embryogenesis (Carrasco et al. 2012) and thereby plays a major role in the development of multiple organs, for instance, the cardiovascular system (Suzuki et al. 1996; Zhao et al. 2008), and the digestive system including the pancreas (Ketola et al. 2004), liver (Zhao et al. 2005), stomach (Deng et al. 2012), small intestine (Aronson et al. 2014), colon (Walker et al. 2014), and lung (Liao et al.) (**Fig 1**).

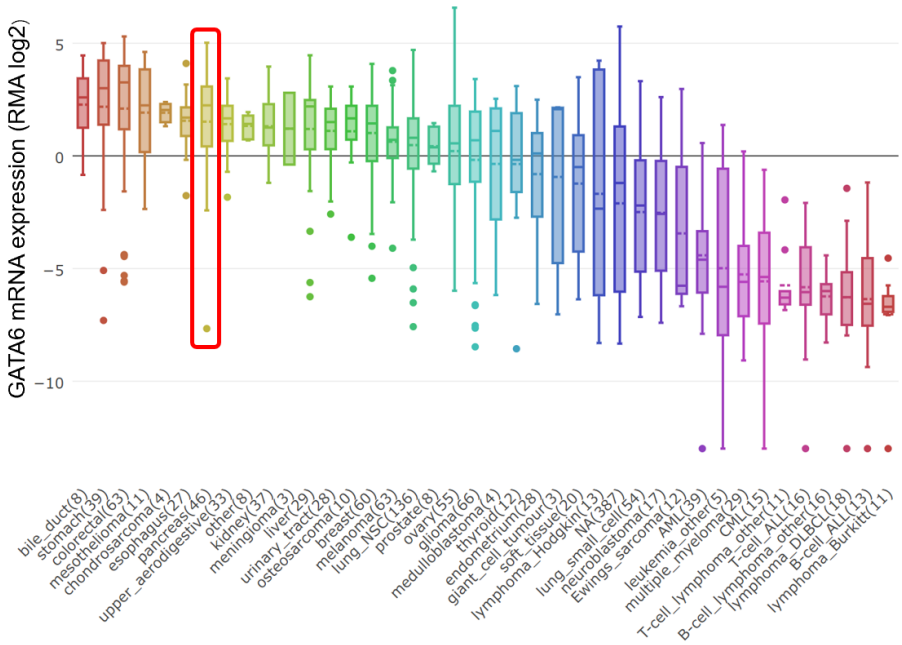

Fig 1. Box and whisker plots show GATA6 mRNA distribution in multiple tumours from CCLE database platform (http://portals.broadinstitute.org/ccle/home). Marked group is GATA6 mRNA expression in pancreatic cancer.

Mutations in this gene are associated with several congenital defects (Xu et al. 2018; Zheng et al. 2012), while overexpression of GATA6 has been shown to participate in the progression of several cancers including cholangiocarcinoma (Tian et al. 2013), colorectal cancer (Belaguli et al. 2010), cutaneous T-cell lymphoma (Kamijo et al. 2018), and pancreatic cancer (Kwei et al. 2008).

GATA6 is required for acinar cell differentiation and maintenance and GATA6 inactivation may cause acinar-to-ductal metaplasia (ADM) and fat replacement (Martinelli et al. 2013) (**Fig 2**). It exerts tumour-suppressor-like activity that stimulates

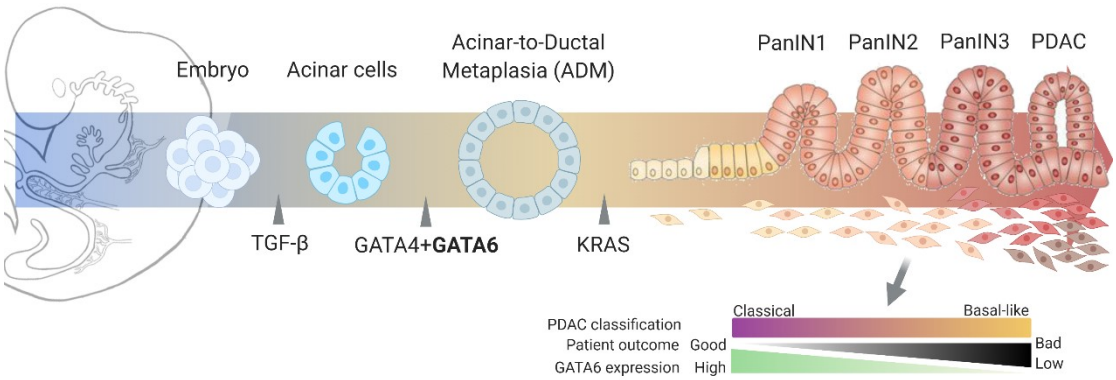

Fig 2. GATA6 plays an important role in pancreatic cancer development. The figureiary was self-drawn and partially inspired by Morris et al (Morris et al. 2010).

acinar cell differentiation and inhibits EMT (Martinelli et al. 2017). Chromosome locus 18q11.2, which contains the GATA6 gene, has selective amplification in pancreatic cancer, especially in well-differentiated tumours (Birnbaum et al. 2011; Fu et al. 2008). This indicates that GATA6 could be a marker for pancreatic cancer differentiation and patient prognosis (Collisson et al. 2011). This was confirmed in the prospective COMPASS trial in patients with advanced PDAC which showed that tumour GATA6 RNA in situ hybridization expression was able to differentiate classical and basal-like PDAC subtypes (Aung et al. 2018). The trial also found that objective tumour responses to first-line chemotherapy were significantly better in patients with the classical PDAC subtype determined by RNA-seq compared with those with the basal-like subtype (Aung et al. 2018). The best progression-free survival was observed in patients with the classical subtype treated with mFOLFIRINOX (Aung et al. 2018).
GATA6 protein expression by immunohistochemistry could also discriminate pancreatic cancer from normal pancreas, and semi-quantitatively classify classical and basal-like subtypes: classical subtype with strong and moderate GATA6 staining, while basal-like subtype with no or weak staining (Kwei et al. 2008).

hENT1

Human equilibrative nucleoside transporter 1 (hENT1), also known as Solute Carrier Family 29 Member 1 (SLC29A1), is a transmembrane glycoprotein located in plasma and mitochondrial membranes and is responsible for nucleoside transport (Beal et al. 2004). Nucleosides and their chemical analogues can only go through the plasma membrane with the help of nucleoside transporters (NTs) due to their hydrophilic nature. Equilibrative nucleoside transporters (ENTs) are passive transporters activated by nucleoside concentration gradient across the membrane. They are broadly-selective carrier proteins that transport both pyrimidines and purines (Huber-Ruano and Pastor-Anglada 2009), and some nucleobases as well (Yao et al. 2011). The ENT family has four members: ENT1-4, among which ENT1 and ENT3 have high sensitivity to inhibition by adenosine analogue nitrobenzylthioinosine (NBMPR), but not ENT2 and

ENT4 (Sundaram et al. 2001). ENT1 and ENT2 are localized to the basolateral membrane and are responsible for nucleoside transport, while ENT3 and ENT4 are localized to the intracellular organelles and are responsible for nucleoside uptake (Endo et al. 2007). Human ENT is widely distributed in various tissues with diverse expression levels (**Fig 3**). It is associated with disease states involving altered adenosine transporter

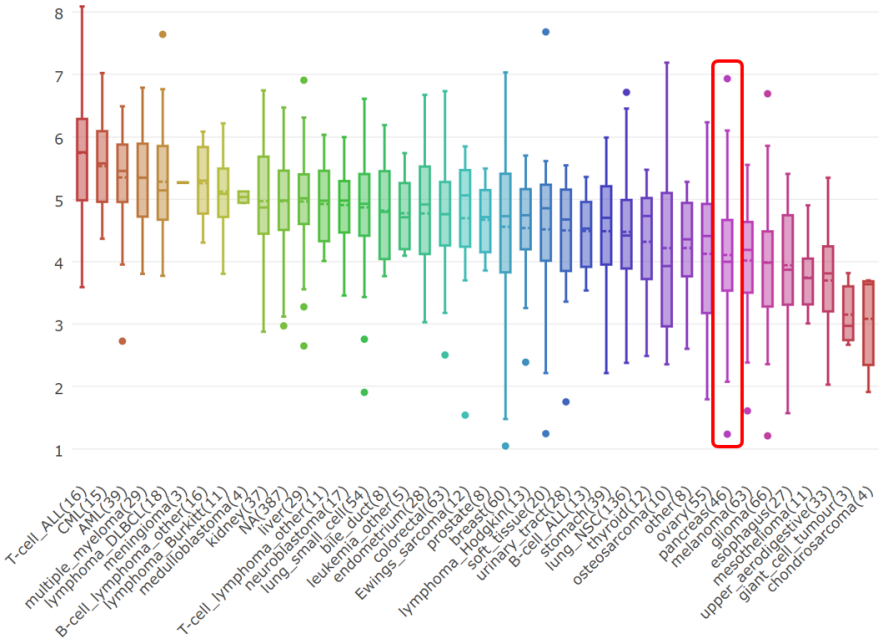

Fig 3. Box and whisker plots show hENT1 mRNA distribution in multiple tumours from CCLE database (http://portals.broadinstitute.org/ccle/home). Marked group is hENT1 mRNA expression in pancreatic cancer.

function, such as diabetes mellitus and hypertension (Pastor-Anglada and Pérez-Torras 2018). Moreover, its prominent role in nucleoside transport makes ENT a promising indicator for nucleoside analogue anticancer therapy. The ENT expression level will directly influence nucleoside analogue drug permeation and cause individual pharmacokinetic variety (Cano-Soldado and Pastor-Anglada 2012). hENT1 expression level significantly influences gemcitabine uptake efficiency (**Fig 4**). hENT1 has been shown to predict response to gemcitabine-based therapy in patients with pancreatic cancer (Bird et al. 2017), non-small cell lung cancer (Oguri et al. 2007), biliary tract cancer (Kim et al. 2018), and mantle cell lymphoma (Marcé et al.)

The ESPAC-3 Trial showed that the median survival for patients with resected PDAC

treated with adjuvant gemcitabine was 17.1 months in those with tumours with hENT1 low-expression vs 26.2 months in those with tumours with hENT1 high-expression (Greenhalf et al. 2014). The RTOG9704 Trial also found that hENT1 high tumour expression was associated with overall and disease-free survival of patients who underwent gemcitabine adjuvant therapy (Farrell et al. 2009).

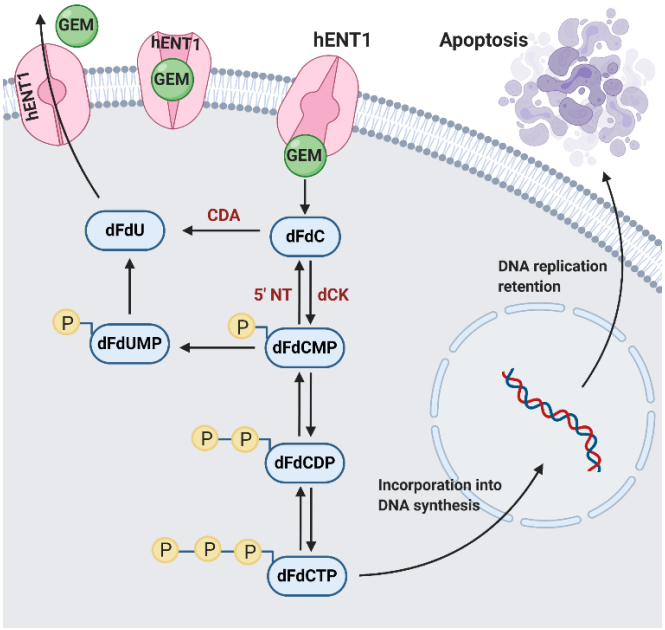

Fig 4. hENT1 transfer gemcitabine into cell plasma (self-drawn).

CYP3A5

CYP3A5 is a member of the cytochrome P450 superfamily of monooxygenases which catalyse many reactions involved in up to 75% of all drug metabolism (Guengerich 2008). CYP3A4 participates in the synthesis of multiple lipids, such as cholesterol and steroids, and is mainly found in adult human liver with higher expression levels than the other isoforms (Waring 2020). CYP3A5 shows a wider distribution than CYP3A4 not only in adult human liver and small intestines, but also in fetal liver, kidney and lung (Aoyama et al. 1989; Wrighton et al. 1990) (**Fig 5**). There is a wide variation in expression levels between different ethnic groups (Hsu and Johnson 2019). CYP3A5 expression is low in around 91% of Caucasians due to a SNP within intron 3 (A6986G) termed the CYP3A5*3 variant allele, causing alternative splicing and protein truncation, while individuals with at least one CYP3A5*1 allele have high expression

levels (Kuehl et al. 2001). The cytochrome P450 family is involved in numerous physiological processes and pathophysiological conditions. In hypertension CYP3A5 converts cortisol to a 6β-hydroxylated which causes sodium and water retention and contributes to hypertension (Bochud et al. 2009; Zhang et al. 2014). In the prostate gland, CYP3A5 catalyses the 6β-hydroxylation of testosterone, converting this it into the less active 6β-hydroxy testosterone. There is an androgen response element in the proximal promoter

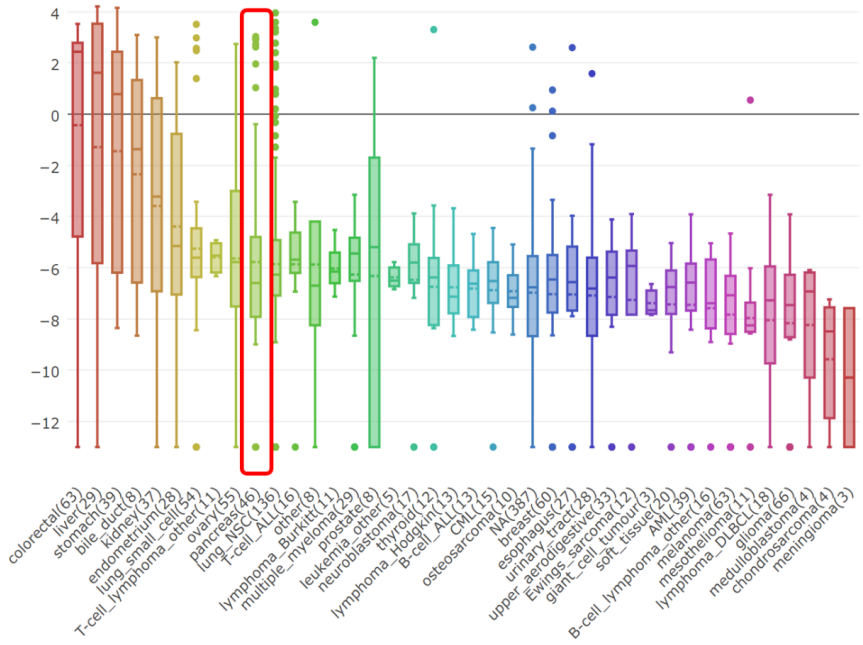

Fig 5. Box and whisker plots show CYP3A5 mRNA distribution in multiple tumours from CCLE analysis (http://portals.broadinstitute.org/ccle/home). Marked group is CYP3A5 mRNA expression in pancreatic cancer.

of CYP3A5, forming an autoregulatory feedback loop controlling prostate cell exposure to androgens, implicated in prostate cancer (Mitra and Goodman 2015; Moilanen et al. 2007). In hepatocellular carcinoma (HCC) CYP3A5 functions as a tumour suppressor of pathogenesis and metastasis by regulating the ROS/mTORC2/Akt signalling pathway (Jiang et al. 2015).

CYP3A5 is involved in the metabolism of numerous drugs used for cancer chemotherapy including the mitosis inhibitors vincristine and paclitaxel (Skiles et al. 2018)), the tyrosine-kinase inhibitors lapatinib (Towles et al. 2016) and erlotinib (Noll et al. 2016), and the DNA topoisomerase I inhibitor irinotecan (Buck et al. 2019).

Irinotecan is hydrolysed by carboxylesterase 2 (CES2) into the active metabolite 7-ethyl-10-hydroxy-camptothecin (SN-38) which inhibits topoisomerase I, leading to DNA breaks and cell death, and CES2 tumour expression is predictive of response to irinotecan using patient-derived PDAC xenograft (PDX) models (Capello et al. 2020; Capello et al. 2015). Irinotecan is deactivated by CYP3A4- and CYP3A5-dependent oxidation to the inactivate metabolites 7-ethyl-10-[4-N-(5-aminopentanoicacid)-1-piperidino] carbonyloxycamptothecin (APC), 7-ethyl-10[4-amino-1-piperidino] carbonyloxy-camptothecin (NPC) and M4 (**Fig 6**). SN38 itself is inactivated and detoxified by UDP-glucuronosyltransferase (UGT) enzymes notably UGT1A1, UGT1A6 and UGT1A10 to SN38G. The UGT1A1*28 polymorphism, results in decreased UGT1A1 enzyme expression and a reduced glucuronidation of the active metabolite SN38, leading to irinotecan-induced severe neutropenia. Extracellular transport by the ATP-binding cassette transporters (ABC transporters) also regulates the intercellular levels of irinotecan (ABCB1 and ABCB2), and SN38 (ABCB1, ABCC1, ABCC2, and ABCG2).

Hepatocyte nuclear factor 1-alpha (HNF1A) is a master transcriptional regulator that influences the expression of several key genes involved in drug metabolism and including UGT and ABCC2 with improved progression-free survival in irinotecan-treated metastatic colorectal cancer patients carrying the HNF1A coding variant p.I27L (Labriet et al. 2017).

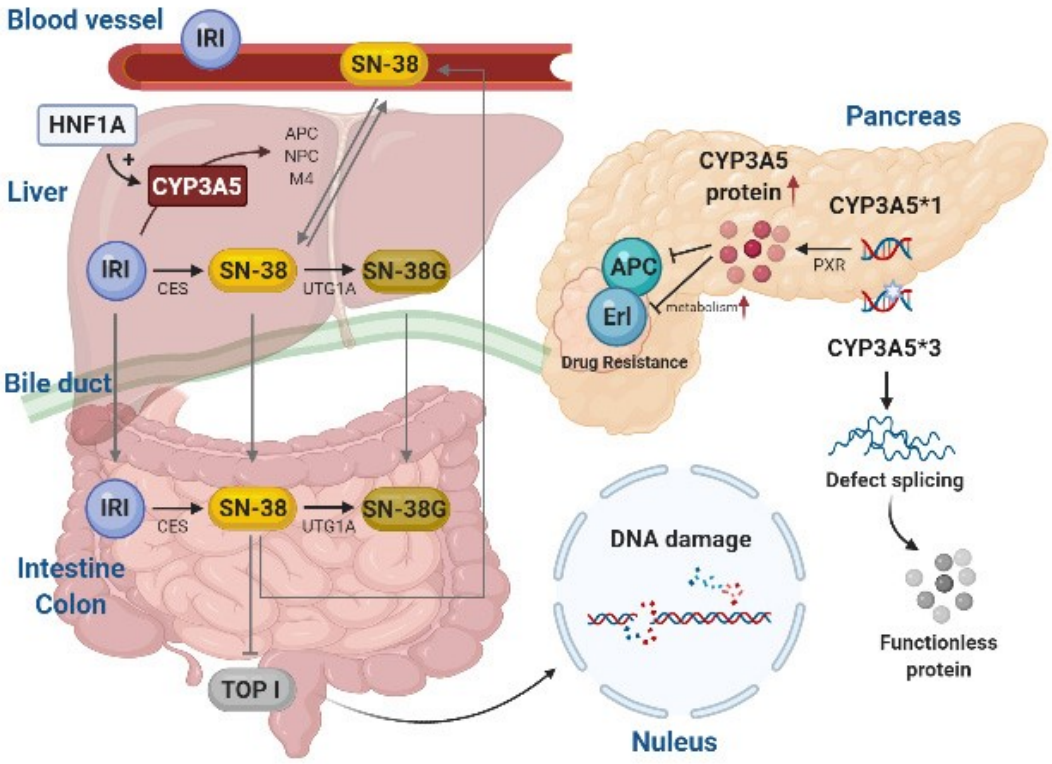

Fig 6. CYP3A5's function in drug metabolism. CYP3A5 causes irinotecan resistance by oxidizing activate metabolite SN-38 into APC, NPC or M4 (self-drawn).

Noll and colleagues showed that in pancreatic cancer, the Collisson exocrine-like subtype was resistant to dasatinib, erlotinib, and paclitaxel, and that each of these drug-xenobiotics caused upregulation of CYP3A5-dependent drug detoxification (Noll et al. 2016). Whereas the nuclear receptor transcription factors hepatocyte nuclear factor 4 alpha (HNF4A) and the pregnane X receptor (PXR), also known as the steroid and xenobiotic sensing nuclear receptor (SXR) or nuclear receptor subfamily 1, group I, member 2 (NR1I2) control the basal expression of CYP3A family members only the NR1I2 initiates transcription in response to xenobiotics such as dasatinib, erlotinib, and paclitaxel (Noll et al. 2016). Further understanding of the clinical relevance of the findings by Noll and colleagues is required since around 90% of Caucasians have the inactive CYP3A5*3 isoform (Ingelman-Sundberg and Lauschke 2020).

HNF1A and KRT81

Hepatocyte nuclear factor 1 homeobox A (HNF1A), also known as TCF1, is a

transcription factor expressed in the human liver, pancreatic islets, kidney and gut (Harries et al. 2006) (**Fig 7**).

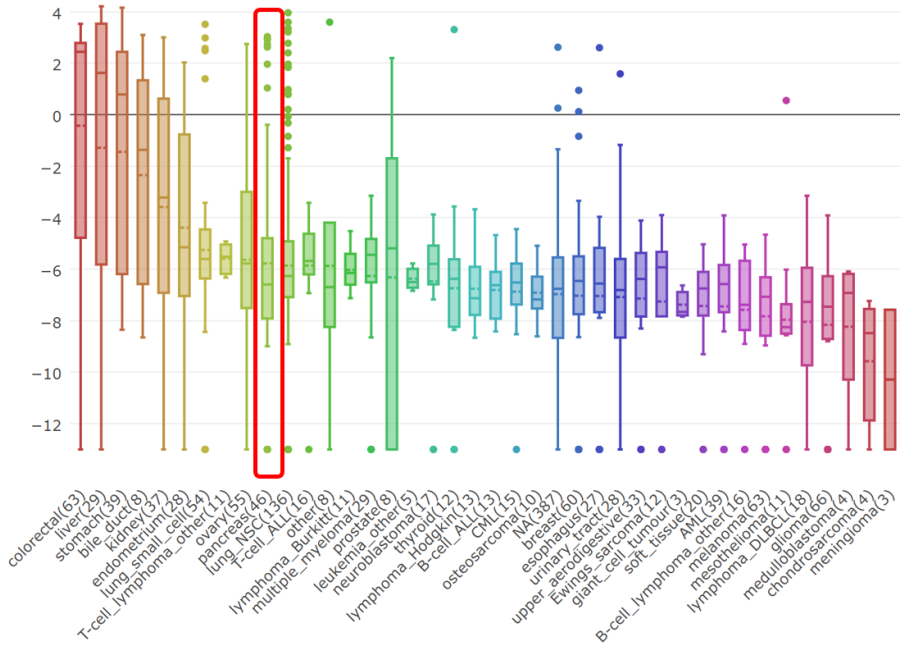

Fig 7. Box and whisker plots show HNF1A mRNA distribution in multiple tumours from CCLE analysis (http://portals.broadinstitute.org/ccle/home). Marked group is HNF1A mRNA expression in pancreatic cancer.

HNF family numbers have a close relationship with maturity-onset diabetes of the young (MODY), a monogenic form of diabetes mellitus. HNF4A, HNF1A and HNF1B mutations can result in MODY1, 3 and 5 respectively (Fajans et al. 1994; Yamagata et al. 1996). MODY is caused by glucose-stimulated insulin secretion impairment, suggesting that HNF1A and HNF4A mutations are related to pancreatic β-cell disfunction (Leahy et al. 1993; Yamagata 2014). Mutations of HNF1A are the most common cause of MODY. The HNF1A gene contains 10 exons and codes for a 631 amino acid homeoprotein, and there are 414 different mutations in almost all the regions of the HNF1A gene, including the promoter region, the DNA-binding domain (Haliyur et al. 2019), and the transactivation domain (Colclough et al. 2013), with P291fsinsC taking dominance (Yamagata et al. 1998). The HNF1A protein is found in both endocrine and exocrine pancreatic cells with three isoforms, HNF1A(A), HNF1A(B), and HNF1A(C). HNF1A expression supports β-cell number maintenance and in turn contributes to insulin secretion by regulating multiple genepathway-rel

related genes, including SlC2A2 (Ban et al. 2002), atedPklr (Párrizas et al. 2001), Tmem27 (Akpinar et al. 2005), and HNF4A (Boj et al. 2001). Mutation of HNF1A in the Hnfia$^{-/-}$ mice model suppressed glucagon secretion from pancreatic α-cells (Yoshifumi Sato 2020).

Genome-wide association studies (GWAS) found that HNF1A SNPs were strongly related to pancreatic cancer, indicating that HNF1A was a susceptibility locus (Pierce and Ahsan 2011). HNF1A is a tumour suppressor gene in pancreatic cancer and is downregulated in PDAC (Hoskins et al. 2014; Luo et al. 2015). KDM6A encodes lysine-specific demethylase which is a component of the MLL/COMPASS transcriptional co-regulatory complex that catalyses the demethylation of histone H3K27me3, associated with polycomb-mediated repression controlling multiple differentiation pathways during development; up to 18% of PDAC tumours carry mutations in KDM6A (Waddell et al. 2015). HNF1A recruits KDM6A to genomic binding sites forming a transcriptional complex which activates an acinar differentiation program (FOXA3, DEPTOR, GSTP1, and PTPRJ) that indirectly suppresses core oncogenic pathways including EMT gene programs and MAPK signa (Bärthel et al. 2020; Kalisz et al. 2020). In transformed cells with oncogenic KRAS signalling, loss of HNF1A and/or KDM6A induces upregulation of mesenchymal gene sets (FOXA2, HOXB8, MYC, and ΔNp63) and leads to a sarcomatoid differentiated PDAC (Bärthel et al. 2020; Kalisz et al. 2020). HNF1A can also promote long noncoding RNA-CASC2 expression through direct binding to a CASC2-HNF1A response element, leading to suppression of pancreatic cancer cell proliferation through the PTEN/Akt-mTOR signalling pathway (Yu et al. 2019). Bailey et al found that HNF1A expression along with PDX1, GATA6, MNX1, HNF4G, HNF4A, HNF1B, FOXA2, FOXA3 and HES1 were identified as transcriptional networks defining the pancreatic progenitor or classical subtype whereas MYC, RUNX2, CK17, and ΔNp63 defined the squamous or basal subtype (Bailey et al. 2016).

KRT81 is a member of the keratin gene family encoding cytokeratins which are differentially expressed in various epithelial cells (Langbein et al. 2001; Langbein and

Schweizer 2005) (**Fig 8**).

Noll and colleagues used HNF1A and KRT81 expression to classify Collisson's PDAC subtypes: $KRT81^{+}HNF1A^{-}$ for the quasi-mesenchymal (QM-PDA) subtype, $KRT81^{-}HNF1A^{+}$ for the exocrine-like subtype, and $KRT81^{-}HNF1A^{-}$ for the classical subtype (Noll et al. 2016; Scott and Wilkinson 2016).

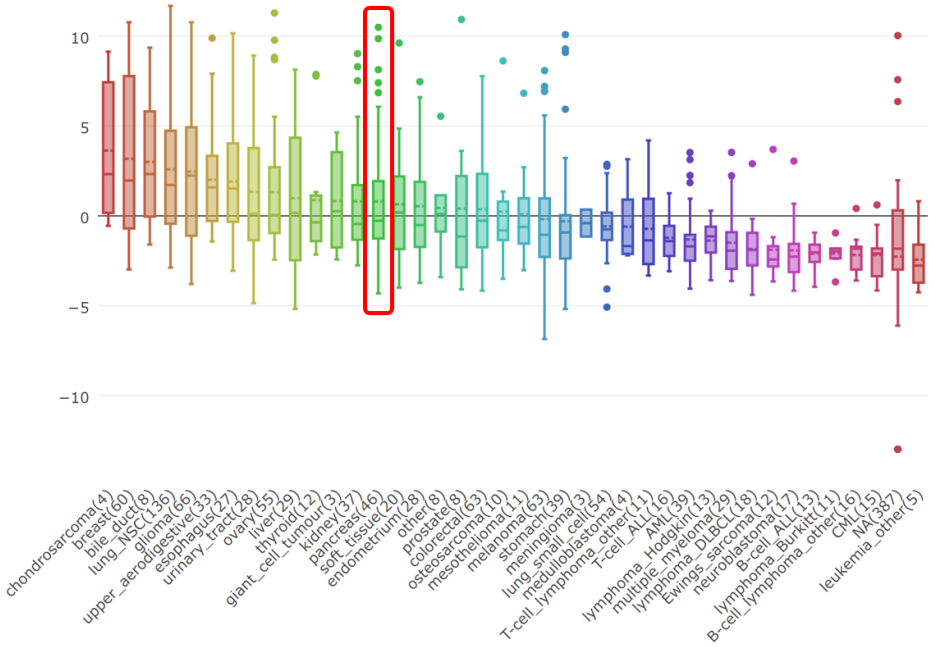

Fig 8. Box and whisker plots show KRT81 mRNA distribution in multiple tumours from CCLE analysis (http://portals.broadinstitute.org/ccle/home). Marked group is KRT81 mRNA expression in pancreatic cancer.

In subsequent clinical studies the $HNF1A^{+}$ subtype showed the best survival in resected PDAC, the $KRT81^{+}$ subtype the worst, and the $KRT81^{-}HNF1A^{-}$ subtype had intermediate survival, whilst $KRT81^{+}$ patients treated only with chemotherapy also had the worst prognosis (Muckenhuber et al. 2018).

1.7 Aim

In this study, we aimed to investigate tumour biomarkers that identify molecular subtypes and best survivors/responders to surgery and standard chemotherapy regimens in patients with pancreatic ductal adenocarcinoma. There are many potential biases in a study such as this. We chose patients that underwent surgery so that we could work with representative samples of fresh cancer tissue, along with baseline

demographic, pathological, and clinical information and documentation on any subsequent additional treatment and clinical follow-up. We used time to death from surgery as the measure for the clinical outcome as this is a hard endpoint. Previous investigations have included patients that may have had chemoradiotherapy as well surgery and chemotherapy. Chemoradiotherapy is a major confounder for pathological and molecular analyses, so we excluded all such cases. Thus, we were very careful to select only fresh tumour samples that came from patients that fell into two groups: patients that had upfront (neoadjuvant) chemotherapy then surgery with follow-up, in order to study the effect of chemotherapy on tumour tissue; and (2) patients that had upfront surgery and then (adjuvant) chemotherapy with follow up, so that we had access to chemo-naïve tissue acting as a control to the first group. Laser capture microdissection was conducted on chemo-naïve samples prior to adjuvant therapy for tumour cell enrichment. The aim was to explore the discovery of biomarkers that could be used to optimize clinical treatment selection.

2. MATERIALS AND METHODS

2.1 Materials

2.1.1 Laboratory Equipment

Analytical balance	KERN
Autoclaves	Systec
Distilled water purification system	Heraeus
Electronic balance	Sarrtorius
Fluorescence and H&E imaging system	TISSUE GNOSTICS
Fluorescence microscope	Carl Zeiss
Freezer -20°C	LIEBHERR
Freezer -80°C	SANYO
Glassware washer	Miele
High-speed centrifuge	Eppendorf
Ice machine	HOSHIZAKI
Light microscope	Leica
Low-speed centrifuge	Heraeus
Magnetic stirrer	Heidolph
Microtome	Leica
Microwave oven	SHARP
Mini-rocker shaker	Biosan
Mini-spin	Eppendorf
Orbital shaker	Heidolph
PH meter	HANNA
Refrigerator 4°C	LIEBHERR
Roller mixer	Couler
Thermal oven	Mennert
Thermomixer	Eppendorf
UV illuminator system	Viber Lourmat
Water bath	Medingen

Confocal Microscope	Leica
Laser Microdissection System LMD7000	Leica
Incubator oven (180°C)	Memmert
Microcentrifuge (with rotor for 2ml tubes)	
QIAcube Connect	QIAGEN

2.1.2 Laboratory Consumables

Accupette pipettes	neoLab
Pipette tips (0.1-10 µl, 1-200 µl)	AHN Biotechnology
Pipette tips (1000µl)	Gilson
Microcentrifuge tubes (1.5 ml, 2 ml)	SARSTEDT
Microscope cover glasses	MARIENFELD
Microscope slides	Thermo Scientific
Pasteur capillary pipettes (230mm)	VBGL Scientific
Pipettes	Gilson
Stripettes (5 ml, 10 ml, 25 ml)	Costar
Weighing paper	neoLab
DAKO pen	Dako
Ethanol resistant pen	SARSTEDT
Membrane slides	Carl Zeiss
(1.0 PEN membrane-covered)	
DNase/RNase-free 50 ml tubes	Sarstedt
AdhesiveCap 500 opaque (500µl)	Carl Zeiss
Syringe filter (PVDF, sterile)	ROTH
Safe-lock microcentrifuge tubes (2 ml)	Eppendorf

2.1.3 Reagents

Antibody diluents	Dako, USA
(with background reducing components)	
Bromophenol blue	ROTH, Germany
DAPI	Sigma, St. Louis, USA

DPBS	Gibco, Paisley, UK
Eosin	ROTH, Germany
Ethanol (70%, 100%)	ROTH, Germany
UltraCruz Blocking reagent	ChemCruz, Germany
Hematoxylin	Merck, Germany
HCl (37%)	ROTH, Germany
Methanol	ROTH, Germany
Milk powder	ROTH, Germany
Mounting medium	ROTH, Germany
NaOH	J.T. Baker, Holland
RNaseZAP	Sigma, St. Louis, USA
Acetic Acid (100%)	ROTH, Germany
Roticlear	ROTH, Germany
Saponin	Fluka, Steinheim, Germany
Sodium citrate buffer (10×)	Nordic MUbio, The Netherlands
Tween-20	Sigma, St. Louis, USA
RLT lysis buffer	QIAGEN, Germany
Xylene	ROTH, Germany
Cresyl Violet acetate	Sigma, St. Louis, USA
β-mercaptoethanol (14.3 M)	
AllPrep DNA/RNA/miRNA Universal Kit	QIAGEN, USA

2.1.4 Buffers and Solutions

10 × PBS – 1 L (pH 7.4)

NaCl	80 g
Na_2HPO_4	14.4g
KCl	2 g
K_2HPO_4	2.4 g

Dissolve and adjust pH to 7.4 with 37% HCl. Add dH_2O to final volume of 1 L. Before use: dilute as1:10 with dH_2O and adjust pH to 7.4 if necessary.

0.05% TBS-T

0.5 ml Tween-20 in 1 L 1 × TBS

5% Eosin

1.5g Eosin in 300 ml 96% ethanol with 6 drops of. Filter before use.

0.1% Saponin

0.2g Saponin in 200 ml 1 × TBS

1% Cresyl Violet

0.5 g Cresyl Violet in 50 ml Ethanol overnight. Filter before use.

2.1.5 Antibodies

Primary Antibodies

The primary antibodies are shown in **Table 1**, were diluted in antibody diluents (with Background Reducing Components) and used for immunofluorescence (IF).

Table 1. The list of primary antibodies.

Primary Antibodies	Company	Catalog No.	Dilution Ratio	Source
CK19	Santa Cruz Biotechnology	sc-376126	1/400	Mouse
CK19	Abcam	ab52625	1/400	Rabbit
CYP3A5	Abcam	ab108624	1/200	Rabbit
GATA6	R&D System	AF1700	1/100	Goat
hENT1	Creative Biolabs	TAB-023CT	1/100	Mouse
HNF1A	Santa Cruz Biotechnology	sc-393925	1/100	Mouse
KRT81	Santa Cruz Biotechnology	sc-100929	1/50	Mouse

Secondary Antibodies

The secondary antibodies are shown in **Table 2** for IF and were diluted in antibody diluents.

Table 2. The list of secondary antibodies.

Secondary Antibodies	Conjugate	Company	Catalog No.	Dilution Ratio	Source
Anti-Goat IgG	DyLight 594	Thermo	SA5-10088	1/100	Donkey
Anti-Rabbit IgG	Alexa Fluor 555	Fisher	A31572	1/400	Donkey
Anti-Mouse IgG	DyLight 550	Scientific	SA5-10173	1/200	Goat

2.1.6 Human Subjects

This study was approved by the Ethics Committee of Heidelberg University: Pancreatic cancer tissue (S-708/2019). All the patients were informed that their tissue would be used for research purposes and signed the ethical consent form. PDAC tissue and

corresponding blood samples were collected by the Biobank service of the European Pancreas Centre (EPZ), which is part of the Department of Surgery of the University Clinic Heidelberg according to the inclusion criteria (**Table 3**).

Table 3. Inclusion criteria.

Adjuvant Chemotherapy Samples	Neoadjuvant Chemotherapy Samples
• No prior therapy. • PDAC resection only-M0. • Adjuvant CTX: FOLFIRINOX or GEM-based therapy, no chemo-radiation. • Known recurrence (date) or not (last known date). • Known last follow-up or death. • Standard demographics and pathology.	• PDAC resection only-M0. • Neoadjuvant CTX: FOLFIRINOX or GEM-based therapy, no chemoradiation. • Known recurrence (date) or not (last known date) • Known last follow-up or death. • Standard demographics and pathology.

Both cryopreserved and formalin-fixed, paraffin-embedded (FFPE) tissues were examined by a specialist pancreas pathologist. Sixty-eight snap-frozen cryopreserved samples were collected from chemo-naïve patients after surgical resection. After surgery, fifty-five patients received gemcitabine (GEM)-based chemotherapy, eleven patients received FOLFIRINOX (FFX) chemotherapy, and two patients received GEM/FFX sequential chemotherapy. Thirty-five of the sixty-eight cryopreserved samples from chemo-naïve patients underwent LCM for tumour cell enrichment. Thirty-seven snap-frozen cryopreserved samples were collected from the patients who received neoadjuvant therapy prior to surgical resection. The neoadjuvant/post-treatment group included 23 patients with gemcitabine-based therapy, 21 patients with FOLFIRINOX (FFX) chemotherapy, and three patients had FFX/GEM sequential chemotherapy. Corresponding blood samples were treated with EDTA and stored immediately at -80°C. The cryopreserved tissue samples were for RNA sequencing. Patient characteristics were extracted from the clinical database with anonymized patients' names for research use only, shown in **Table 5**.

Seventy-seven formalin-fixed, paraffin-embedded (FFPE) samples were collected from chemo-naïve patients after surgical resection, including 57 patients with gemcitabine-based therapy, nine with FFX therapy, seven with sequential chemotherapy (five with GEM/FFX, two with FFX/GEM) and four had unknown treatment regimens. Fifty-one FFPE samples were collected from patients who had received neoadjuvant chemotherapy, including 22 patients with gemcitabine-based chemotherapy, 23 with FFX, three with FFX/GEM sequential therapy, and two had unknown treatment regimens. Nine normal pancreas samples were obtained from organ donors as healthy controls.

The FFPE samples were used for immunofluorescence (IF) assays to determine marker protein expression levels. Patient treatment details and outcomes were extracted from the clinical database with anonymized patients' names for research use only. The data are not shown here.

2.2 Methods

2.2.1 Formalin-Fixed, Paraffin-Embedded (FFPE) Tissue

Fresh tissue samples were fixed in 4% formalin (DPBS buffered) at room temperature for 24 hours. The samples were then immersed in 70% ethanol for 2 to 3 days and embedded by paraffin into blocks. The blocks were stored at 4℃ and were put at -20℃ on the day before use. The blocks were cut into 4 μm thick by microtome and the sections were mounted on adhesive-coated slides. The slides were dried out and kept at 4℃ for further use.

2.2.2 Hematoxylin & Eosin (H&E) Staining

H&E staining for FFPE tissue slides

1. Incubate the slides at 60℃ for 10 minutes.
2. Deparaffinization and rehydration.

Immerse the slides in the following solutions one after another.

- Roticlear, 3×10 minutes;
- 100% ethanol, 3×3 minutes;
- 95% ethanol, 1×3 minutes;
- 70% ethanol, 1×10 minutes;
- 50% ethanol, 1×3 minutes;
- Distilled water, 1×3 minutes.

3. Incubate the slides in filtered hematoxylin solution for 2 minutes.
4. Rinse the slides with running tap water for 15 minutes.
5. Immerse the slides in 5% eosin solution for 2 seconds.
6. Dehydration.

Immerse the slides in the following solutions one after another.

- 70% ethanol, 2×5 seconds;
- 95% ethanol, 1×3 minutes;
- 100% ethanol, 3×3 minutes;
- Roticlear, 3×3 minutes.

7. Mount the sections with mounting medium and coverslips. Incubate the slides at 37℃ overnight to dry out.

The slides were scanned by the Tissue Gnostics imaging system to acquire H&E staining images.

H&E staining for cryo-tissue slides

1. De-freeze the slides at room temperature (RT) for 1 minute.
2. Immerse the slides in filtered hematoxylin for 16 seconds.
3. Rinse the slides in tap water, 2×3 seconds.
4. Immerse the slides in 5% eosin for 4 seconds.
5. Dehydration.

Immerse the slides in the following solutions one after another.

- 70% ethanol, 1-2 seconds;
- 95% ethanol, 1×3 minutes;
- 100% ethanol, 3×3 minutes;
- Roticlear, 3×5 minutes.

6. Mount the sections with mounting medium and coverslips. Incubate the slides at

37°C overnight to dry out.

The slides were scanned by the Tissue Gnostics imaging system to acquire H&E staining images.

2.2.3 Histopathological Evaluation

H&E and cresyl violet staining tissue slides were examined by an experienced pancreas specialist pathologist who was blinded to patient clinical information. Tumour type (e.g., PDAC, IPMN and PanIN), tumour area and proportion, and whether there was inflammation were included in the evaluation. The samples were then selected for further study according to this pathology report.

2.2.4 Immunofluorescence (IF)

Immunofluorescence for GATA6, hENT1, CYP3A5, HNF1A and KRT81 expression was performed on FFPE sections, which were double-stained with the epithelial cell marker CK19, taken as a ductal tumour cell marker. The IF procedure was performed as follows:

1. Incubate the slides at 60°C for 10 minutes.
2. Deparaffinization and rehydration.
   - Roticlear, 3×10 minutes;
   - 100% ethanol, 3×10 minutes;
   - 95% ethanol, 1×10 minutes;
   - 70% ethanol, 1×10 minutes;
     50% ethanol, 1×10 minutes;
   - Distilled water, 1×5 minutes.
3. Antigen retrieval.
   - Boil the slides in preheated 1×sodium citrate buffer (10 mM, pH6.0) in a microwave oven (800W) for 10 minutes.
   - Incubate the slides in preheated sodium citrate buffer in a 98°C-water bath for 20 minutes.
   - Cool down the slides within the buffer in RT for 30 minutes.

4. Rinse the slides in TBS for 5 minutes.
5. Permeabilization.

Incubate the slides in 0.1% Saponin at RT for 20 minutes.

6. Rinse the slides in 0.05% TBS-T for 2×2 minutes, and then in TBS for 5 minutes.
7. Blocking.
   - Draw a hydrophobic circle around the tissue with a Dako pen and put the slide back into PBS. Repeat the same procedure until all the sections are circled.
   - Place the slides in a flat dark humid chamber.
   - Suck out extra TBS on the tissue and add 60-100 µl ultra-blocking reagent. Make sure that the tissue is completely covered. Repeat the same procedure until all the sections are blocked.
   - Incubate the slides in RT for 30 minutes.
8. Primary antibody incubation.

Suck out the blocking reagent without rinsing. Add 60-100 µl primary antibodies (diluted in antibody diluents) drop-wise on the tissue. The dilution ratio is shown in Table 1 according to the antibody datasheet. For double staining, the antibodies from different sources were mixed together. For negative control sections, the same volume of antibody diluents without primary antibodies was added to eliminate the influence of the non-specific binding from secondary antibodies. Incubate the slides in humid chamber at 4℃ overnight (16-18 h).

9. Rinse the slides in 0.05% TBS-T for 3×5 minutes.
10. Secondary antibody incubation.

Suck out extra TBS-T from the tissue. Add 60-100 µl secondary antibodies (diluted in antibody diluents, dilution ratio shown in **Table 2**) drop-wise on the tissue. The secondary antibodies were conjugated with fluorophores (fluorescent dye Cy3 or Cy5) raised against the host species of the primary antibodies. For double staining, the antibodies were also mixed together. Incubate the slides in dark humid chamber at RT for 1 hour.

11. Rinse the slides in 0.05% TBS-T for 3×5 minutes.
12. DAPI staining.

Suck off extra TBS-T, add 60-100 µl DAPI solution (1:1000 diluted in PBS) on the

tissue. Incubate the slides in dark humid chamber at RT for 20 minutes.

13. Rinse the slides in 0.05% TBS-T for 3×5 minutes and distilled water.
14. Immerse the slides in 100% ethanol for 5 minutes and leave them to dry out in the dark.

15 Mount the slides with Fluoromount-G mounting medium and coverslip. Store the slides in a dark place at 4℃ for further use.

2.2.5 Images Acquisition and Analysis

The imaging system consisted of a fluorescence microscope (Observer. Z1, Zeiss), illumination unit (X- Cite® Series 120PC Q), and TissueFAXS software (Tissue Gnostics, Vienna, Austria). H&E images were acquired using a 20X objective lens using bright field. IF images were acquired using a 20X objective lens with light emitting diodes (LED) with specific light filters, exposure time and sensitivity threshold for DAPI, Cy3 and Cy5 (Chroma Technology, USA) respectively. The image analysis was performed using StrataQuest software (Tissue Gnostics), which can locate and calculate the intensity of the fluorescence signals in the region of interest (ROI). Nuclei and cellular size were adjusted to achieve specific tissue cell type detection. StrataQuest was used to plot the mean intensity of Cy3 and Cy5 the against mean DAPI intensity as a scattergram. IF images of negative control sections were used to set the appropriate gating to exclude any background immunofluorescence and non-specific binding signals. The expression of each marker protein was co-determined on each section with DAPI and CK19 expression, using signals from the latter to indicate the tumour cell ROI. The expression level of each marker protein was calculated by the percentage of protein positive stained cells in DAPI and/or CK19 positive cells.

2.2.6 Laser capture microdissection (LCM)

LCM was performed on 35 cryopreserved tissue samples from patients after resection and prior to any adjuvant therapy. LCM was not undertaken on tissue samples after neoadjuvant chemotherapy as the tumour cells were difficult to identify and often

widely scattered across the stroma cells to enable any meaningful tumour cell enrichment.

Cutting Procedure

1. Before use, the slides are placed under UV irradiation (220 nm-260 nm) for 30 minutes. Label and precool the slides at -20℃ before cutting sections.
2. The first section is for a quick look to ensure that there is tissue in the section before cutting further sections (‘general validation’), using an adhesion slide. Dip the slide in hematoxylin for 1min and wash with tap water. Examine under microscope the estimate the tumour percentage.
3. The second slide is prepared for tissue validation by the specialist pathologist (‘precise validation’) on another adhesion side. Cut 2 sections on the SuperFrost Plus adhesion slide marked with ‘patient ID-1’ and store it at -80℃ for H&E staining later.
4. Each 1.0 PEN membrane slide will have 6-8 sections (depending on the size of the tissue pieces) that have been further cut. The thickness of the sections is 12 μm. The slides are labelled with ‘patient ID- ‘, ‘patient ID-2’, and so on.
5. The slides may be temporarily stored in the slide box at -80℃ prior to LCM.
6. After preparing the first 5 X 1.0 PEN membrane slides, to further check that the block contains adequate tissue a general validation and a precise validation adhesion slide is also prepared as above. The sequence of slide preparation is shown in **Fig 9**.

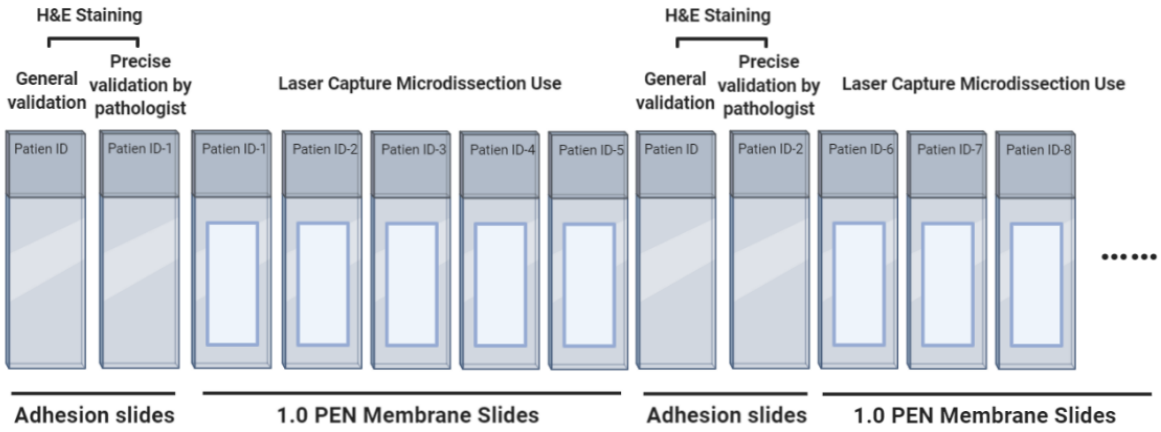

Fig 9. Slide Arrangement.

The number of membrane slides prepared for each tumour sample

For large diameter tissue blocks, there would be 4-6 sections to fully occupy one 1.0 PEN membrane slide. For small diameter tissue blocks, 10-12 sections would be required to fully occupy one 1.0 PEN membrane slide. The sections are placed in the same orientation as the sections for H&E staining. The number of membrane slides required to obtain sufficient tumour cells for quality-controlled RNA-seq is dependent on the tumour content in the original sample. The estimates shown in **Table 4** was established empirically by preliminary studies.

Table 4. Sections to prepare according to tumour percentage.

Tumour Content	Sections on each slide	Number of Membrane Slides
80%-90%	6	3-4
40%-60%	6	5-8
10%-40%	6	10-12
5%-10%	6	16-20

Samples with very low tumour percentage (less than 5%) are excluded as it was found that insufficient tumour could be obtained for quality-controlled RNA-seq. The range of the proportion of tumour cells in different tissue samples is illustrated in **Fig 10 (i)**.

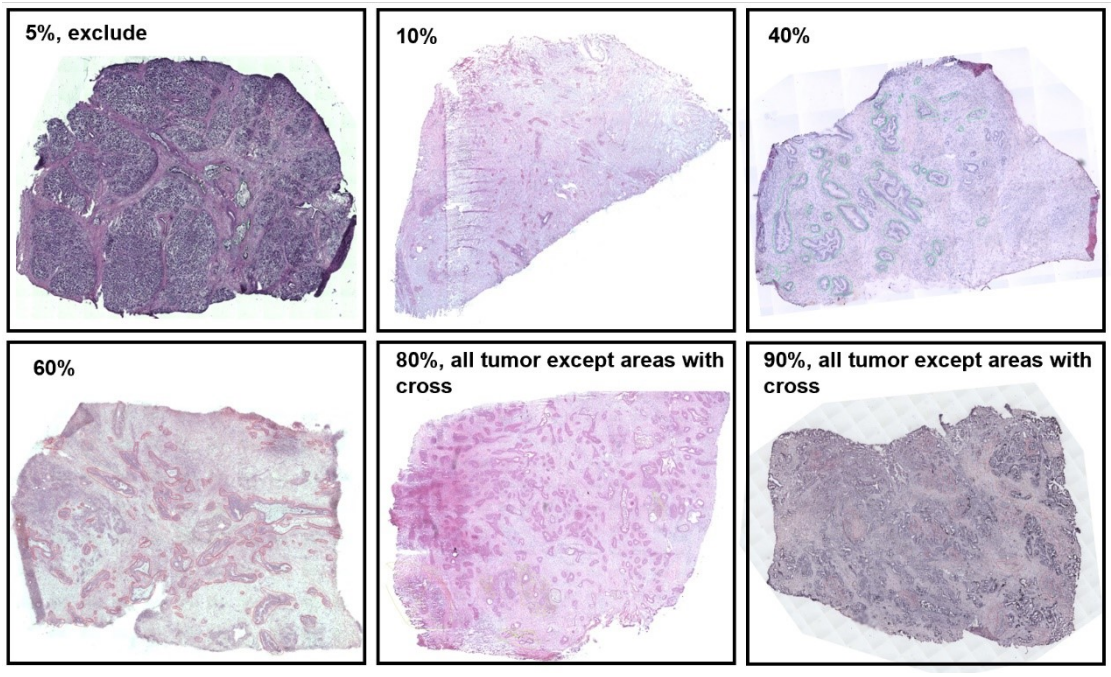

Fig 10 (i). The range of the proportion of tumour cells in different tissue samples determined by the specialist pathologist.

H&E Staining Procedure

The same procedure as in section 2.2.2 hematoxylin & eosin (H&E) staining/ H&E staining for cryopreserved tissue slides is used. This procedure is only needed for the sections on standard adhesion slides used for H&E validation, but not for the sections on membrane slides used for laser capture microdissection.

Cresyl Violet Staining Procedure

This quick cresyl violet staining procedure was used on snap frozen tissue slides just before laser capture microdissection was undertaken. The incubation steps were kept as brief as possible to minimize the influence of RNase.

1. Rehydration: incubate the slides in 100% ethanol, 2×30 seconds.
2. Incubate the slides in filtered cresyl violet for 30 seconds.
3. Dehydration.
   - 50% ethanol, 30 seconds;
   - 75% ethanol, 30 seconds;
   - 95% ethanol, 30 seconds;
   - 100% xylene, dip for several times;
   - 100% xylene, 5 minutes;

Air dry slides briefly for 1-2 minutes.

LCM Procedure

1. Turn on the laser key and the microscope controller, open the LCM program on desktop, and wait for autocalibration.
2. Unload the slide holder and clean it with RNaseZAP. Mount the sample(s) (face down, maximum 4 slides) on the tray holder and carefully put the holder back on the stage. It will click when it is in the proper location.
3. Unload the collector holder and clean it with RNaseZAP. Mount 0.5 ml microtube(s) on the holder. Put the holder back.
4. Reference point calibration.

Select 5x lens magnification. Click “Go to reference point”. Adjust the white hole (reference point) to the centre of the image view window by clicking the four orientation arrow buttons. Click “OK” to finish the calibration.

5. Laser calibration

Select 10x or 20x lens magnification. Find a field without region of interest and focus. Click “Calibration” under the laser menu. Follow the instruction to click the centre of each cross.

6. Focus on the sample and use the mouse to draw out the region of interest. Choose the collector position. Adjust power, aperture and speed on the laser parameter panel.

   Click “start” to begin the microdissection procedure.

7. Repeat step 6 to harvest enough tissue on the tube cap. Carefully unload the microtube and add 200-400 µl RLT buffer in the tube. Carefully close the cap and let the tissue soaked in the buffer. Store the tube at -80°C for further use. The final volume of the sample should be 600 µl.
8. After use, clean up the holders by RNaseZAP, close the software, the microscope and switch off the laser controller.

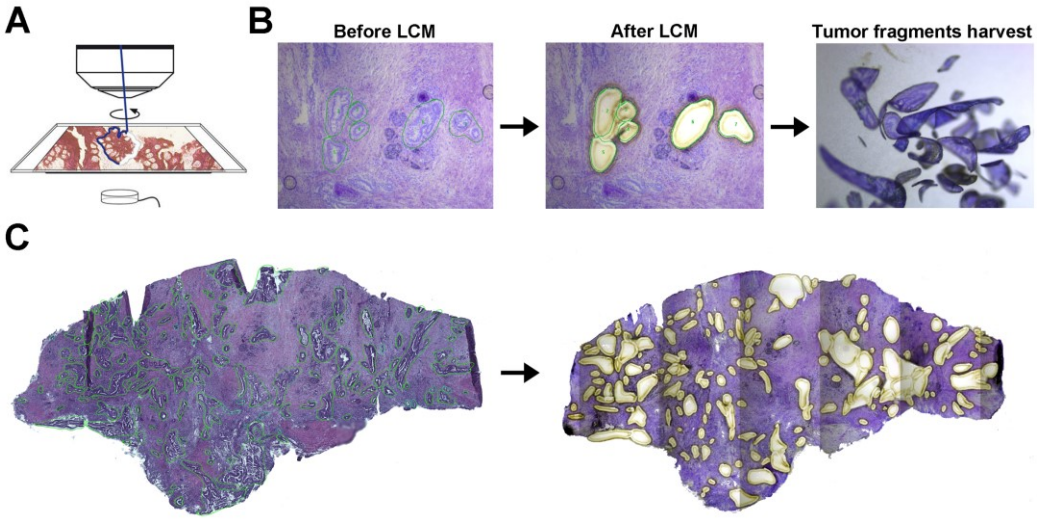

Fig 10 (ii). LCM procedure. **(A)** Schematic diagram of LCM. **(B)** An example of the LCM procedure from regions of interest before LCM, after LCM and tumour fragments harvested in the adhesive cap (Patient ID: HD 7603). **(C)** Comparison between pathological validation image and the image after-LCM - the same patient as (B).

2.2.7 DNA and RNA Extraction

DNA and RNA extraction procedure was performed in National Centre for Tumour Diseases Heidelberg (NCT).

DNA Extraction

1. Disrupt tissue in 600 µl RLT buffer, add appropriate β-mercaptoethanol in the buffer (10 µl β-mercaptoethanol in 1 ml RLT buffer) to eliminate the influence of RNase.
2. Transfer the homogenized lysate to an AllPrep DNA spin column placed in a 2 ml collection tube. Close the lid gently and centrifuge at full speed (17,000 rpm) for 3 minutes.
3. Purification.
   - Add 350 µl buffer AW1 to the AllPrep DNA spin column.
   - Add 20 µl Proteinase K to 60 µl Buffer AW1, mix gently and apply the mixture to the AllPrep DNA spin column membrane. Incubate for 5 minutes at room temperature.
   - Add 500 µl buffer AW1 to the DNA spin column. Centrifuge for 15 seconds.
   - Add 500 µl buffer AW2 to the DNA spin column. Centrifuge for 2 minutes.
   - Place the spin column in a new 1.5 ml collection tube. Add 100 µl buffer EB directly to the column membrane. Centrifuge for 1 minute at 10,000 rpm to elute the DNA.
   - Repeat last step to elute further DNA. To achieve a higher DNA concentration, elute with 2×50 µl buffer EB, but the final DNA yield may be reduced.
4. After purification, move DNA solution into a labelled 1.5 ml DNase/RNase-free tube and store at -80℃ for further use.

Total RNA Extraction

1. Disrupt tissue in 600 µl RLT buffer, add appropriate β-mercaptoethanol in the buffer (10 µl β-mercaptoethanol in 1 ml RLT buffer) to eliminate the influence of RNase.
2. Transfer the homogenized lysate to an AllPrep DNA spin column placed in a 2 ml collection tube. Close the lid gently and centrifuge at full speed (17,000 rpm) for 3 minutes.
3. Purification.
   - Add 80 µl Proteinase K to the DNA spin column and mix well.
   - Add 350 µl of 96%-100% ethanol and mix well. Incubate the solution at room temperature for 10 minutes.

- Add 750 µl of 96%-100% ethanol and mix well.
- Transfer up to 700 of 96%-100% ethanol to the mixture and mix well. Of the sample, including any precipitate that may have formed to a RNeasy spin column placed in a 2 ml collection tube. Centrifuge for 15 seconds, repeat until the complete lysate is used.
- Add 500 µl buffer RPE to the RNeasy spin column. Centrifuge for 15 seconds.
- Add 10 µl DNase I stock solution to 70 µl buffer RDD. Mix gently by inverting the tube. Add 80 µl DNase I incubation mix directly to the RNeasy spin column membrane and place on the bench top for 15 minutes.
- Add 500 µl buffer FRN to the RNeasy spin column. Centrifuge for 15 seconds. Save the flow-through. Place the RNeasy spin column in a new 2 ml collection tube. Reapply the flow-through to the spin column and centrifuge for 15 seconds.
- Add 500 µl Buffer RPE to the RNeasy spin column. Centrifuge for 15 seconds.
- Add 500 µl of 96–100% ethanol to the RNeasy spin column. Centrifuge for 2 minutes.
- Place the RNeasy spin column in a new 1.5 ml collection tube. Add 30-50 µl RNase-free water directly to the spin column membrane. Centrifuge for 1 minute at 17,000 rpm to elute the RNA. Repeat this step to further elute the RNA.

4. After purification, move RNA solution into a labelled 1.5 ml DNase/RNase-free tube and store at -80°C for further use.

DNA/RNA concentrations were determined by using fluorometric kits (Quant-iT dsDNA or RNA broad range assay). DNA/RNA quality was tested by using an automated electrophoresis system (genomic DNA/RNA Screentape for Tapestation System). Quality control criteria for sequencing was as follows:

DNA with DIN ≥ 7; RNA with RIN > 6, 28S/18S area > 0.8, and DV200 > 70%.

2.2.8 RNA-sequencing

The RNA extractions of the snap-frozen samples were sent to the Genomics and Proteomics Core Facility, DKFZ for Systems integration bulk RNA sequencing by using STAR Version 2.5.3a via the internal NGS-data processing system (ref: http://dx.doi.org/1016/j.jbiotec.2017.08.006).

2.2.9 Statistical Analysis

The RNA-seq results were analysed by bioinformatic specialists (Prof. Peter Bailey, Department of General Surgery, University Clinic Heidelberg, Germany and the University of Glasgow; Prof. Benedikt Brors and Dr Roma Kurilov, German Cancer Research Centre (DKFZ), Heidelberg, Germany). The batch-effect of the RNA-seq count data was corrected by Combat as implemented by the SVA R package. The DESeq2 package was used to normalize batch corrected count files and to generate LogR normalized gene expression values. Downstream statistical analyses were performed using LogR normalized values. Heatmaps were generated using the ComplexHeatmap package in R. PCA analysis was performed using the DESeq2 package.

The mRNA expression profile of the biomarkers was extracted from the RNA-seq data. The boxplots and Kaplan-Meier curves were generated by GraphPad Prism 8.

TissueFAXS software was used to calculate the immunofluorescence intensity and the data was analysed by Student's t-Test and Wilcoxon Test. The boxplots and Kaplan-Meier curves were also generated by GraphPad Prism 8.

The results were considered as significant difference when $p \leq 0.05$ and were marked with significant scores (*$p < 0.05$; **$p < 0.01$; ***$p < 0.001$; ****$p < 0.0001$). The detailed results were reported as mean ± SEM (standard error of the mean) or normalized to the control samples as indicated in the figures.

3. RESULTS

3.1 Patient Characteristics.

To explore the classification and potential biomarkers for PDAC, snap-frozen, and FFPE samples were obtained from the Biobank of EPZ of the Surgery Department. Among 115 recruited cases, 47 patients received chemotherapy before surgery (Neoadjuvant group) and 68 patients after surgery (Adjuvant group). General characteristics of all patients in this cohort were listed in **Table 5**.

3.2 Transcriptional Profile of PDAC Patients

Bulk RNA-seq was performed on three subsets of patient samples, namely: a) adjuvant/chemo-naïve, b) LCM-enriched adjuvant/chemo-naïve; and c) neoadjuvant/ post-chemotherapy to determine and compare the transcriptional profiles of PDAC patients that had received either adjuvant or neoadjuvant therapy. LCM was performed on chemo-naïve samples to eliminate the influence of stromal tissue and to enrich tumour-specific signals. Principal component analysis using Log normalized RNA expression values demonstrated that treatment naïve and post-treatment samples are transcriptional distinct and form two separable groups (**Fig 11**). This analysis also demonstrated that LCM samples cluster together within the treatment naïve group.

Table 5. Demographic, clinicopathological and surgical characteristics according to treatment group.

	Post=chemotherapy group (N=47)	**Chemo-naïve group (N=68)**
Gender ratio (m / f)	24 / 23 (51.1 / 48.9)	42 /26 (61.8 / 38.2)
Age in years*	63.1 (56.9 – 70.9)	61.6 (57.4 – 67.3)
BMI (kg/m^2) *	23.9 (21.8 – 25.5)	25.3 (22.8 – 27.8)
ASA classification		
ASA 1	1 (2.2)	7 (10.8)
ASA 2	29 (64.4)	42 (64.6)
ASA 3	15 (33.3)	16 (24.6)
CA 19-9 (U/mL) *	78.2 (10.5 – 371.8)	280.6 (85.2 – 885.8)
Type of operation		

Pancreatoduodenectomy	18 (38.3)	39 (57.4)
Distal pancreatectomy	10 (21.3)	13 (19.1)
Total pancreatectomy	19 (40.4)	16 (23.5)
Arterial resection	11 (23.4)	5 (7.4)
PV/SMV resection	28 (59.6)	24 (35.3)
Tumour size		
≤2cm (8^{th} T1)	3 (6.4)	5 (7.6)
>2-≤4cm (8^{th} T2)	22 (46.8)	39 (59.1)
>4cm (8^{th} T3)	18 (38.3)	20 (31.8)
Arterial infiltration (8^{th} T4)	4 (8.5)	1 (1.5)
Missing size	0	3
Positive node count		
0 (8^{th} N0)	15 (31.9)	13 (19.1)
1-3 (8^{th} N1)	15 (31.9)	28 (41.2)
≥4 (8^{th} N2)	17 (36.2)	27 (39.7)
M status		
M0	40 (85.1)	60 (88.2)
M1	7 (14.9)	8 (11.8)
UICC (8^{th}) stage		
IA	2 (4.3)	0 (0.0)
IB	7 (14.9)	9 (13.2)
IIA	3 (6.4)	4 (5.9)
IIB	11 (23.4)	24 (35.3)
III	17 (36.2)	23 (33.8)
IV	7 (14.9)	8 (11.8)
R-classification		0
R0	9 (19.1)	10 (14.7)
R1	38 (80.9)	57 (83.8)
Rx	0 (0.0)	1 (1.5)
Chemotherapy		
FOLFIRINOX	21 (44.7)	11 (16.2)
Gemcitabine	23 (48.9)	55 (80.9)
Combination	3 (6.4)	2 (2.9)

Values in parentheses are percentages unless indicated otherwise; *values are median (IQR).

Transcriptomic analysis of the RNA-seq data focused on 2 main areas. Firstly, samples were classified using one of four major transcriptomic classification schemes, namely Moffitt, Bailey, Collisson and Notta. Secondly, the mRNA expression of 5 putative biomarkers (GATA6, CYP3A5, HNF1A, KRT81 and hENT1) - referred to herein as "biomarkers" - were analysed to determine their relative expression between PDAC subtypes and/or association with clinical outcome.

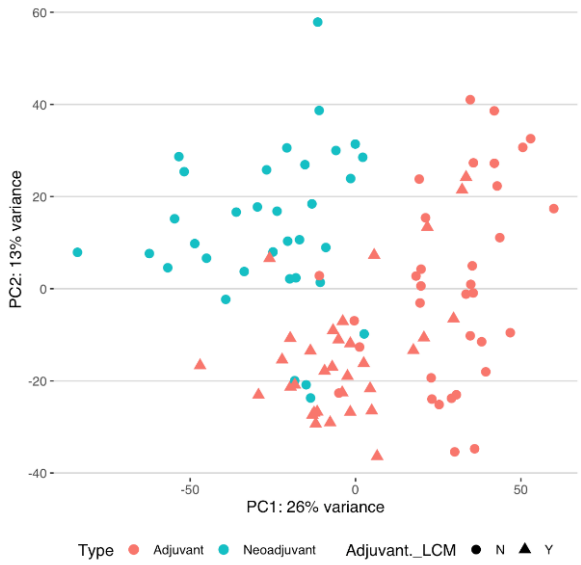

Fig 11. PCA analysis showed clusters of patient samples belonging to adjuvant, LCM-enriched adjuvant (adjuvant LCM) and neoadjuvant samples.

3.2.1 Transcriptomic Profile of PDAC Patients Validated Multiple Classification Schemes.

A comprehensive subtyping analysis was performed on patient samples described herein to define and validate the Moffitt, Collisson, Bailey and Notta classification schemes. Subtyping analysis of treatment naïve samples demonstrated that all patient samples could be classified into at least one PDAC subtype (**Fig 12A**). Further, the Collisson, Bailey and Notta classification schemes exhibited considerable overlap with the consensus Moffitt Classical and Basal-like subtypes. For example, and as previously demonstrated, the Bailey Progenitor and Squamous subtypes showed considerable overlap with the Moffitt Classical and Basal-like subtypes, respectively. Notably, 72% (n=48) of treatment naive samples were identified as belonging to the classical subtype whereas the remaining 28% (n=19) were identified as basal-like (**Fig 12A**).

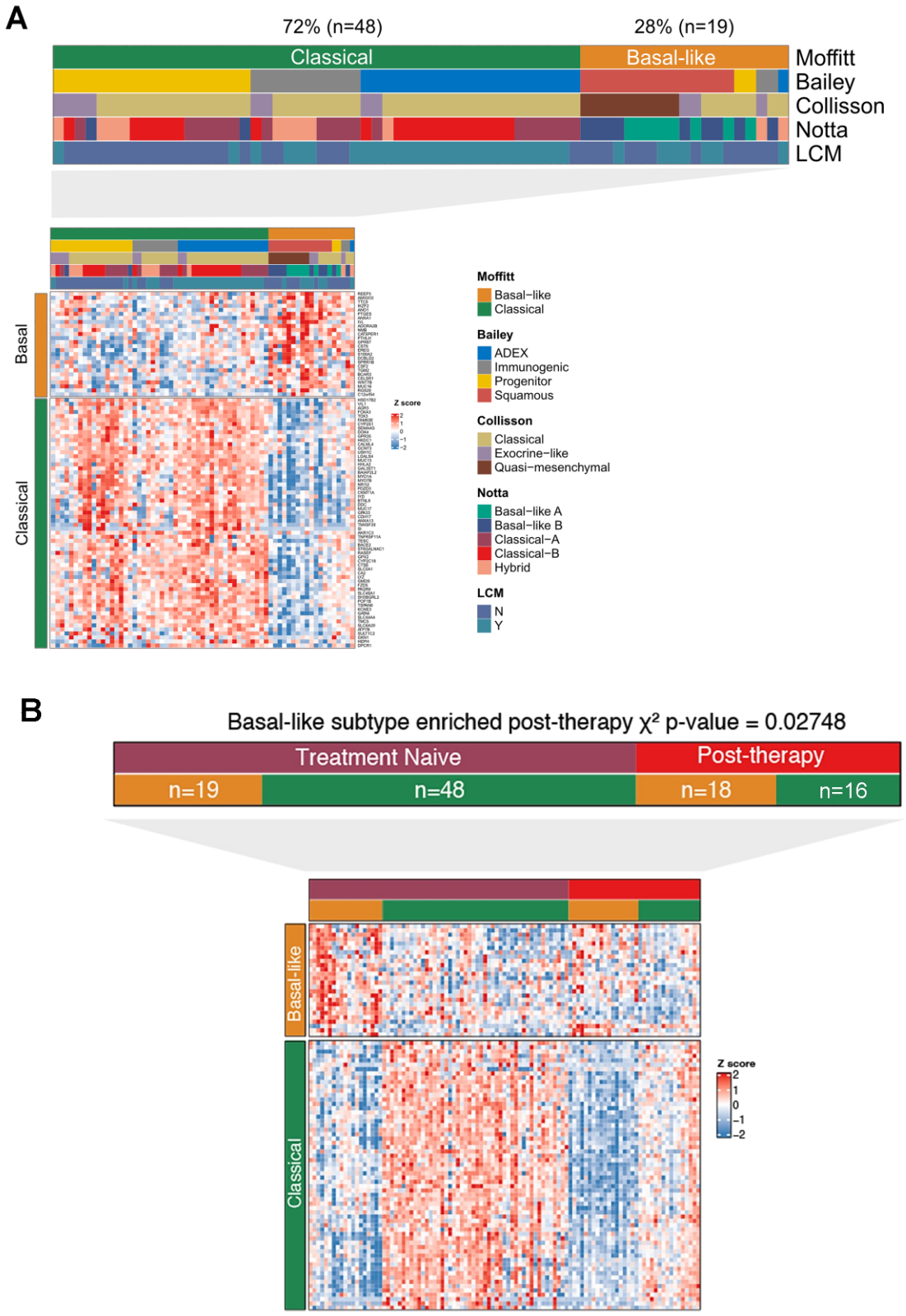

Fig 12. PDAC Subtype analysis of treatment naïve and post treatment samples **(A)** Treatment naïve samples stratified according to the Moffitt, Bailey, Collisson and Notta classification schemes **(B)** Post treatment samples stratified according to the Moffitt classification scheme.

Subtyping analysis of post-treatment resected samples demonstrated that the Moffitt

Classical and Basal-like subtypes persist after therapy, however, in comparison to treatment naive samples, the basal-like subtype was found to be significantly over-represented in post treated samples when compared to the classical subtype (P value = 0.027; X2-Test) (**Fig 12B**).

3.2.2 HNF1A and CYP3A5 Showed lower Expression in PDAC Patients after Neoadjuvant Treatment.

The differential expression of biomarker mRNA between treatment naïve and post-treatment patient samples was assessed. GATA6, HNF1A, CYP3A5 all exhibited a general trend towards lower post-treatment expression with HNF1A and CYP3A5 showing significantly lower expression in post treatment samples (**Fig 13 A**). KRT81, in contrast, showed a significant increase in expression in post treatment samples. No significant change in the expression of hENT1 (SLC29A1) was observed. There was no significant difference found in potential biomarker mRNA according to different neoadjuvant CTX as shown in **Fig 13 B**, indicating that gemcitabine/FOFIRINOX regimens before surgery did not appreciably change biomarker mRNA expression.

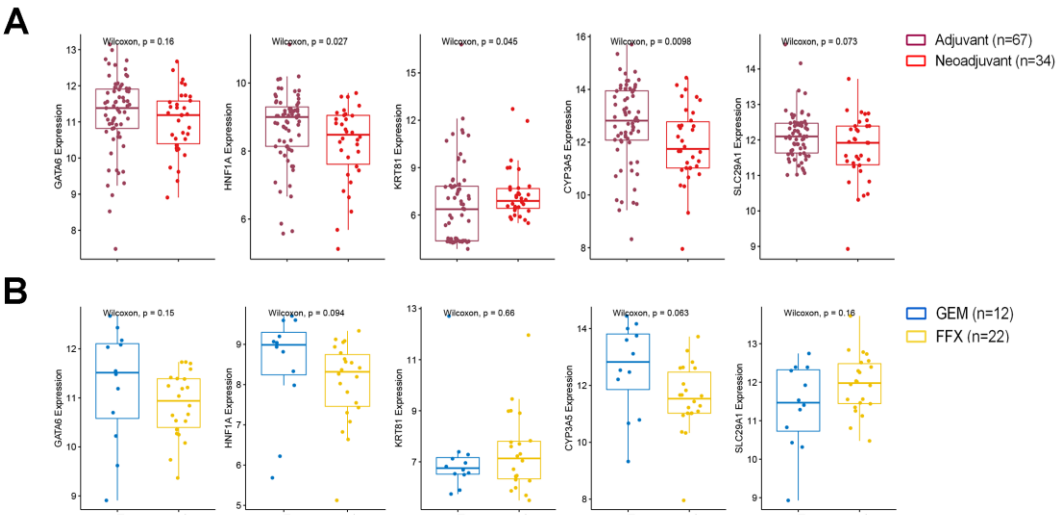

Fig 13. mRNA expression of potential biomarkers stratified by (**A**) pre-/post-chemotherapy treatment (marked as adjuvant/neoadjuvant, Wilcoxon test), and **(B)** different neoadjuvant regimens (Kruskal-Wallis test; ns $p > 0.05$, *$p < 0.05$, **$p < 0.01$, ***$p < 0.001$, ****$p < 0.0001$).

3.2.3 GATA6, CYP3A5 and HNF1A identified classical subtype in Moffitt, Collisson and Notta classifications.

To explore the relationship between the expression of the biomarkers and PDAC subtypes in chemo-naïve and post-treatment samples, biomarker mRNA expression levels were stratified according to the Moffitt, Collisson and Notta subtype classifications. This analysis in the chemo-naïve group demonstrated that GATA6, CYP3A5 and HNF1A had higher mRNA expression in the Moffitt classical subtype, while KRT81 had significantly higher expression in the basal-like subtype. hENT1 showed no difference between the two subtypes in the adjuvant group. GATA6, CYP3A5, and HNF1A were also significantly associated with the classical subtype in the post-chemotherapy group, while the other 2 markers showed no significant subtype enrichment (**Fig 14 A**).

GATA6 and CYP3A5 expression were strongly related to Collisson classification in chemo-naïve group, with high expression in classical subtype and low expression in QM-PDA subtype. Same pattern was found for HNF1A expression with only significant difference in QM-PDA subtype. In post-chemotherapy group, GATA6 and CYP3A5 also showed a significant association with the Collisson classification (GATA6 low expression in QM-PDA subtype and CYP3A5 high expression in classical subtype). hENT1 expression was found to be significantly higher in the exocrine-like group in post chemotherapy samples. KRT81 expression, however, did not change between groups. (**Fig 14 B**).

GATA6, CYP3A5, HNF1A and hENT1 mRNA was also stratified according to the Notta classification in the chemo-naïve group (**Fig 14 C**). GATA6, HNF1A, CYP3A5 were significantly expressed in the classical A/B subtype. These biomarkers, meanwhile, were lowly expressed in basal-like A subtype samples. CYP3A5 was also proved that it could well stratify Notta classification in post-chemotherapy group, followed by HNF1A showing slight significance. These results suggested that GATA6, CYP3A5 and HNF1A were promising biomarkers for classical subtype for all three

classifications, while KRT81 and hENT1 played minor roles in subtyping.

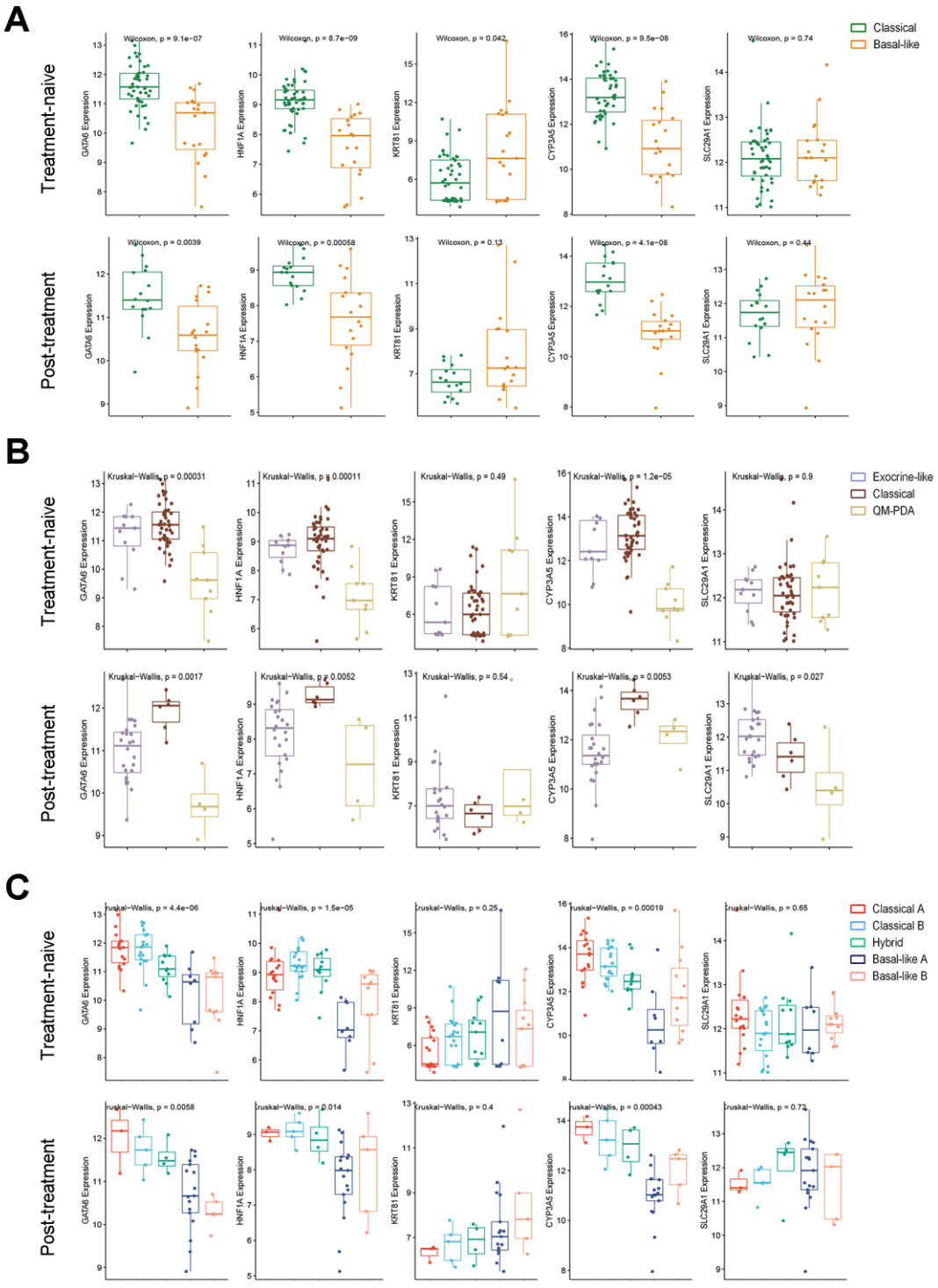

Fig 14. mRNA expression of GATA6, CYP3A5, HNF1A, KRT81 and hENT1 stratified by **(A)** Moffit classification in chemo-naïve group (**upper panel row**) and post-chemotherapy group (**lower panel row**); by Collisson classification **(B)** in chemo-naïve group (**upper panel row**) and post-chemotherapy group (**lower panel row**); by Notta classification **(C)** in chemo-naïve group (**upper panel row**) and post-chemotherapy group (**lower panel row**); (Wilcoxon test and Kruskal-Wallis test; ns $p > 0.05$, *$p < 0.05$, **$p < 0.01$, ***$p < 0.001$, ****$p < 0.0001$).

3.3 Clinical Correlation between mRNA Expression of Potential Biomarkers and Patient Outcome.

To assess whether these biomarkers are prognostic in either treatment naïve or post-treatment samples a comprehensive survival analysis was performed using dichotomized mRNA expression levels.

3.3.1 High GATA6, CYP3A5, HNF1A and KRT81 Expression Were Associated with Good Prognosis of Chemo-naïve PDAC Patients.

The overall survival rate indicated that GATA6, CYP3A5 and HNF1A high mRNA expression level were significantly correlated with good prognosis in patients with adjuvant therapy (**Fig 15 A/B/C**). This matched with the former results showing their roles as classical subtype representatives.

However, KRT81 mRNA high expression was correlated with good prognosis (**Fig 15 D**). This finding was contrary to a previous study by Noll et al., that showed that KRT81 is associated with poor outcome.

Biomarker mRNA expression was found not to be prognostic in patients that had received neoadjuvant therapy (**Fig 15 F-J**).

In addition, no significant associated between biomarker mRNA expression and the outcomes of patients who had received FFX preoperatively was found (**Fig 16**).

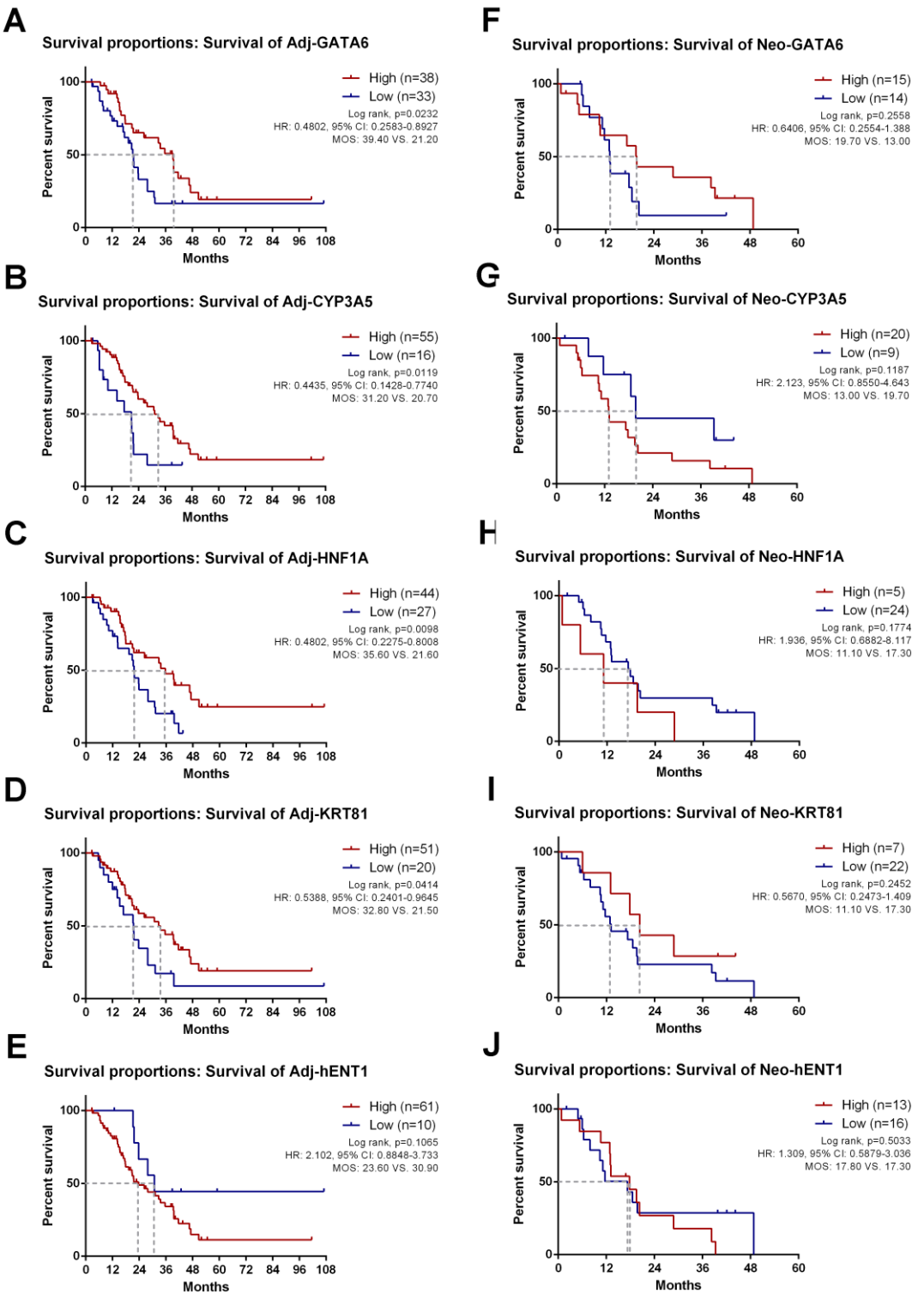

Fig 15. Kaplan-Meier curve showed the overall survival of PDAC patients with chemo-naïve (marked as Adj-, short for adjuvant treatment) and post-chemotherapy treatment (marked as Neo-, short for neoadjuvant treatment). (**A-E**) Overall survival of chemo-naïve patients according to GATA6, CYP3A5, HNF1A, KRT81 and hENT1mRNA expression, respectively. (**F-J**) Overall survival of patients after neoadjuvant treatment according to GATA6, CYP3A5, HNF1A, KRT81 and hENT1mRNA expression, respectively (Log-rank test, $p < 0.05$).

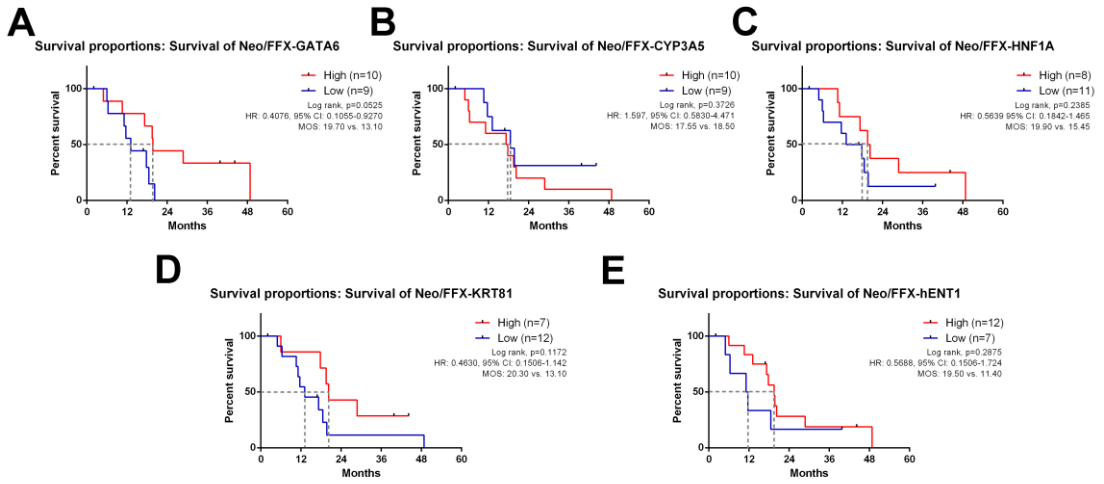

Fig 16. Kaplan-Meier curve showed the overall survival of PDAC patients after FFX neoadjuvant treatment. Overall survival of patients according to (**A**) GATA6, (**B**) CYP3A5, (**C**) HNF1A, (**D**) KRT81 and (**E**) hENT1mRNA expression (Log-rank test, $p < 0.05$).

3.3.2 Moffitt Classical Subtype Was Related to Good Prognosis of Chemo-naïve PDAC Patients.

The overall survival of PDAC patients according to Moffitt, Collisson and Notta classifications was also assessed (**Fig 17**).

These results showed that the Moffit classical subtype was significantly correlated with better prognosis, while the basal-like subtype was correlated with relatively poor prognosis in chemo-naïve patients (**Fig 17 A**).

However, the same trend was not found in the post-chemotherapy group (**Fig 17 D**). Neither Collisson nor Notta classifications were associated with patient outcome in either the treatment naïve or post-treatment groups (**Fig 17 B/C/E/F**).

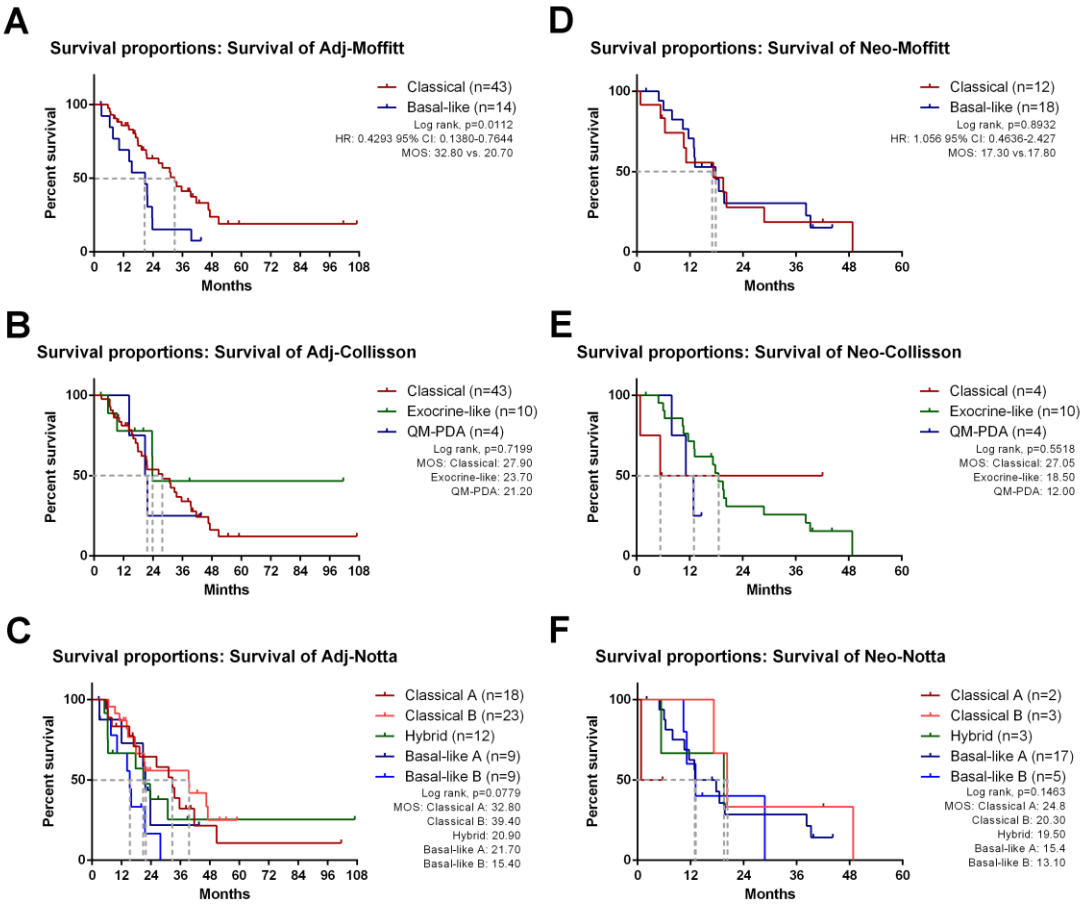

Fig 17. Kaplan-Meier curve showed the overall survival of PDAC patients with FFX neoadjuvant treatment. Overall survival of patients according to (**A**) GATA6, (**B**) CYP3A5, (**C**) HNF1A, (**D**) KRT81 and (**E**) hENT1mRNA expression (Log-rank test, $p < 0.05$).

3.4 Protein Expression of The Potential Biomarkers in PDAC Patients.

The mRNA expression of the 5 biomarkers showed potential utility as surrogates for subtype classification and outcome prediction. However, mRNA expression did not represent the expression profile of the protein, in particular for transcription factors, such as GATA6. Thus, the protein expression of the biomarkers could be a more accurate approach for determining patient outcome. To answer this question, immunofluorescence was performed on tissue sections to provide both a quantitative assessment of protein expression and information about the spatial expression of the given protein. The IF assay was performed in pre- and post-chemotherapy groups

compared to healthy donor pancreas group as controls. The IF cell counts of each marker are listed in **Supplementary Tables 1-5**.

3.4.1 GATA6 Expression Showed Upward Trend in Adjuvant, Neoadjuvant and Normal Pancreas Group.

The protein expression of GATA6 in nuclear, cytosol and in whole cells was analysed in whole tissue sections and specifically in tumour cells ($CK19^+$ cells) displayed the representative images of CK19 and GATA6 staining (**Fig 18 A/B/C)**. GATA6 expression showed upward trend in pre-, post-chemotherapy and normal pancreas group (**Fig 18 D)**.

Narrowed down to $CK19^+$ cells, the results showed that GATA6 nuclear expression was significantly higher in the post-chemotherapy group compared to the chemo-naïve group. However, same difference was not found in either cytosol or whole tissue GATA6 expressions, indicating that neoadjuvant therapy may specifically influence the expression of functional GATA6 in the nucleus rather than storage in the cytosol. As CK19 presented minor signals in the cytoplasm of epithelial cells in normal pancreas tissue, the signals of GATA6 cytosol expression in $CK19^+$ cells were higher in normal pancreas than in other two groups (**Fig 18 E)**.

The GATA6 expression according to different neoadjuvant treatment regimens was also analysed. GATA6 expression in $CK19^+$ cells showed an insignificant downward trend in GEM, FFX and GEM/FFX combination group (**Fig 18 G)**.

This result suggests that GATA6 showed promising role as a drug-response marker after neoadjuvant therapy. High GATA6 expression was a good indicator for a less-malignant classical subtype and better prognosis. However, more research was needed for confirming this result.

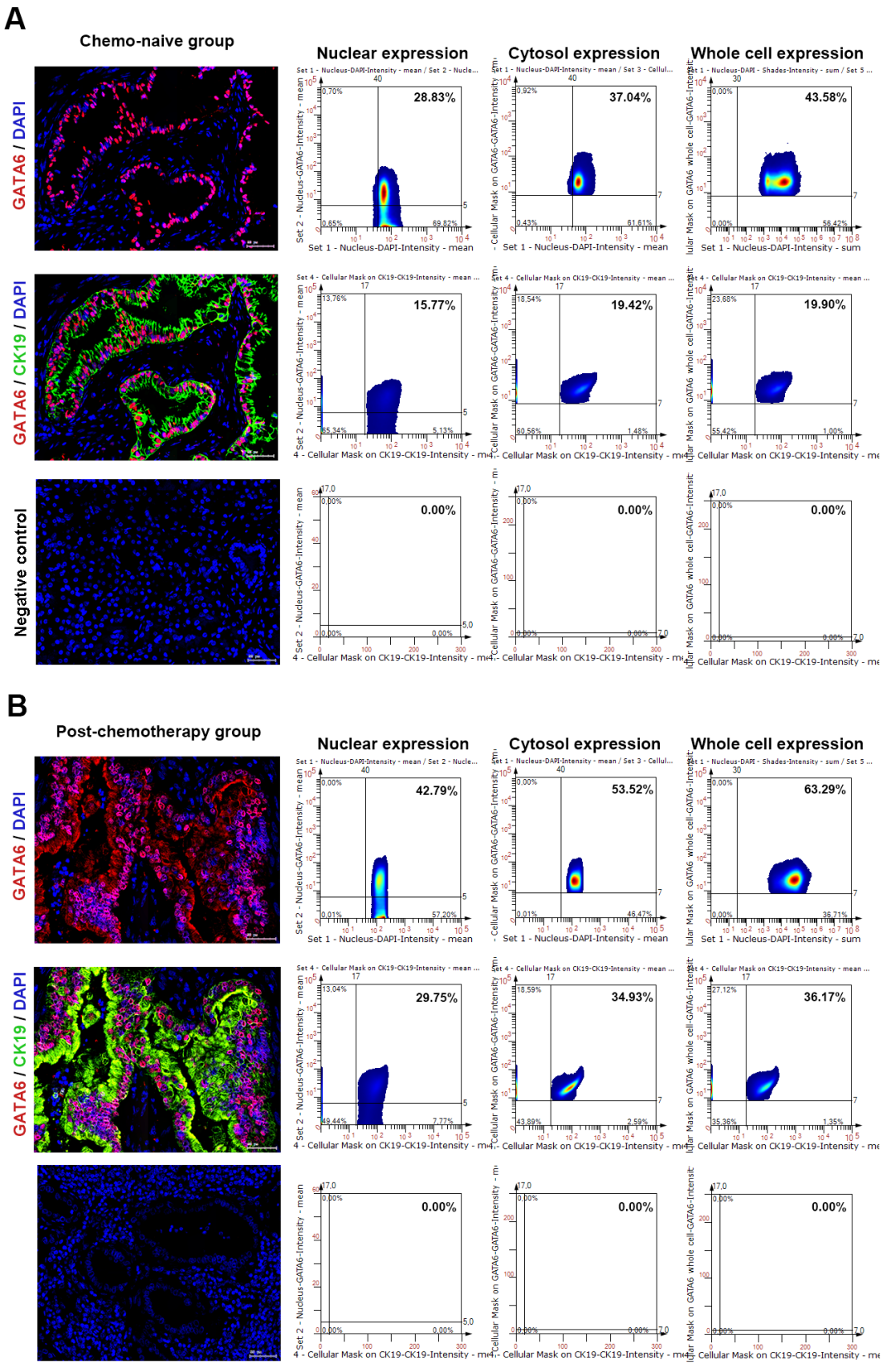
A
Chemo-naive group
Nuclear expression
Cytosol expression
Whole cell expression
GATA6 / DAPI
GATA6 / CK19 / DAPI
Negative control
28.83%
37.04%
43.58%
15.77%
19.42%
19.90%
0.00%
0.00%
0.00%
B
Post-chemotherapy group
Nuclear expression
Cytosol expression
Whole cell expression
GATA6 / DAPI
GATA6 / CK19 / DAPI
42.79%
53.52%
63.29%
29.75%
34.93%
36.17%
0.00%
0.00%
0.00%

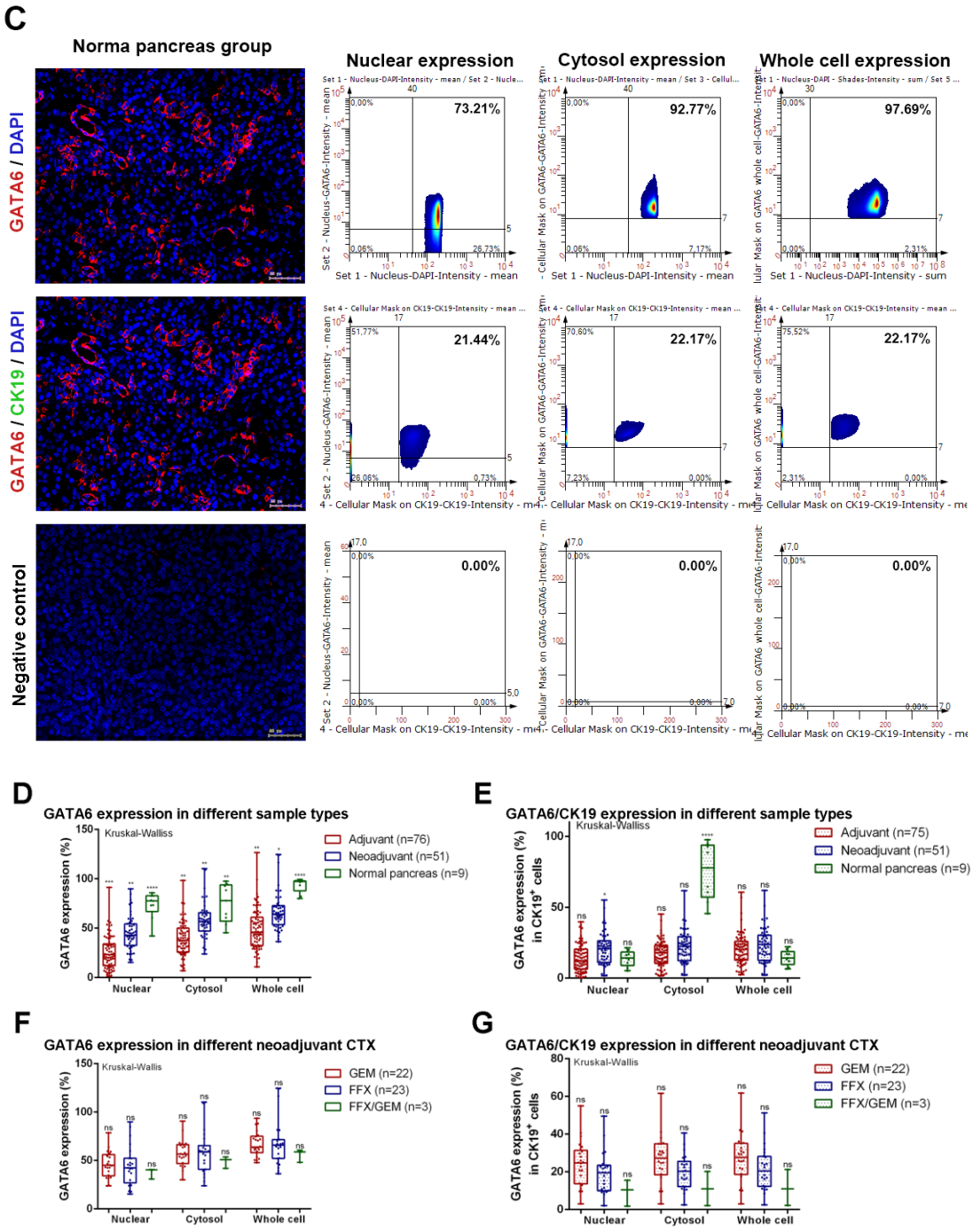

Fig 18. Representative IF colocalization images (20X objective; scale bar = 50 μm) stained for GATA6 (red), CK19 (green) and DAPI (blue) with corresponding FACS-like scattergrams for co-expression quantitation in patients with adjuvant treatment **(A)**, neoadjuvant treatment **(B)** and normal pancreas samples **(C)**. IF and FACS-like quantitation of GATA6 nuclear, cytosol and whole cell expression in whole tissue section **(D)** and in GATA6/CK19^{+} cells **(E)** according to different sample types. IF and FACS-like quantitation of GATA6 nuclear, cytosol and whole cell expression in whole section **(F)** and in GATA6/CK19^{+} cells **(G)** according to different neoadjuvant CTXs (Kruskal-Wallis test; ns $p > 0.05$, *$p < 0.05$, **$p < 0.01$, ***$p < 0.001$, ****p < 0.0001).

3.4.2 CYP3A5 Expression Was in Tumour Tissue Higher Than in Healthy Pancreas Tissue.

The protein expression of CYP3A5 were analysed both in the whole section and in $CK19^+$ stained tumour cells. **Fig 19 A/B/C** displayed the representative images of CK19 and CYP3A5 co-staining. After quantification, CYP3A5 showed higher expression in both pre- and post-chemotherapy groups compared with the normal pancreas group (**Fig 19 D/E**).

Moreover, CYP3A5 expression was not influenced by neoadjuvant treatment, because there was no difference in expression levels between the chemo-naïve and post-chemotherapy groups. Further analysis showed that CYP3A5 expression was higher after FFX-neoadjuvant treatment compared to gemcitabine-based treatment alone or combination therapy (**Fig 19 F/G**), suggesting that CYP3A5 might be a predictor to FFX drug response. However, more samples were needed to prove this hypothesis.

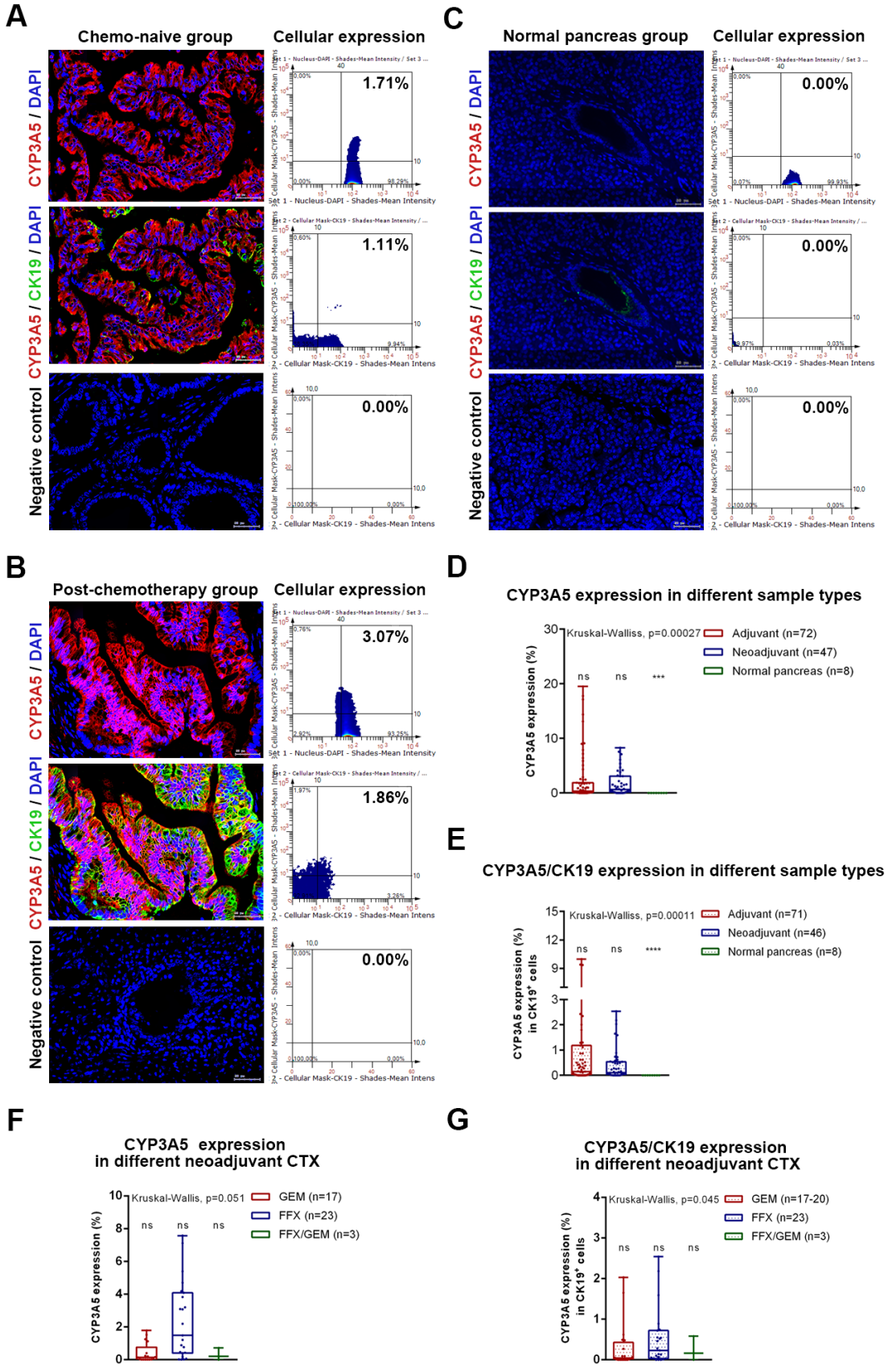

Fig 19. Representative IF colocalization images (20X objective; scale bar = 50μm) stained for CYP3A5 (red), CK19 (green) and DAPI (blue) with corresponding FACS-like scattergrams for co-

expression quantitation in patients with adjuvant treatment **(A)**, neoadjuvant treatment **(B)** and normal pancreas samples **(C)**. IF and FACS-like quantitation of CYP3A5 expression in whole section **(D)** and in $CK19^+$ cells **(E)** according to different sample types. IF and FACS-like quantitation of CYP3A5 expression in whole section **(F)** and in $CK19^+$ cells **(G)** according to different neoadjuvant CTXs (Kruskal-Wallis test; ns $p > 0.05$, *$p < 0.05$, **$p < 0.01$, ***$p < 0.001$, ****$p < 0.0001$).

CYP3A5 showed selective expression in tumour cells according to IF images (**Fig 20**), indicating that CYP3A5 has a potential to be a steady tumour specific index in certain tumour cells. The H&E staining showed no pathological difference between these two tumour cell clusters.

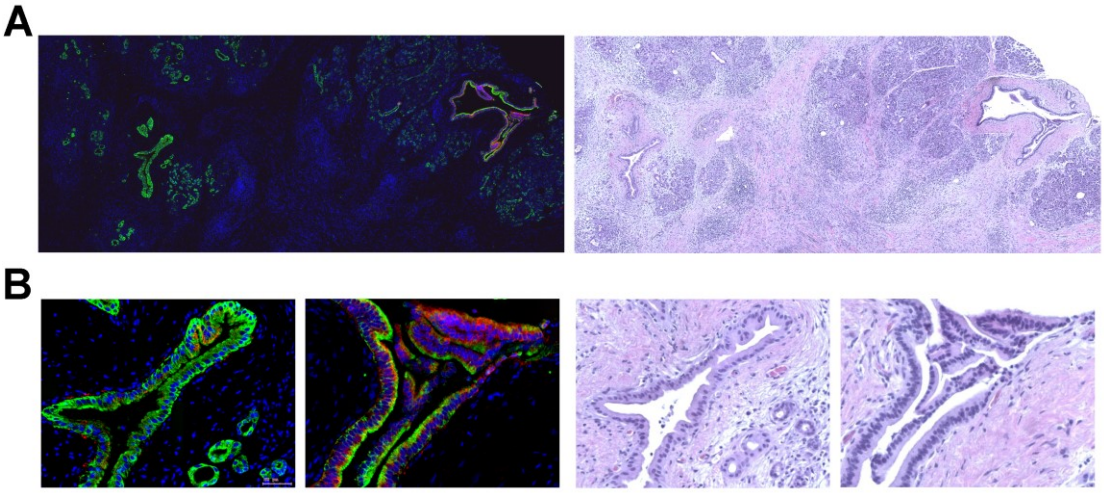

Fig 20. (A) Representative IF colocalization images stained for CYP3A5 (red), CK19 (green) and DAPI (blue) with corresponding H&E images (20X objective; scale bar = 500μm). **(B)** Detailed IF and corresponding H&E images of tumour cell clusters with weak/strong CYP3A5 staining (20X objective; scale bar = 50 μm).

3.4.3 HNF1A Expression Was Higher after Neoadjuvant-therapy Compared to Adjuvant Chemo-naïve and Normal Pancreas Tissue.

The protein expression of HNF1A in nuclear, cytosol and in whole cell were analysed both in the whole section and specifically in tumour cells ($CK19^+$ cells). **Fig 21 A/ B/C** displayed the representative images of CK19 and HNF1A co-staining. The results showed that HNF1A expression was significantly higher after neoadjuvant therapy

compared to chemo-naïve samples as well as normal pancreas samples (**Fig 21 D)**. The same trend was also found in $CK19^{+}$ tumour cells, with a significantly in nuclear and cytosol HNF1A expression. Whole cell analysis showed no significant difference in HNF1A expression (**Fig 21 E)**. There was no HNF1A expression differences related to neoadjuvant CTX therapy (**Fig 21 F/G)**, suggesting that the responsive increase of HNF1A expression was irrelevant with the type of drug therapy.

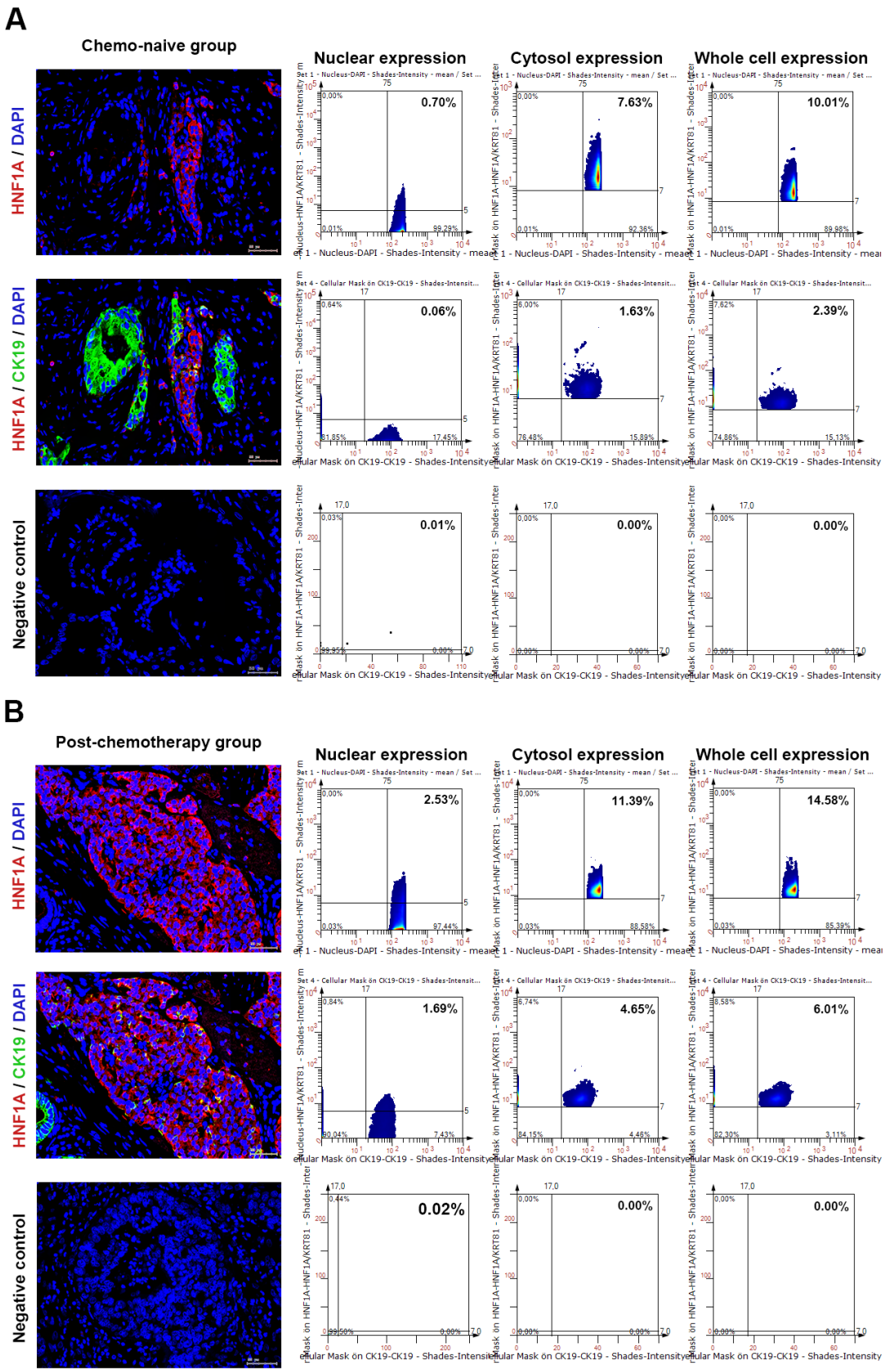
A
Chemo-naive group
Nuclear expression
Cytosol expression
Whole cell expression
HNF1A / DAPI
HNF1A / CK19 / DAPI
Negative control
0.70%
7.63%
10.01%
0.06%
1.63%
2.39%
0.01%
0.00%
0.00%
B
Post-chemotherapy group
Nuclear expression
Cytosol expression
Whole cell expression
HNF1A / DAPI
HNF1A / CK19 / DAPI
Negative control
2.53%
11.39%
14.58%
1.69%
4.65%
6.01%
0.02%
0.00%
0.00%

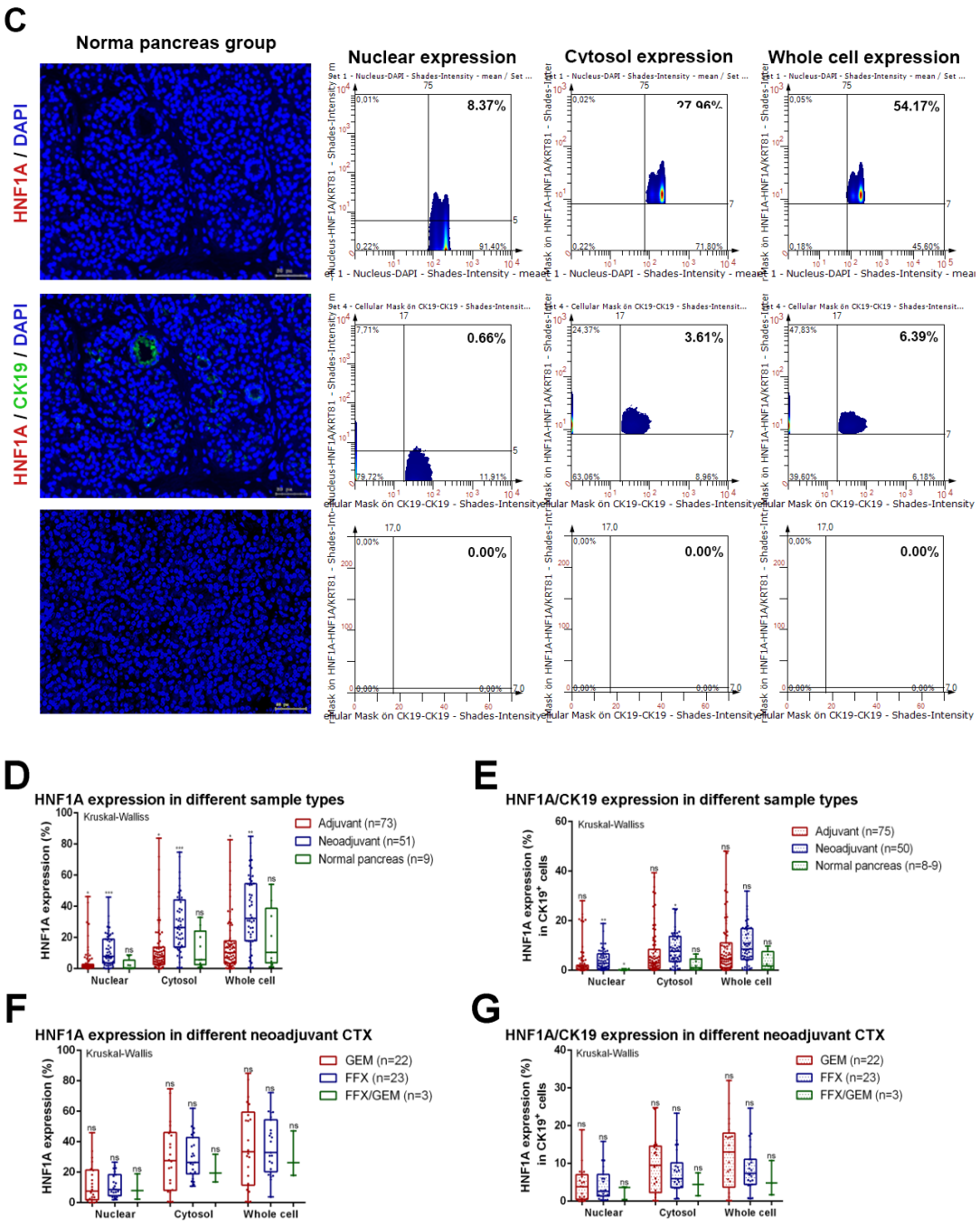

Fig 21. Representative IF colocalization images (20X objective; scale bar = 50 μm) stained for HNF1A (red), CK19 (green) and DAPI (blue) with corresponding FACS-like scattergrams for co-expression quantitation in chemo-naïve patients **(A)**, post-chemotherapy patients **(B)** and normal pancreas donors **(C)**. IF and FACS-like quantitation of HNF1A nuclear, cytosol and whole cell expression in whole section **(D)** and in $CK19^+$ cells **(E)** according to different sample types. IF and FACS-like quantitation of HNF1A nuclear, cytosol and whole cell expression in whole section **(F)** and in $CK19^+$ cells **(G)** according to different neoadjuvant CTXs (Kruskal-Wallis test; ns $p > 0.05$, *$p < 0.05$, **$p < 0.01$, ***$p < 0.001$).

The IF staining of HNF1A showed strong signals in certain tumour cell clusters with weak CK19 signals (**Fig 22 A)**.

These cells were more acinar-like (**Fig 22 B/D/E**) than epithelial/ductal-like (**Fig 22 C**) as shown in the images of paralleled H&E staining.

This finding indicated that HNF1A might be an index for acinar or less-differentiated feature.

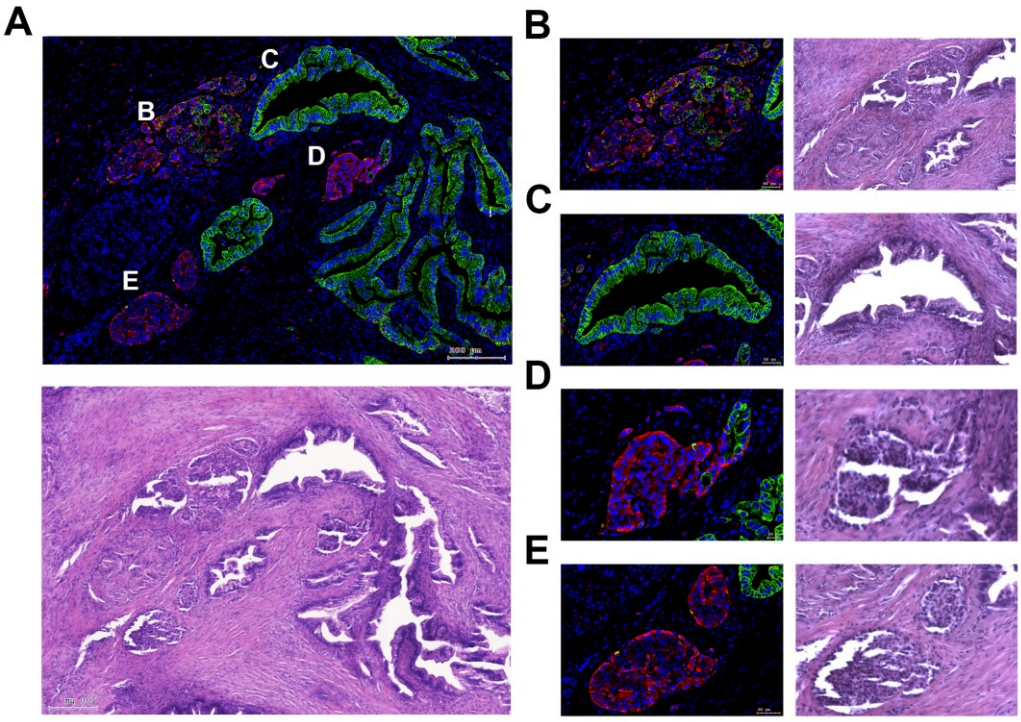

Fig 22. (A) Representative IF colocalization images stained for HNF1A (red), CK19 (green) and DAPI (blue) with corresponding H&E images (20X objective; scale bar = 200µm). **(B-E)** Detailed IF and corresponding H&E images of HNF1A$^{+/-}$ cell clusters (20X objective; scale bar = 50 µm).

3.4.4 KRT81 Expression Was High in Neoadjuvant-treated Samples and Low in Normal Pancreas Samples.

The protein expression of HNF1A was analysed both in the whole section and specifically in tumour cells (CK19^{+} cells). **Fig 23 A/B/C** displays the representative images of CK19 and HNF1A staining.

HIF1A showed significantly high expression in post-chemotherapy group and low expression in normal pancreas group (**Fig 23 D/E**). This suggested that KRT81 may be

a biomarker for PDAC and was increased after neoadjuvant treatment.

However, there was no expression difference correlated to chemotherapy regimens (**Fig 23 F/G**).

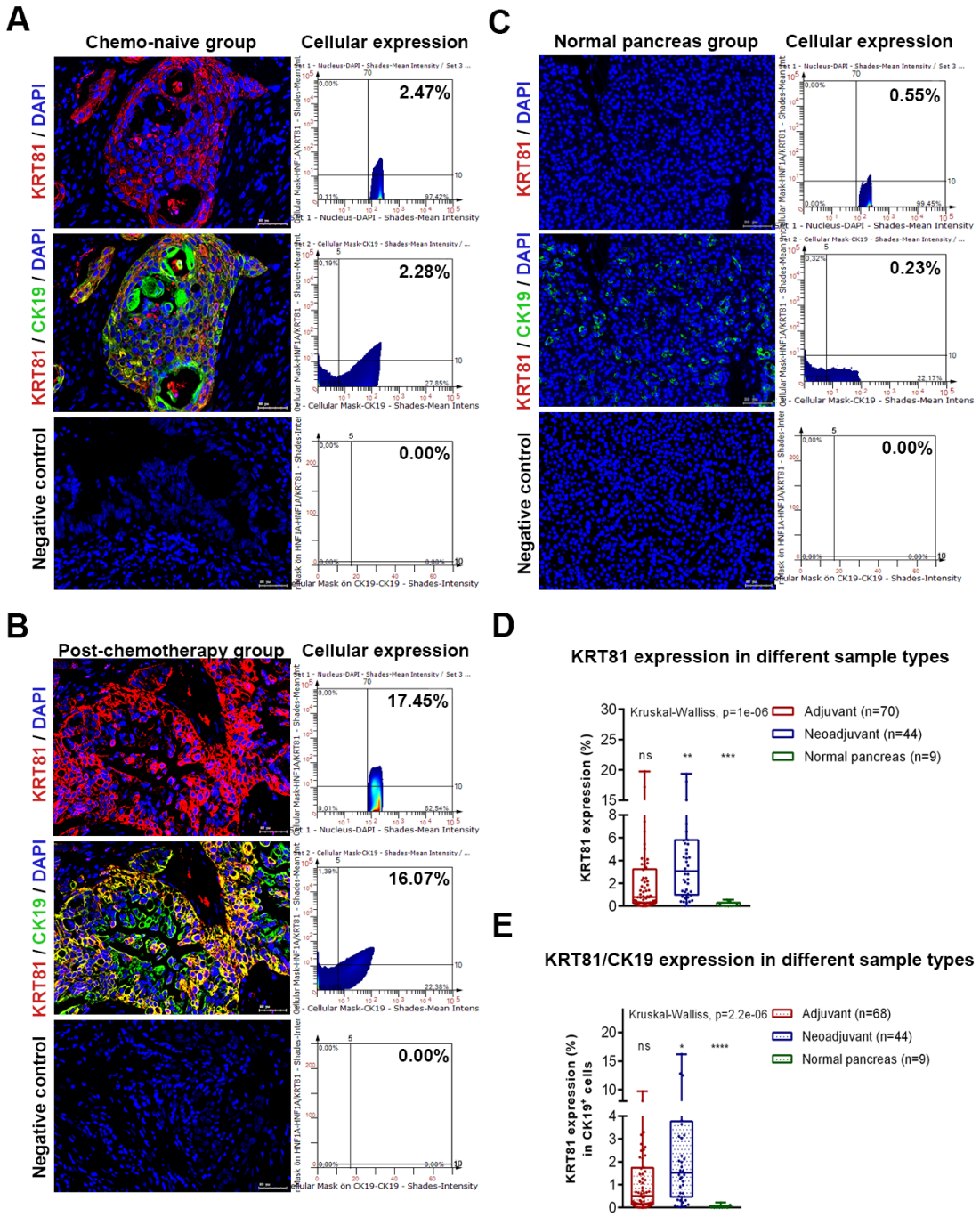

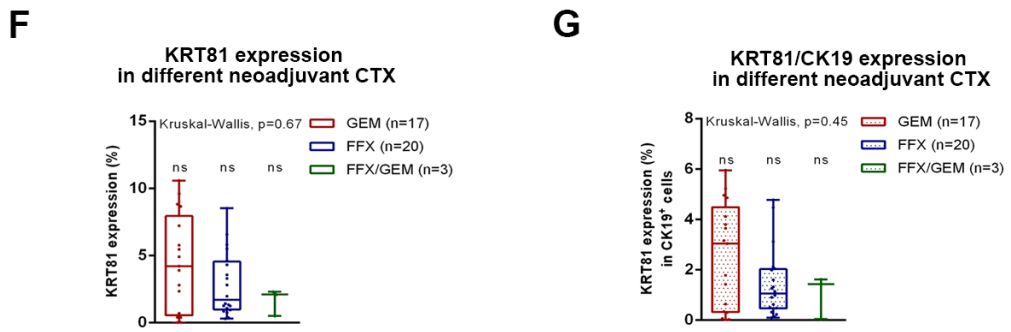

Fig 23. Representative IF colocalization images (20X objective; scale bar = 50 μm) stained for KRT81 (red), CK19 (green) and DAPI (blue) with corresponding FACS-like scattergrams for co-expression quantitation in chemo-naïve patients **(A)**, post-chemotherapy patients **(B)** and normal pancreas donors **(C)**. IF and FACS-like quantitation of KRT81 expression in whole section **(D)** and in $CK19^+$ cells **(E)** according to different sample types. IF and FACS-like quantitation of KRT81 expression in whole section **(F)** and in $CK19^+$ cells **(G)** according to different neoadjuvant CTXs (Kruskal-Wallis test; ns $p > 0.05$, *$p < 0.05$, **$p < 0.01$, ***$p < 0.001$, ****$p < 0.0001$).

3.4.5 hENT1 Expression in Tumour Samples Was Higher Than in Normal Pancreas Samples.

The protein expression of hENT1 was analysed both in the whole section and specifically in tumour cells ($CK19^+$ cells).

Fig 24 A/B/C displayed the representative images of CK19 and hENT1 co-staining. hENT1 showed the same trend as CYP3A5: higher expression in both pre- and post-chemotherapy tissue compared to normal pancreas (**Fig 24 D/E**), while the expression in chemo-treated samples was irrelevant with different neoadjuvant CTXs (**Fig 24 F/G**). hENT1 was reported as a predictor of gemcitabine-based treatment response (Bird et al. 2017). However, this study failed to confirm this correlation.

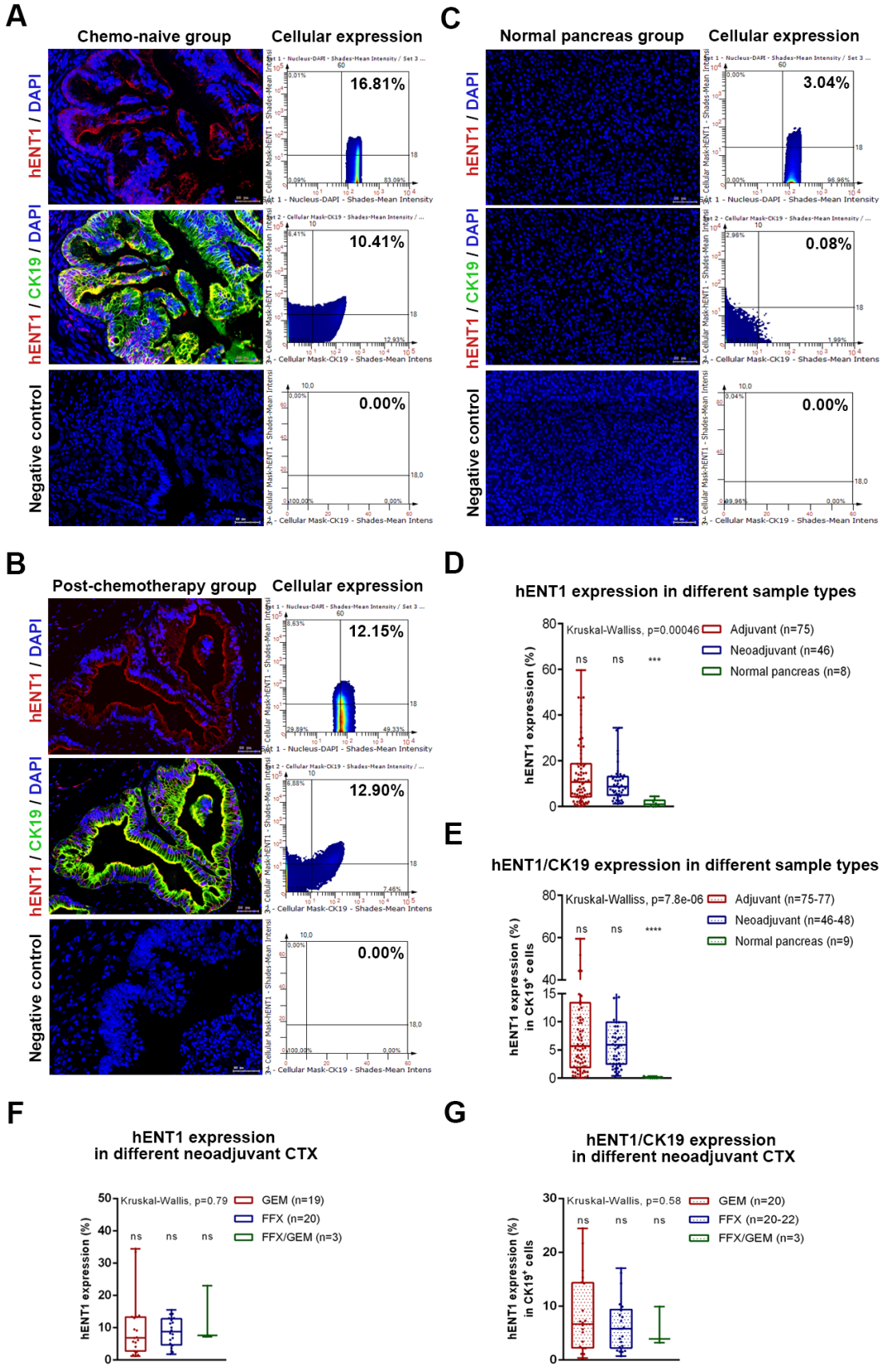

Fig 24. Representative IF colocalization images (20X objective; scale bar = 50 μm) stained for hENT1 (red), CK19 (green) and DAPI (blue) with corresponding FACS-like scattergrams for co-

expression quantitation in chemo-naïve patients **(A)**, post-chemotherapy patients **(B)** and normal pancreas donors **(C)**. IF and FACS-like quantitation of hENT1 expression in whole section **(D)** and in $CK19^+$ cells **(E)** according to different sample types. IF and FACS-like quantitation of hENT1 expression in whole section **(F)** and in $CK19^+$ cells **(G)** according to different neoadjuvant CTXs (Kruskal-Wallis test; ns $p > 0.05$, *$p < 0.05$, **$p < 0.01$, ***$p < 0.001$, ****$p < 0.0001$).

3.4.6 The Potential Biomarkers Couldn't Well Classify Moffitt, Collisson and Notta Subtypes.

The protein expression of the five biomarkers were detected according to the Moffitt, Collisson and Notta classifications in both chemo-naïve (adjuvant group) and neoadjuvant-treated (neoadjuvant group) tissue samples. No biomarker showed detectable differential expression levels in certain subtypes (**Supplementary Fig 1-3)**.

3.5 Clinical Correlation Between Protein Expression of Potential Biomarkers and Patient Outcome

The mRNA expression of the potential biomarkers showed good correlation properties with patient outcome. However, the transcriptional mRNA levels of the biomarkers were not always equal to protein expression profiles, presumably because of the post-transcriptional regulation, nuclear translocation and enzyme activities. Kaplan-Meier curve analysis was further performed to explore the relationship between the potential biomarkers and patient outcome in protein level.

3.5.1 GATA6 Protein Expression Showed Inverse Correlation with Patient Prognosis in Chemo-naïve and Post-chemotherapy Group.

GATA6 high expression exhibited a good prognosis correlation, especially in GATA6 nuclear expression (**Fig 25 A**), GATA6 whole cell expression (**C**) and GATA6 nuclear expression in $CK19^+$ cells (**D**). The survival curves after neoadjuvant therapy showed

that low expression of GATA6 was strongly correlated with a good prognosis no matter in CK19^{+} cells or not (**G-L**). This prognostic correlation was not detected on the GATA6 mRNA expression level, indicating that mRNA expression profiles alone may not be accurate in considering a prognosis correlation.

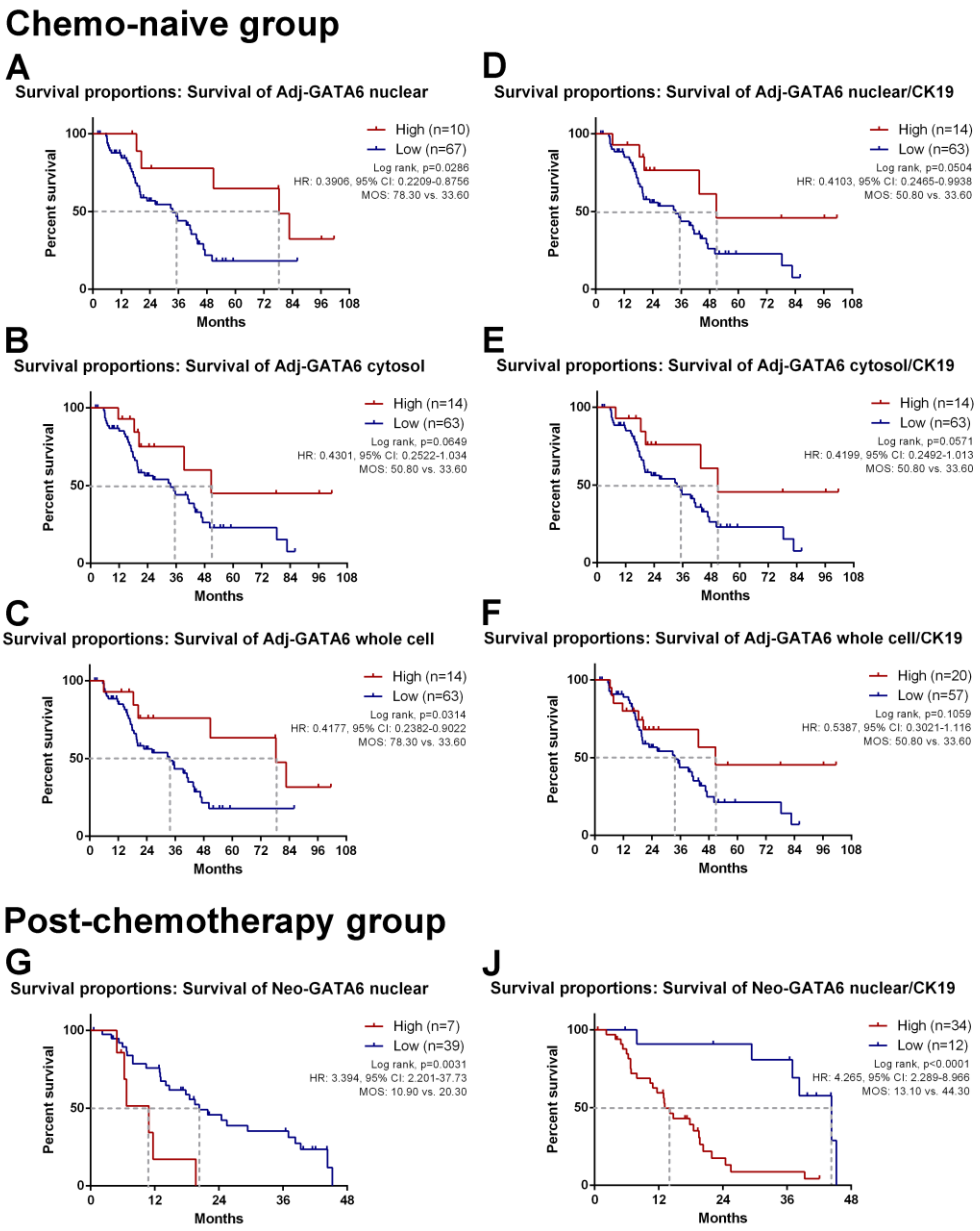

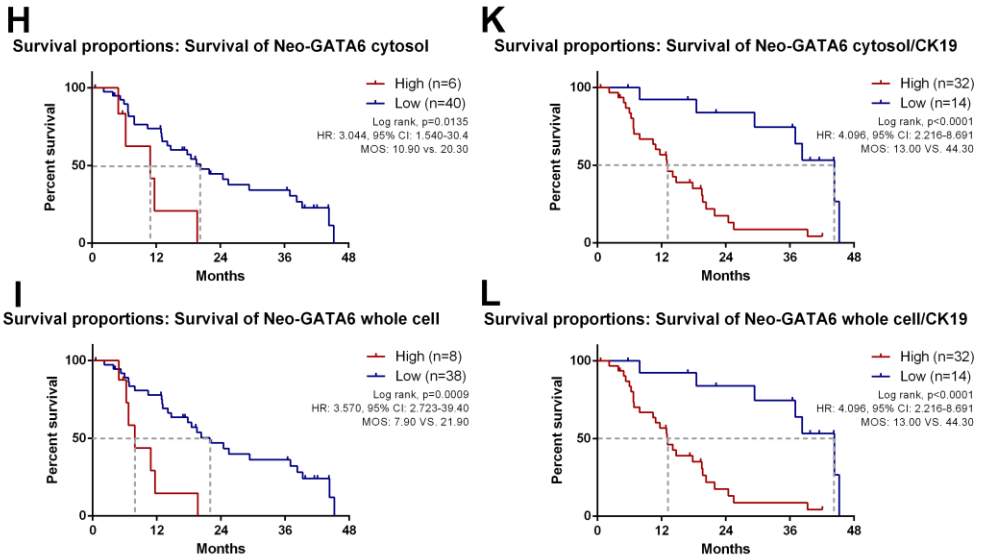

Fig 25. (**A-F**) Kaplan-Meier curve showed the overall survival of chemo-naïve patients according to GATA6 nuclear, cytosol, whole cell expression (**A-C**) and GATA6 expression in $CK19^+$ cells (**D-F**), respectively. (**G-L**) Overall survival of patients after neoadjuvant treatment according to GATA6 nuclear, cytosol, whole cell expression (**G-I**) and GATA6 expression in $CK19^+$ cells (**J-L**), respectively (Log-rank test, $p < 0.05$).

To further discover the clinical correlation between GATA6 expression and chemotherapy regimens, the patients with neoadjuvant treatment were separated into GEM and FFX group (**Fig 26**).

GATA6 high expression was not significantly associated with good prognosis in patients with gemcitabine-based treatment, while it was significantly associated with poor prognosis in patients with FFX treatment.

This result suggested that GATA6 is a potential biomarker for clinical treatment selection, which may further assist a more precise personal medicine and better therapy responsiveness.

Neoadjuvant-GEM group

A

Survival proportions: Survival of Neo/GEM-GATA6 nuclear

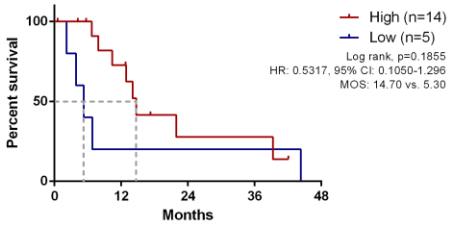

D

Survival proportions: Survival of Neo/GEM-GATA6 nuclear/CK19

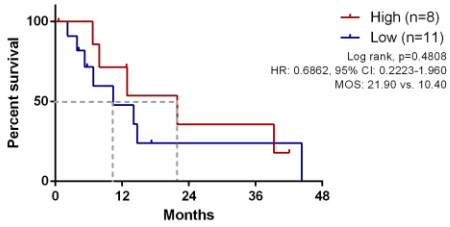

B

Survival proportions: Survival of Neo/GEM-GATA6 cytosol

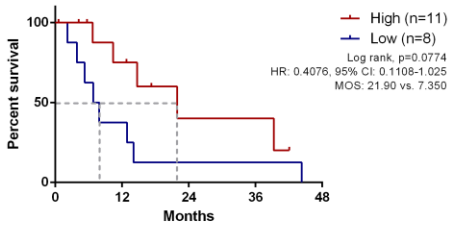

E

Survival proportions: Survival of Neo/GEM-GATA6 cytosol/CK19

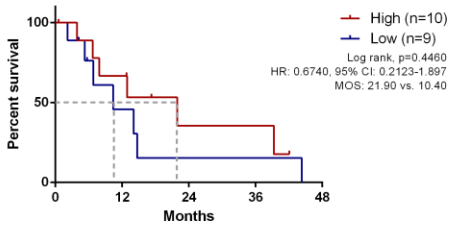

C

Survival proportions: Survival of Neo/GEM-GATA6 whole ce

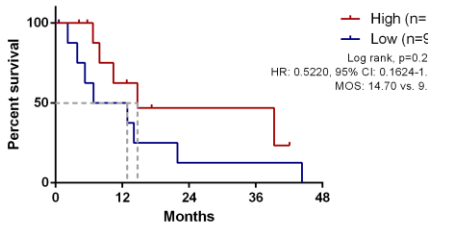

F

Survival proportions: Survival of Neo/GEM-GATA6 whole cell/CK19

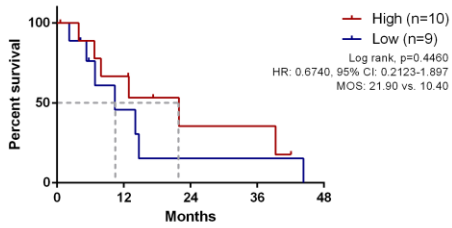

Neoadjuvant-FFX group

G

Survival proportions: Survival of Neo/FFX-GATA6 nuclear

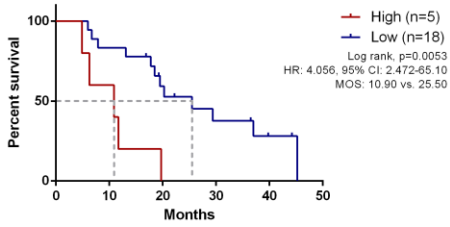

J

Survival proportions: Survival of Neo/FFX-GATA6 nuclear/CK19

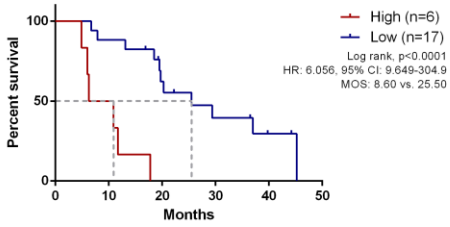

H

Survival proportions: Survival of Neo/FFX-GATA6 cytosol

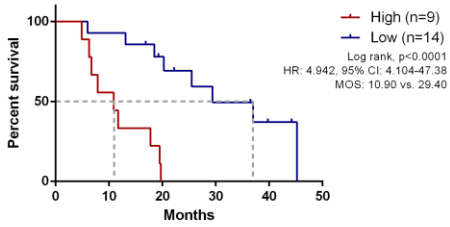

K

Survival proportions: Survival of Neo/FFX-GATA6 cytosol/CK19

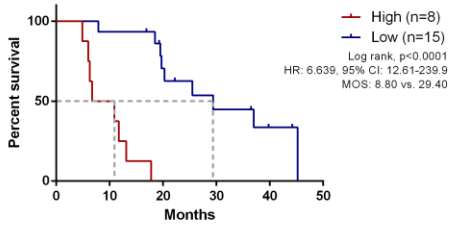

I

Survival proportions: Survival of Neo/FFX-GATA6 whole cell

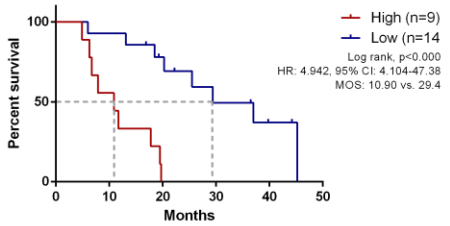

L

Survival proportions: Survival of Neo/FFX-GATA6 whole cell/CK19

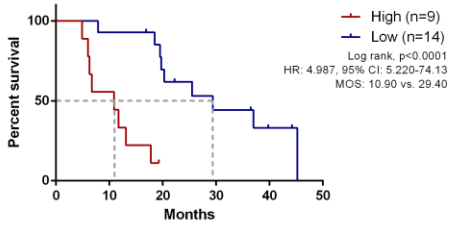

Fig 26. (**A-F**) Kaplan-Meier curve showed the overall survival of patients with gemcitabine-based neoadjuvant treatment according to GATA6 nuclear, cytosol, whole cell expression (**A-C**) and GATA6 expression in $CK19^+$ cells (**D-F**), respectively. (**G-L**) Overall survival of patients with FFX neoadjuvant treatment according to GATA6 nuclear, cytosol, whole cell expression (**G-I**) and GATA6 expression in $CK19^+$ cells (**J-L**), respectively (Log-rank test, $p < 0.05$).

3.5.2 Low CYP3A5 Expression Was Correlated with Good Prognosis in Neoadjuvant-treated Patients.

Kaplan-Meier curves showed that CYP3A5 was not significantly associated with good prognosis in the adjuvant group (**Fig 27 A/B**). However, low expression of CYP3A5 was significantly associated with good prognosis after neoadjuvant therapy (**C/D**). This result indicated that CYP3A5 expression may be a chemotherapy efficacy marker considering its role in drug resistance.

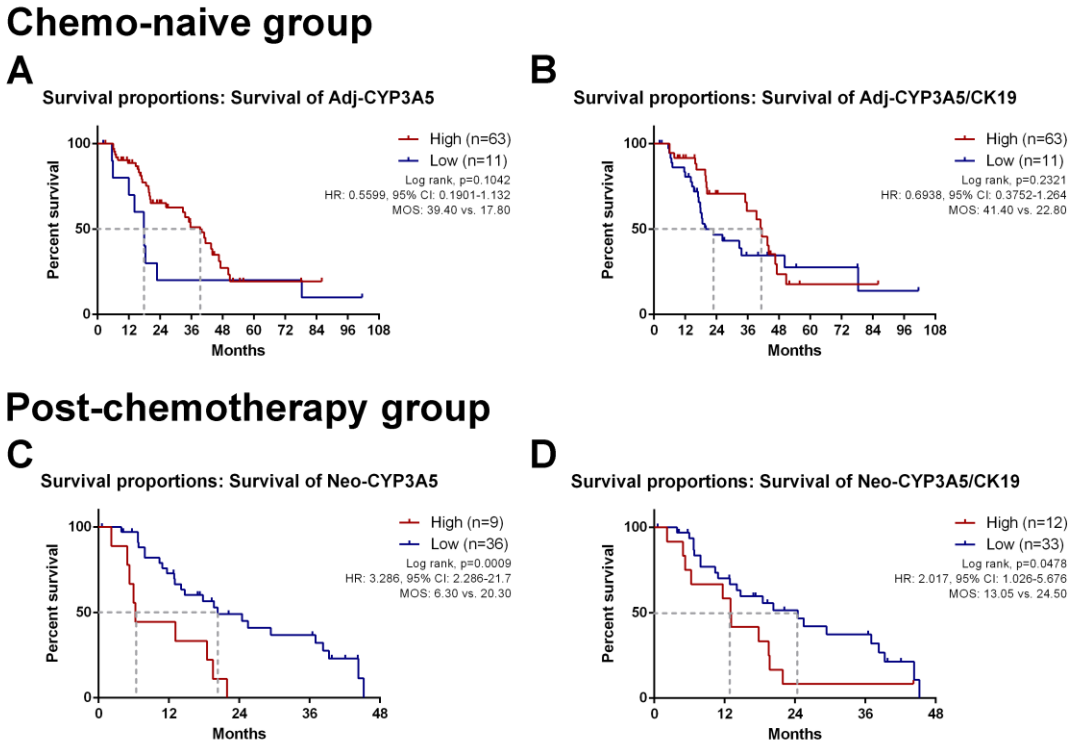

Fig 27. Kaplan-Meier curve showed the overall survival of chemo-naïve PDAC patients according to CYP3A5 expression (**A**) and its expression in $CK19^+$ cells (**B**), in post-chemotherapy group according to CYP3A5 expression (**C**) and its expression in $CK19^+$ cells (**D**) (Log-rank test, $p < 0.05$)

CYP3A5 expression was further correlated with different chemotherapy regimens. The results showed that CYP3A5 low expression was significantly correlated with

good prognosis in patients who had received FFX neoadjuvant therapy (**Fig 28 C/D**). This finding demonstrated that patients with low CYP3A5 expression have better outcomes after FFX treatment. Further study was needed to confirm this assumption considering the limited sample size.

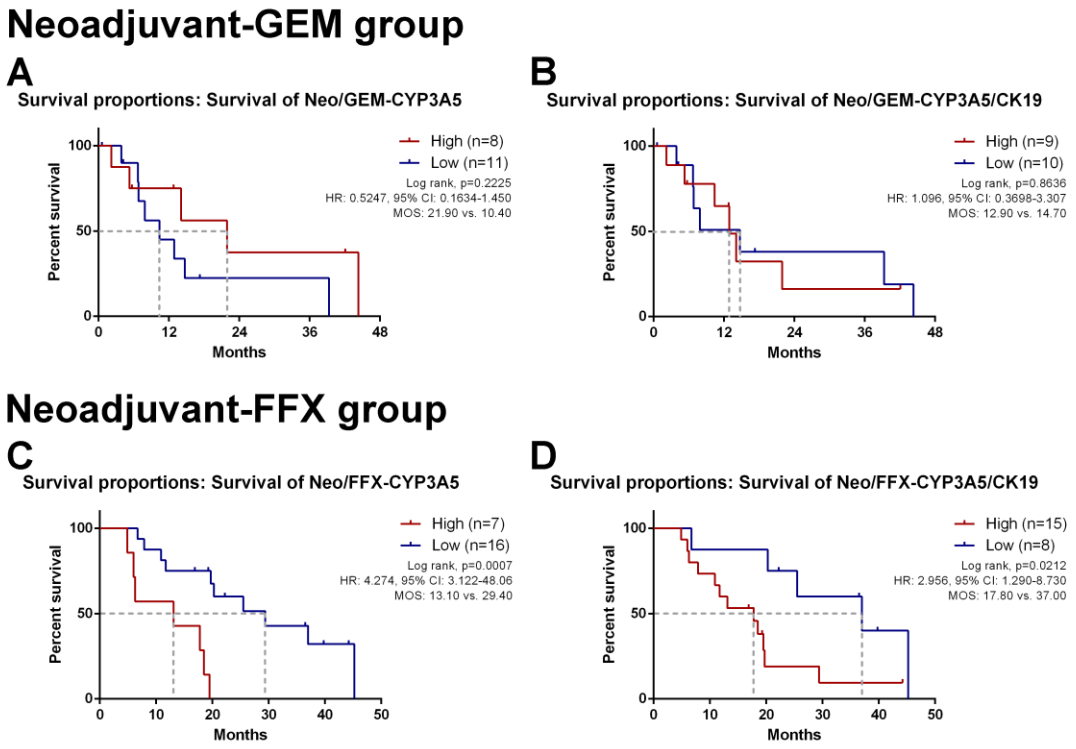

Fig 28. Kaplan-Meier curve showed the overall survival of patients with GEM neoadjuvant therapy according to CYP3A5 expression (**A**) and its expression in $CK19^{+}$ cells (**B**), and patients with FFX neoadjuvant therapy according to CYP3A5 expression (**C**) and its expression in $CK19^{+}$ cells (**D**) (Log-rank test, $p < 0.05$).

3.5.3 HNF1A Protein Expression Did Not Correlate with Patient Outcome.

Overall survival of patients was analysed according to HNF1A protein expression. It showed that HNF1A was not significantly correlated to patient outcome in both adjuvant and neoadjuvant groups, as well as in GEM/FFX neoadjuvant sub-groups (**Supplementary Fig 4-5**).

3.5.4 KRT81 Expression in CK19^{+} Cells Correlated with Good Prognosis after Neoadjuvant-treated Patients.

The overall survival curves showed that high KRT81 expression in CK19^{+} cells was associated with good prognosis in patients after neoadjuvant therapy (**Fig 29 D**).

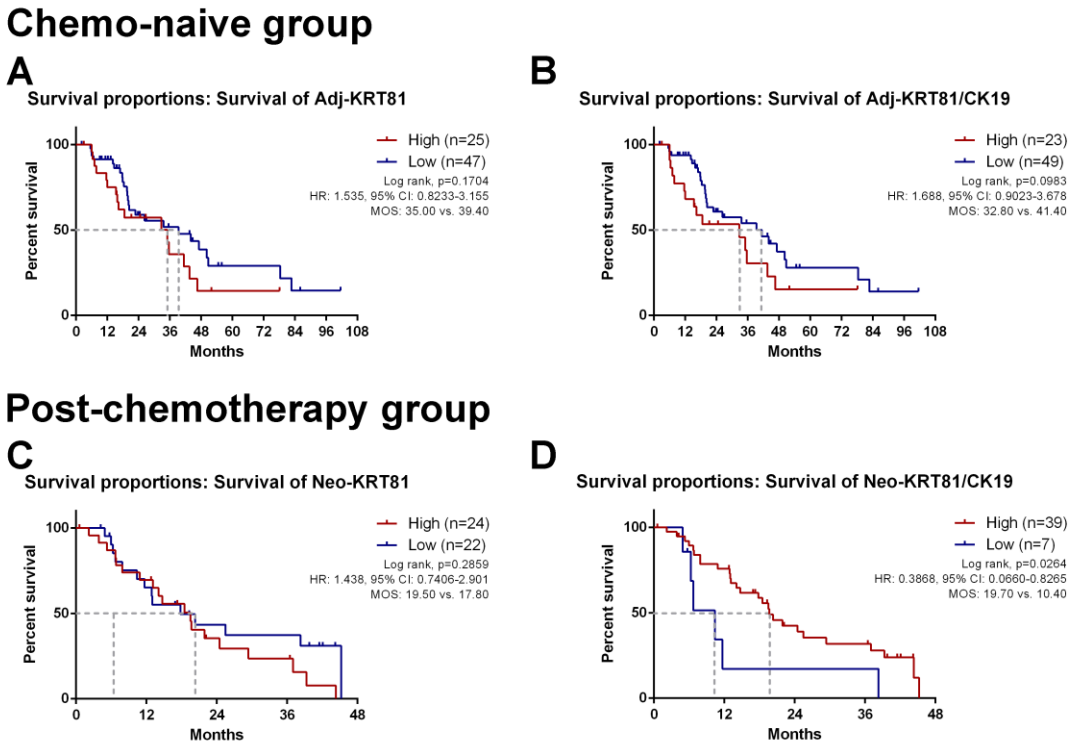

Fig 29. Kaplan-Meier curve showed the overall survival of PDAC patients in adjuvant group according to KRT81 expression (**A**) and its expression in CK19^{+} cells (**B**), in neoadjuvant group according to KRT81 expression (**C**) and its expression in CK19^{+} cells (**D**) (Log-rank test, $p < 0.05$).

High KRT81 expression in CK19^{+} cells was especially more significantly associated with good prognosis in neoadjuvant patients after FFX treatment (**Fig 30 D**).

This result indicated that high KRT81 expression was associated with better survival especially after FFX neoadjuvant therapy.

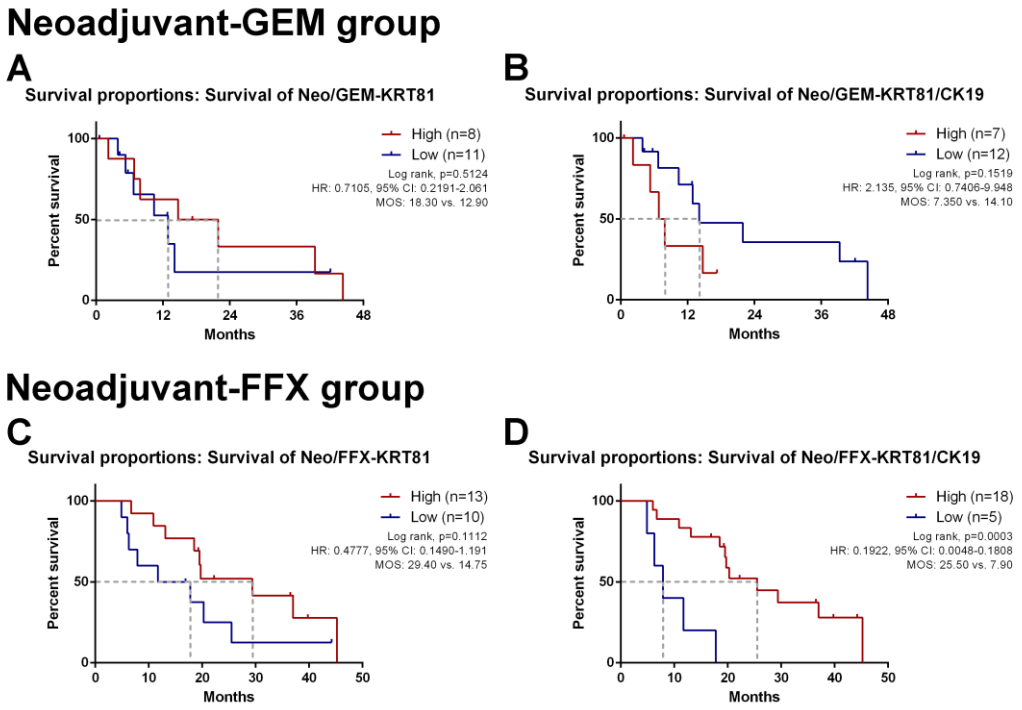

Fig 30. Kaplan-Meier curve showed the overall survival of patients with GEM neoadjuvant therapy according to KRT81 expression (**A**) and its expression in $CK19^+$ cells (**B**), and patients with FFX neoadjuvant therapy according to KRT81 expression (**C**) and its expression in $CK19^+$ cells (**D**) (Log-rank test, $p < 0.05$).

3.5.5 hENT1 Expression in $CK19^+$ Cells was Correlated with Poor Prognosis in Neoadjuvant-treated Patients.

The overall survival curves showed that high hENT1 expression in $CK19^+$ cells was significantly associated with poor prognosis in patients after neoadjuvant treatment (**Fig 31 D**).

However, no significant correlation was found between hENT1 expression and GEM/FFX neoadjuvant therapy (**Supplementary Fig 6**).

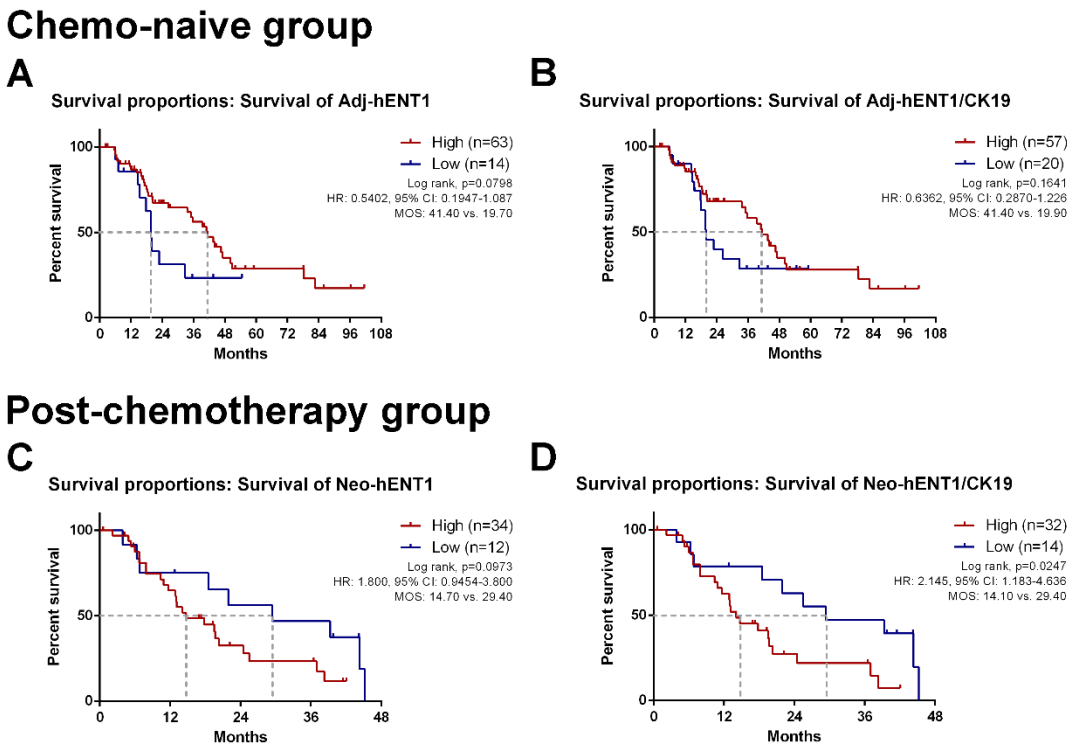

Fig 31. Kaplan-Meier curve showed the overall survival of PDAC patients in chemo-naïve group according to hENT1 expression **(A)** and its expression in $CK19^{+}$ cells **(B)**, in post-chemotherapy group according to hENT1 expression **(C)** and its expression in $CK19^{+}$ cells **(D)** (Log-rank test, $p < 0.05$).

4. Discussion

Pancreatic ductal adenocarcinoma is a highly lethal malignancy, which has now become the seventh most common cause of cancer death in the world, with the highest mortality rates in Europe and North America. Although the 5-year overall survival has been improved from 2.5% to 10% in North America, it is still relatively poor progress compared to other cancer types (Siegel et al. 2021). This modest improvement in prognosis is largely due to three reasons: (1) the development of more advanced surgical approaches, (2) the greater use of adjuvant chemotherapy after resection, and (3) the increased use of neoadjuvant chemotherapy for borderline and locally advanced pancreatic cancer. The application of chemotherapy before surgery may increase the resectability of PDAC from 20-30% to almost half of the borderline and unresectable tumour cases. However, even after successful treatment with surgery and chemotherapy most patients develop recurrence. Targeting different therapies to individual patients or particular subgroups of patients may enhance the overall therapeutic effect and reduce the rate of drug-resistance, but this approach requires effective selection procedures.

We are now able to recognize different PDAC subtypes based on various molecular characteristics. However, the evolution of molecular targeted therapies based on pancreatic cancer subtyping has so far been met with only limited progress. The most commonly accepted PDAC classifications are those from Collisson, Moffit, and Bailey that set a benchmark in pancreatic cancer molecular subtyping (Bailey et al. 2016; Collisson et al. 2019; Moffitt et al. 2015). These subtyping schemes appear to identify prognostic subgroups reasonably well in resectable tumours but perform less well in the advanced setting. The Notta classification was derived using non-negative matrix factorization (NMF) to extract four tumour-specific expression signatures, which were then used for consensus clustering into five subtypes, comprising Classical A, Classical B, Hybrid, Basal-like A and Basal-like B subtypes (Chan-Seng-Yue et al. 2020).

LCM enriched tumour content of the samples.

In this study, the most common subtypes were defined by using LCM on chemo-naïve PDAC tissue samples in the adjuvant setting to guarantee a high tumour cell component. Samples of PDAC tissues from patients in the neoadjuvant setting were also recruited to explore the influence of chemotherapy. Lase capture microscopy, however, was not performed on this subgroup, as the tissue architecture was largely destroyed following the chemotherapy along with tumour cell scattering amongst a massive stromal reaction, making it difficult to identify tumour cells for LCM. The tumour cell percentage in PDAC tissue samples after neoadjuvant therapy was also relatively much lower than in chemo-naïve samples, making it harder to harvest sufficient tumour fragments for RNA-seq. Therefore, in this post-chemotherapy group, bulk tissue with tumour cell percentage >20% was used for investigation.

Commonality of transcriptomic signatures

Subtyping analysis demonstrated that all treatment naïve patient samples could be classified into the Moffit, Collisson, Bailey, and Notta PDAC subtypes. There was substantial congruity between the Collisson, Bailey and Notta classification subtypes and the consensus Moffitt Classical and Basal-like subtypes. This is illustrated for example by the Bailey Progenitor and Squamous subtypes overlapping with the Moffitt Classical and Basal-like subtypes, respectively. The treatment naïve samples were dominated by the Classical subtype found in 72% (n=48) of the PDAC samples compared to 28% (n=19) Basal-like. The Basal-like subtype was significantly enriched in post-treatment subsets increasing to 53% (n=18) of the PDAC samples compared to 47% (n=16) with the Classical-like subtype, suggesting that chemotherapy may influence subtype signatures. This could be further supported by studying molecular profiling in patient-derived pancreatic cancer organoids (PDO) before and after chemotherapy. There may be additional variables to consider however in this system, as the process of generating PDOs may also subject them to adopting an altered molecular phenotype in vitro from the original patient sample in vivo. To demonstrate chemotherapy driven molecular subtyping transformation more concretely it will be necessary to undertake pre- and post-treatment tumour sampling for molecular

profiling in future clinical studies.

GATA6 and CYP3A5 as Classical-subtype biomarkers

The identification of representative biomarkers of each subtype would facilitate the development of clinical decision making based on therapy dependent molecular subtypes. The potential biomarkers identified in this research could be categorized into three types:

- Classical-like subtype associated biomarkers: GATA6, CYP3A5 and HNF1A
- Basal-like subtype associated biomarker: KRT81
- Drug-response related biomarkers: CYP3A5 for FFX therapy and hENT1 for GEM therapy

GATA6, CYP3A5 and HNF1A had higher mRNA expression levels in the Moffitt Classical subtype in the chemo-naïve group, while KRT81 had significantly higher expression levels in the Basal-like subtype group of patients. hENT1 mRNA expression showed no difference between the two subtypes in the adjuvant group of patients. GATA6, CYP3A5, and HNF1A mRNA expression levels were also significantly associated with the Classical subtype in the post-chemotherapy group, while KRT81 and hENT1 mRNA expression showed no significant subtype enrichment. The association between GATA6 high mRNA expression in the Classical subtype and better overall survival in the adjuvant setting is consistent with the studies of Collisson, Moffitt, and Bailey (Brunton et al. 2020; Collisson et al. 2019; Moffitt et al. 2015), as well as the COMPASS trial (Aung et al. 2018; O'Kane et al. 2020).

The overall survival rates in patients given adjuvant therapy were significantly correlated with good prognosis in those with high tumour CYP3A or HNF1A mRNA expression levels, consistent with previous studies by Noll et al. (Muckenhuber et al. 2018; Noll et al. 2016; Scott and Wilkinson 2016). On the other hand, we found contrary results in patients with high KRT81 mRNA expressing tumours as this was also correlated with a good prognosis following adjuvant therapy (Muckenhuber et al. 2018; Noll et al. 2016; Scott and Wilkinson 2016). KRT81 expression was identified as a Moffitt Basal-like biomarker in this study, whilst Knoll et al. found this to be more

associated the Collisson QM-PDA subtype (Noll et al. 2016). In any case KRT81 mRNA expression seems to be of borderline significance and might be subject to a more complex modulation, for example in a convoluted interaction with stromal activity.

As expected, the Classical subtype, which is associated with a well-differentiated tumour type, was linked to longer patient survival compared to those with a Basal-like subtype, which is associated with poorly differentiated tumour types. The GATA6/ CYP3A/HNF1A-high mRNA expressing tumours were all associated with the Classical subtype and showed better clinical outcome, thus strengthening their potential value as biomarkers. Contrary to expectation high KRT81 mRNA expression, which paradoxically was associated with the Basal-like sub-type, was also correlated with good prognosis. This indicates the need for a deeper functional understanding of molecular profiles, along with exploration of additional candidate biomarkers in this role such as CK5,CK17 and S100A2 (Li et al. 2021; Lu et al. 2021; Roa-Pena et al. 2019).

Protein expression of the biomarkers showed no potential in PDAC classification

Although the mRNA expression of the five biomarkers showed potential utility as surrogates for molecular subtype classification and clinical outcome prediction, the protein expression profiles did not match the mRNA expression profiles. Protein expression is influenced by multiple post-transcriptional modification and degradation mechanisms including mRNA splicing and siRNA post-transcriptional gene silencing. Protein levels may also be more susceptible to signals from the stromal environment and so weaken the predictive function of the biomarker protein expression compared to mRNA levels. Post-chemotherapy samples were found to have an altered tumour microenvironment compared to chemo-naïve samples with an enhanced immune response shown by enrichment of B cells, $CD4^+$ and $CD8^+$ T cells and DC cells. GATA6 nuclear expression (in $CK19^+$ cells) was significantly higher in the post-chemotherapy group compared to the chemo-naïve group, but altered GATA6 protein levels were not found in either the cytosol or whole cells. This suggests that neoadjuvant therapy may

specifically influence the expression of functional GATA6 in the nucleus rather than storage in the cytosol.

GATA6, HNF1A, and CYP3A5 expressing cells persistent post-chemotherapy

We found that GATA6, HNF1A, and CYP3A5 showed higher protein expression in the tumours of post-chemotherapy patient subsets compared with those from pre-treatment patient subsets. Whilst biomarker mRNA expression in post-chemotherapy tumours showed no association with patient outcome, high protein expression of GATA6 and CYP3A5 were each significantly associated with poor prognosis, especially in those treated with FFX (FOLFIRINOX). These $GATA6^{+}$ and $CYP3A5^{+}$ expressing cells enriched after chemotherapy may be identified as persistent cancer cells (Shen et al. 2020). Persistent cancer cells are characterized by their slow proliferation, highly flexible energy consumption, adaptation to their microenvironment, and phenotypic plasticity that survive cancer drug treatment and may represent a major cause of treatment failure (Shen et al. 2020). The discovery of such persistent cancer cells might be the reason of poor drug response, drug resistance or even eventually increases the unpredictable risk of metastatic relapses (Shen et al. 2020). CYP3A isoforms play a major role in drug metabolism and resistance, notably for irinotecan used as a component of the FOLFIRINOX regimen, and which (along with ABCC1 and ABCC2 transporters and TOP1) are under the transcriptional regulation of HNF1A (Capello et al. 2020; Capello et al. 2015). Since around 90% of Caucasians have the inactive CYP3A5*3 isoform it will be necessary to determine whether other isoforms such as CYP3A4 and CYP3A7 have a functional role as persister cancer cells after chemotherapy in pancreatic cancer (Ingelman-Sundberg and Lauschke 2020).

5. Summary

Pancreatic ductal adenocarcinoma (PDAC) is a lethal malignancy with limited response to current therapies. Molecular subtyping of PDAC has been found to be associated with clinical drug response and patient prognosis. The Classical-like subtype is related to a relatively good prognosis, whilst the Basal-like/QM-PDA subtype is correlated with a poor prognosis and paradoxically to a good response from chemotherapy. The investigation of representative biomarkers for each molecular subtype is still at an early stage of development. This study refined the transcriptomic profiling of PDAC by using laser capture microscopy in chemo-naïve tumours and in so doing confirmed the canonical subtyping schemes of Moffitt, Collisson, Bailey and Notta. GATA6, CYP3A5 and HNF1A were identified as biomarkers at the mRNA level for Classical-like subtype tumours as well as being shown to be prognostic indicators. KRT81 expression at the mRNA level was correlated with the Moffitt Basal-like subtype, but in this case, it was not a significant prognostic indicator. Following neoadjuvant chemotherapy patients with high GATA6 and CYP3A5 protein expressing tumours tended to have relatively poor outcome, especially in those treated with FFX (FOLFIRINOX). These $GATA6^{+}$ and $CYP3A5^{+}$ expressing cells that were enriched in the tumour tissues after chemotherapy may represent persister cancer cells, potentially contributing to poor drug response and drug resistance, and the promotion of tumour metastases.

The discovery of further representative biomarkers of molecular phenotypes will contribute to improving the drive towards more precise and more personalized treatment. Further understanding of the nature of pancreatic cancer persister cells after chemotherapy should lead to the discovery of more effective therapeutic strategies and so help to help provide longer survival for affected patients.

Zusammenfassung

Das duktale Adenokarzinom der Bauchspeicheldrüse (PDAC) ist eine tödliche Erkrankung, die auf die derzeitigen Therapien nur begrenzt anspricht. Es hat sich gezeigt, dass die molekulare Subtypisierung von PDAC mit dem klinischen Ansprechen auf Medikamente und der Prognose der Patienten zusammenhängt. Der Classical-like Subtyp ist mit einer relativ guten Prognose verbunden, während der Basal-like/QM-PDA-Subtyp mit einer schlechten Prognose und paradoxerweise mit einem guten Ansprechen auf die Chemotherapie korreliert. Die Untersuchung repräsentativer Biomarker für jeden molekularen Subtyp befindet sich noch in einem frühen Stadium der Entwicklung. In dieser Studie wurde das Transkriptom Profil von PDAC mit Hilfe der Laser-Capture-Mikroskopie in chemo-naiven Tumouren verbessert und die kanonischen Subtypisierungsschemata von Moffitt, Collisson, Bailey und Notta bestätigt. GATA6, CYP3A5 und HNF1A wurden als Biomarker auf mRNA-Ebene für Tumoure des Classical-like Subtyps identifiziert und erwiesen sich als prognostische Indikatoren. Die Expression von KRT81 auf mRNA-Ebene korrelierte mit dem Moffitt Basal-like Subtyp, war aber in diesem Fall kein signifikanter prognostischer Indikator. Nach einer neoadjuvanten Chemotherapie hatten PDAC Patienten, die viel GATA6 und CYP3A5 Proteine exprimieren, tendenziell ein relativ schlechteres Ansprechen, insbesondere nach einer FFX (FOLFIRINOX) Behandlung. Diese $GATA6^{+}$ und $CYP3A5^{+}$ exprimierenden Zellen, die nach der Chemotherapie im Tumourgewebe angereichert waren, könnten persistierende Krebszellen darstellen, die möglicherweise zu einem schlechten Ansprechen auf Medikamente und zu einer Medikamentenresistenz sowie zur Förderung von Tumourmetastasen beitragen.

Die Entdeckung weiterer repräsentativer Biomarker für molekulare Phänotypen wird zu verbesserten Vorhersagen beitragen, um eine präzisere und stärker personalisierte Behandlung zu erzielen. Ein besseres Verständnis zur Beschaffenheit der Persistenzzellen des Bauchspeicheldrüsenkrebses nach einer Chemotherapie sollte zur

Entwicklung wirksamerer therapeutischer Strategien führen und so dazu beitragen, dass die betroffenen Patienten mit dieser Krankheit länger überleben.

6. References

Ahmed, S., Sami, A. and Xiang, J. (2015). **HER2-directed therapy: current treatment options for HER2-positive breast cancer**. Breast Cancer (Tokyo, Japan) *22 (2)*, 101-116, doi: 10.1007/s12282-015-0587-x.

Akpinar, P., Kuwajima, S., Krützfeldt, J. and Stoffel, M. (2005). **Tmem27: A cleaved and shed plasma membrane protein that stimulates pancreatic β cell proliferation**. Cell Metabolism *2 (6)*, 385-397, doi: 10.1016/j.cmet.2005.11.001.

Alexandrov, L. B., Nik-Zainal, S., Wedge, D. C., Campbell, P. J. and Stratton, M. R. (2013). **Deciphering signatures of mutational processes operative in human cancer**. Cell Rep *3 (1)*, 246-259, doi: 10.1016/j.celrep.2012.12.008.

Amadou, A., Waddington Achatz, M. I. and Hainaut, P. (2018). **Revisiting tumour patterns and penetrance in germline TP53 mutation carriers: temporal phases of Li–Fraumeni syndrome**. Current Opinion in Oncology *30 (1)*, 23-29, doi: 10.1097/CCO.0000000000000423.

Aoki, M. N., Amarante, M. K., de Oliveira, C. E. C. and Watanabe, M. A. E. (2018). **Biomarkers in Non-Small Cell Lung Cancer: Perspectives of Individualized Targeted Therapy**. Anti-Cancer Agents in Medicinal Chemistry *18 (15)*, 2070-2077, doi: 10.2174/1871520618666180827102101.

Aoyama, T., Yamano, S., Waxman, D. J., Lapenson, D. P., Meyer, U. A., Fischer, V., Tyndale, R., Inaba, T., Kalow, W. and Gelboin, H. V. (1989). **Cytochrome P-450 hPCN3, a novel cytochrome P-450 IIIA gene product that is differentially expressed in adult human liver. cDNA and deduced amino acid sequence and distinct specificities of cDNA-expressed hPCN1 and hPCN3 for the metabolism of steroid hormones and cyclosporine**. The Journal of Biological Chemistry *264 (18)*, 10388-10395.

Aronson, B. E., Stapleton, K. A. and Krasinski, S. D. (2014). **Role of GATA factors in development, differentiation, and homeostasis of the small intestinal epithelium**. American Journal of Physiology - Gastrointestinal and Liver Physiology *306 (6)*, G474-G490, doi: 10.1152/ajpgi.00119.2013.

Aung, K. L., Fischer, S. E., Denroche, R. E., Jang, G.-H., Dodd, A., Creighton, S., Southwood, B., Liang, S.-B., Chadwick, D., Zhang, A., O'Kane, G. M., Albaba, H., Moura, S., Grant, R. C., Miller, J. K., Mbabaali, F., Pasternack, D., Lungu, I. M., Bartlett, J. M. S., Ghai, S., Lemire, M., Holter, S., Connor, A. A., Moffitt, R. A., Yeh, J. J., Timms, L., Krzyzanowski, P. M., Dhani, N., Hedley, D., Notta, F., Wilson, J. M., Moore, M. J., Gallinger, S. and Knox, J. J. (2018). **Genomics-Driven Precision Medicine for Advanced Pancreatic Cancer: Early Results from the**

COMPASS Trial. Clinical Cancer Research: An Official Journal of the American Association for Cancer Research *24 (6)*, 1344-1354, doi: 10.1158/1078-0432.CCR-17-2994.

Bailey, P., Chang, D. K., Nones, K., Johns, A. L., Patch, A.-M., Gingras, M.-C., Miller, D. K., Christ, A. N., Bruxner, T. J. C., Quinn, M. C., Nourse, C., Murtaugh, L. C., Harliwong, I., Idrisoglu, S., Manning, S., Nourbakhsh, E., Wani, S., Fink, L., Holmes, O., Chin, V., Anderson, M. J., Kazakoff, S., Leonard, C., Newell, F., Waddell, N., Wood, S., Xu, Q., Wilson, P. J., Cloonan, N., Kassahn, K. S., Taylor, D., Quek, K., Robertson, A., Pantano, L., Mincarelli, L., Sanchez, L. N., Evers, L., Wu, J., Pinese, M., Cowley, M. J., Jones, M. D., Colvin, E. K., Nagrial, A. M., Humphrey, E. S., Chantrill, L. A., Mawson, A., Humphris, J., Chou, A., Pajic, M., Scarlett, C. J., Pinho, A. V., Giry-Laterriere, M., Rooman, I., Samra, J. S., Kench, J. G., Lovell, J. A., Merrett, N. D., Toon, C. W., Epari, K., Nguyen, N. Q., Barbour, A., Zeps, N., Moran-Jones, K., Jamieson, N. B., Graham, J. S., Duthie, F., Oien, K., Hair, J., Grützmann, R., Maitra, A., Iacobuzio-Donahue, C. A., Wolfgang, C. L., Morgan, R. A., Lawlor, R. T., Corbo, V., Bassi, C., Rusev, B., Capelli, P., Salvia, R., Tortora, G., Mukhopadhyay, D., Petersen, G. M., Australian Pancreatic Cancer Genome, I., Munzy, D. M., Fisher, W. E., Karim, S. A., Eshleman, J. R., Hruban, R. H., Pilarsky, C., Morton, J. P., Sansom, O. J., Scarpa, A., Musgrove, E. A., Bailey, U.-M. H., Hofmann, O., Sutherland, R. L., Wheeler, D. A., Gill, A. J., Gibbs, R. A., Pearson, J. V., Waddell, N., Biankin, A. V. and Grimmond, S. M. (2016). **Genomic analyses identify molecular subtypes of pancreatic cancer**. Nature *531 (7592)*, 47-52, doi: 10.1038/nature16965.

Ban, N., Yamada, Y., Someya, Y., Miyawaki, K., Ihara, Y., Hosokawa, M., Toyokuni, S., Tsuda, K. and Seino, Y. (2002). **Hepatocyte nuclear factor-1alpha recruits the transcriptional co-activator p300 on the GLUT2 gene promoter**. Diabetes *51 (5)*, 1409-1418, doi: 10.2337/diabetes.51.5.1409.

Bärthel, S., Schneider, G. and Saur, D. (2020). **Blocking the road to de - differentiation: HNF1A/KDM6A complex safeguards epithelial integrity in pancreatic cancer**. The EMBO Journal *39 (9)*, doi: 10.15252/embj.2020104759.

Beal, P. R., Yao, S. Y. M., Baldwin, S. A., Young, J. D., King, A. E. and Cass, C. E. (2004). **The equilibrative nucleoside transporter family, SLC29**. Pflügers Archiv European Journal of Physiology *447 (5)*, 735-743, doi: 10.1007/s00424-003-1103-2.

Belaguli, N. S., Aftab, M., Rigi, M., Zhang, M., Albo, D. and Berger, D. H. (2010). **GATA6 Promotes Colon Cancer Cell Invasion by Regulating Urokinase Plasminogen Activator Gene Expression**. Neoplasia (New York, N.Y.) *12 (11)*, 856-865.

Bird, N. T. E., Elmasry, M., Jones, R., Psarelli, E., Dodd, J., Malik, H., Greenhalf, W., Kitteringham, N., Ghaneh, P., Neoptolemos, J. P. and Palmer, D. (2017). **Immunohistochemical hENT1 expression as a prognostic biomarker in patients with resected pancreatic ductal adenocarcinoma undergoing adjuvant gemcitabine-based chemotherapy**. British Journal of Surgery *104 (4)*, 328-336, doi: 10.1002/bjs.10482.

Birnbaum, D. J., Adélaïde, J., Mamessier, E., Finetti, P., Lagarde, A., Monges, G., Viret, F., Gonçalvès, A., Turrini, O., Delpero, J.-R., Iovanna, J., Giovannini, M., Birnbaum, D. and Chaffanet, M. (2011). **Genome profiling of pancreatic adenocarcinoma**. Genes, Chromosomes and Cancer *50 (6)*, 456-465, doi: 10.1002/gcc.20870.

Bochud, M., Bovet, P., Burnier, M. and Eap, C. B. (2009). **CYP3A5 and ABCB1 genes and hypertension**. Pharmacogenomics *10 (3)*, 477-487, doi: 10.2217/14622416.10.3.477.

Boj, S. F., Párrizas, M., Maestro, M. A. and Ferrer, J. (2001). **A transcription factor regulatory circuit in differentiated pancreatic cells**. Proceedings of the National Academy of Sciences of the United States of America *98 (25)*, 14481-14486, doi: 10.1073/pnas.241349398.

Bray, F., Ferlay, J., Soerjomataram, I., Siegel, R. L., Torre, L. A. and Jemal, A. (2018). **Global cancer statistics 2018: GLOBOCAN estimates of incidence and mortality worldwide for 36 cancers in 185 countries**. CA: A Cancer Journal for Clinicians *68 (6)*, 394-424, doi: 10.3322/caac.21492.

Brunton, H., Caligiuri, G., Cunningham, R., Upstill-Goddard, R., Bailey, U.-M., Garner, I. M., Nourse, C., Dreyer, S., Jones, M., Moran-Jones, K., Wright, D. W., Paulus-Hock, V., Nixon, C., Thomson, G., Jamieson, N. B., McGregor, G. A., Evers, L., McKay, C. J., Gulati, A., Brough, R., Bajrami, I., Pettitt, S. J., Dziubinski, M. L., Barry, S. T., Grützmann, R., Brown, R., Curry, E., Glasgow Precision Oncology, L., Australian Pancreatic Cancer Genome, I., Pajic, M., Musgrove, E. A., Petersen, G. M., Shanks, E., Ashworth, A., Crawford, H. C., Simeone, D. M., Froeling, F. E. M., Lord, C. J., Mukhopadhyay, D., Pilarsky, C., Grimmond, S. E., Morton, J. P., Sansom, O. J., Chang, D. K., Bailey, P. J. and Biankin, A. V. (2020). **HNF4A and GATA6 Loss Reveals Therapeutically Actionable Subtypes in Pancreatic Cancer**. Cell Reports *31 (6)*, 107625, doi: 10.1016/j.celrep.2020.107625.

Buck, E., Sprick, M., Gaida, M., Grüllich, C., Weber, T., Herpel, E., Bruckner, T. and Koschny, R. (2019). **Tumour response to irinotecan is associated with CYP3A5 expression in colorectal cancer**. Oncology Letters, doi: 10.3892/ol.2019.10043.

Cano-Soldado, P. and Pastor-Anglada, M. (2012). **Transporters that translocate nucleosides and structural similar drugs: structural requirements for substrate recognition: TRANSPORTERS THAT TRANSLOCATE NUCLEOSIDES**. Medicinal Research Reviews *32 (2)*, 428-457, doi: 10.1002/med.20221.

Capello, M., Fahrmann, J. F., Rios Perez, M. V., Vykoukal, J. V., Irajizad, E., Tripathi, S. C., Roife, D., Bantis, L. E., Kang, Y., Kundnani, D. L., Xu, H., Prakash, L. R., Long, J. P., Katayama, H., Fleury, A., Ferri-Borgogno, S., Baluya, D. L., Dennison, J. B., Aguilar-Bonavides, C., Casabar, J. P., Celiktas, M., Do, K. A., Fiehn, O., Maitra, A., Wang, H., Feng, Z., Chiao, P. J., Katz, M. H.,

Fleming, J. B. and Hanash, S. M. (2020). **CES2 Expression in Pancreatic Adenocarcinoma Is Predictive of Response to Irinotecan and Is Associated With Type 2 Diabetes**. JCO Precis Oncol *4*, 426-436, doi: 10.1200/PO.19.00330.

Capello, M., Lee, M., Wang, H., Babel, I., Katz, M. H., Fleming, J. B., Maitra, A., Wang, H., Tian, W., Taguchi, A. and Hanash, S. M. (2015). **Carboxylesterase 2 as a Determinant of Response to Irinotecan and Neoadjuvant FOLFIRINOX Therapy in Pancreatic Ductal Adenocarcinoma**. J Natl Cancer Inst *107 (8)*, doi: 10.1093/jnci/djv132.

Carrasco, M., Delgado, I., Soria, B., Martín, F. and Rojas, A. (2012). **GATA4 and GATA6 control mouse pancreas organogenesis**. The Journal of Clinical Investigation *122 (10)*, 3504-3515, doi: 10.1172/JCI63240.

Chan-Seng-Yue, M., Kim, J. C., Wilson, G. W., Ng, K., Figueroa, E. F., O'Kane, G. M., Connor, A. A., Denroche, R. E., Grant, R. C., McLeod, J., Wilson, J. M., Jang, G. H., Zhang, A., Dodd, A., Liang, S.-B., Borgida, A., Chadwick, D., Kalimuthu, S., Lungu, I., Bartlett, J. M. S., Krzyzanowski, P. M., Sandhu, V., Tiriac, H., Froeling, F. E. M., Karasinska, J. M., Topham, J. T., Renouf, D. J., Schaeffer, D. F., Jones, S. J. M., Marra, M. A., Laskin, J., Chetty, R., Stein, L. D., Zogopoulos, G., Haibe-Kains, B., Campbell, P. J., Tuveson, D. A., Knox, J. J., Fischer, S. E., Gallinger, S. and Notta, F. (2020). **Transcription phenotypes of pancreatic cancer are driven by genomic events during tumour evolution**. Nature Genetics *52 (2)*, 231-240, doi: 10.1038/s41588-019-0566-9.

Colclough, K., Bellanne-Chantelot, C., Saint-Martin, C., Flanagan, S. E. and Ellard, S. (2013). **Mutations in the genes encoding the transcription factors hepatocyte nuclear factor 1 alpha and 4 alpha in maturity-onset diabetes of the young and hyperinsulinemic hypoglycemia**. Human Mutation *34 (5)*, 669-685, doi: 10.1002/humu.22279.

Collisson, E. A., Bailey, P., Chang, D. K. and Biankin, A. V. (2019). **Molecular subtypes of pancreatic cancer**. Nature Reviews. Gastroenterology & Hepatology *16 (4)*, 207-220, doi: 10.1038/s41575-019-0109-y.

Collisson, E. A., Sadanandam, A., Olson, P., Gibb, W. J., Truitt, M., Gu, S., Cooc, J., Weinkle, J., Kim, G. E., Jakkula, L., Feiler, H. S., Ko, A. H., Olshen, A. B., Danenberg, K. L., Tempero, M. A., Spellman, P. T., Hanahan, D. and Gray, J. W. (2011). **Subtypes of pancreatic ductal adenocarcinoma and their differing responses to therapy**. Nature Medicine *17 (4)*, 500-503, doi: 10.1038/nm.2344.

Conroy, T., Desseigne, F., Ychou, M., Bouché, O., Guimbaud, R., Bécouarn, Y., Adenis, A., Raoul, J.-L., Gourgou-Bourgade, S., de la Fouchardière, C., Bennouna, J., Bachet, J.-B., Khemissa-Akouz, F., Péré-Vergé, D., Delbaldo, C., Assenat, E., Chauffert, B., Michel, P., Montoto-Grillot, C., Ducreux, M., Groupe Tumeurs Digestives of, U. and Intergroup, P. (2011). **FOLFIRINOX versus gemcitabine for metastatic pancreatic cancer**. The New England Journal of Medicine *364 (19)*, 1817-1825, doi: 10.1056/NEJMoa1011923.

Conroy, T., Hammel, P., Hebbar, M., Ben Abdelghani, M., Wei, A. C., Raoul, J.-L., Choné, L., Francois, E., Artru, P., Biagi, J. J., Lecomte, T., Assenat, E., Faroux, R., Ychou, M., Volet, J., Sauvanet, A., Breysacher, G., Di Fiore, F., Cripps, C., Kavan, P., Texereau, P., Bouhier-Leporrier, K., Khemissa-Akouz, F., Legoux, J.-L., Juzyna, B., Gourgou, S., O'Callaghan, C. J., Jouffroy-Zeller, C., Rat, P., Malka, D., Castan, F., Bachet, J.-B., Canadian Cancer Trials, G. and the Unicancer, G. P. G. (2018). **FOLFIRINOX or Gemcitabine as Adjuvant Therapy for Pancreatic Cancer**. The New England Journal of Medicine *379 (25)*, 2395-2406, doi: 10.1056/NEJMoa1809775.

Consortium, I. T. P.-C. A. o. W. G. (2020). **Pan-cancer analysis of whole genomes**. Nature *578 (7793)*, 82-93, doi: 10.1038/s41586-020-1969-6.

Cremin, C., Howard, S., Le, L., Karsan, A., Schaeffer, D. F., Renouf, D. and Schrader, K. A. (2018). **CDKN2A founder mutation in pancreatic ductal adenocarcinoma patients without cutaneous features of Familial Atypical Multiple Mole Melanoma (FAMMM) syndrome**. Hereditary Cancer in Clinical Practice *16*, doi: 10.1186/s13053-018-0088-y.

DaVee, T., Coronel, E., Papafragkakis, C., Thaiudom, S., Lanke, G., Chakinala, R. C., González, G. M. N., Bhutani, M. S., Ross, W. A., Weston, B. R. and Lee, J. H. (2018). **Pancreatic cancer screening in high-risk individuals with germline genetic mutations**. Gastrointestinal Endoscopy *87 (6)*, 1443-1450, doi: 10.1016/j.gie.2017.12.019.

Deng, N., Goh, L. K., Wang, H., Das, K., Tao, J., Tan, I. B., Zhang, S., Lee, M., Wu, J., Lim, K. H., Lei, Z., Goh, G., Lim, Q.-Y., Tan, A. L.-K., Sin Poh, D. Y., Riahi, S., Bell, S., Shi, M. M., Linnartz, R., Zhu, F., Yeoh, K. G., Toh, H. C., Yong, W. P., Cheong, H. C., Rha, S. Y., Boussioutas, A., Grabsch, H., Rozen, S. and Tan, P. (2012). **A comprehensive survey of genomic alterations in gastric cancer reveals systematic patterns of molecular exclusivity and co-occurrence among distinct therapeutic targets**. Gut *61 (5)*, 673-684, doi: 10.1136/gutjnl-2011-301839.

Derissen, E. J., Jacobs, B. A., Huitema, A. D., Rosing, H., Schellens, J. H. and Beijnen, J. H. (2016). **Exploring the intracellular pharmacokinetics of the 5-fluorouracil nucleotides during capecitabine treatment**. Br J Clin Pharmacol *81 (5)*, 949-957, doi: 10.1111/bcp.12877.

Ellison, T. A., Wolfgang, C. L., Shi, C., Cameron, J. L., Murakami, P., Mun, L. J., Singhi, A. D., Cornish, T. C., Olino, K., Meriden, Z., Choti, M., Diaz, L. A., Pawlik, T. M., Schulick, R. D., Hruban, R. H. and Edil, B. H. (2014). **A single institution's 26-year experience with nonfunctional pancreatic neuroendocrine tumours: a validation of current staging systems and a new prognostic nomogram**. Annals of Surgery *259 (2)*, 204-212, doi: 10.1097/SLA.0b013e31828f3174.

Endo, Y., Obata, T., Murata, D., Ito, M., Sakamoto, K., Fukushima, M., Yamasaki, Y., Yamada, Y., Natsume, N. and Sasaki, T. (2007). **Cellular localization and functional characterization**

of the equilibrative nucleoside transporters of antitumour nucleosides. Cancer Science *98 (10)*, 1633-1637, doi: 10.1111/j.1349-7006.2007.00581.x.

Fajans, S. S., Bell, G. I., Bowden, D. W., Halter, J. B. and Polonsky, K. S. (1994). **Maturity-onset diabetes of the young**. Life Sciences *55 (6)*, 413-422, doi: 10.1016/0024-3205(94)90052-3.

Farrell, J. J., Elsaleh, H., Garcia, M., Lai, R., Ammar, A., Regine, W. F., Abrams, R., Benson, A. B., Macdonald, J., Cass, C. E., Dicker, A. P. and Mackey, J. R. (2009). **Human Equilibrative Nucleoside Transporter 1 Levels Predict Response to Gemcitabine in Patients With Pancreatic Cancer**. Gastroenterology *136 (1)*, 187-195, doi: 10.1053/j.gastro.2008.09.067.

Ferrone, C. R., Marchegiani, G., Hong, T. S., Ryan, D. P., Deshpande, V., McDonnell, E. I., Sabbatino, F., Santos, D. D., Allen, J. N., Blaszkowsky, L. S., Clark, J. W., Faris, J. E., Goyal, L., Kwak, E. L., Murphy, J. E., Ting, D. T., Wo, J. Y., Zhu, A. X., Warshaw, A. L., Lillemoe, K. D. and Fernández-del Castillo, C. (2015). **Radiological and surgical implications of neoadjuvant treatment with FOLFIRINOX for locally advanced and borderline resectable pancreatic cancer**. Annals of Surgery *261 (1)*, 12-17, doi: 10.1097/SLA.0000000000000867.

Fu, B., Luo, M., Lakkur, S., Lucito, R. and Iacobuzio-Donahue, C. A. (2008). **Frequent genomic copy number gain and overexpression of GATA-6 in pancreatic carcinoma**. Cancer Biology & Therapy *7 (10)*, 1593-1601, doi: 10.4161/cbt.7.10.6565.

Ghaneh, P., Palmer, D.H., Cicconi, S., Halloran, C.M., Psarelli, E.E., Rawcliffe, C.L., Sripadam, R., Mukherjee, S., Wadsley, J., Al-Mukhtar, A., Jiao, L.R., Wasan, H.S., Carter, R., Graham, J.S., Ammad, F., Evans, J.P., Tjaden, C., Hackert, T., Bũchler, M.W., & Neoptolemos, J.P. (2020). **ESPAC-5F: Four-arm, prospective, multicentre, international randomized phase II trial of immediate surgery compared with neoadjuvant gemcitabine plus capecitabine (GEMCAP) or FOLFIRINOX or chemoradiotherapy (CRT) in patients with borderline resectable pancreatic cancer.** . Journal of Clinical Oncology *38:15_suppl*, 4505, doi: 10.1200/JCO.2020.38.15_suppl.4505.

Go, V. L. W., Gukovskaya, A. and Pandol, S. J. (2005). **Alcohol and pancreatic cancer**. Alcohol *35 (3)*, 205-211, doi: 10.1016/j.alcohol.2005.03.010.

Greenhalf, W., Ghaneh, P., Neoptolemos, J. P., Palmer, D. H., Cox, T. F., Lamb, R. F., Garner, E., Campbell, F., Mackey, J. R., Costello, E., Moore, M. J., Valle, J. W., McDonald, A. C., Carter, R., Tebbutt, N. C., Goldstein, D., Shannon, J., Dervenis, C., Glimelius, B., Deakin, M., Charnley, R. M., Lacaine, F., Scarfe, A. G., Middleton, M. R., Anthoney, A., Halloran, C. M., Mayerle, J., Oláh, A., Jackson, R., Rawcliffe, C. L., Scarpa, A., Bassi, C. and Büchler, M. W. (2014). **Pancreatic Cancer hENT1 Expression and Survival From Gemcitabine in Patients From the ESPAC-3 Trial**. JNCI: Journal of the National Cancer Institute *106 (1)*, doi: 10.1093/jnci/djt347.

Greenhalf, W., Levy, P., Gress, T., Rebours, V., Brand, R. E., Pandol, S., Chari, S., Jorgensen, M. T., Mayerle, J., Lerch, M. M., Hegyi, P., Kleeff, J., Castillo, C. F., Isaji, S., Shimosegawa, T., Sheel, A., Halloran, C. M., Garg, P., Takaori, K., Besselink, M. G., Forsmark, C. E., Wilcox, C. M., Maisonneuve, P., Yadav, D., Whitcomb, D., Neoptolemos, J. and Working group for the International Consensus Guidelines for Chronic, P. (2020). **International consensus guidelines on surveillance for pancreatic cancer in chronic pancreatitis. Recommendations from the working group for the international consensus guidelines for chronic pancreatitis in collaboration with the International Association of Pancreatology, the American Pancreatic Association, the Japan Pancreas Society, and European Pancreatic Club**. Pancreatology *20 (5)*, 910-918, doi: 10.1016/j.pan.2020.05.011.

Guengerich, F. P. (2008). **Cytochrome p450 and chemical toxicology**. Chemical Research in Toxicology *21 (1)*, 70-83, doi: 10.1021/tx700079z.

Guldberg, P., Straten, P. t., Ahrenkiel, V., Seremet, T., Kirkin, A. F. and Zeuthen, J. (1999). **Somatic mutation of the Peutz-Jeghers syndrome gene, LKB1/STK11 , in malignant melanoma**. Oncogene *18 (9)*, 1777-1780, doi: 10.1038/sj.onc.1202486.

Hackert, T., Sachsenmaier, M., Hinz, U., Schneider, L., Michalski, C. W., Springfeld, C., Strobel, O., Jager, D., Ulrich, A. and Buchler, M. W. (2016). **Locally Advanced Pancreatic Cancer: Neoadjuvant Therapy With Folfirinox Results in Resectability in 60% of the Patients**. Ann Surg *264 (3)*, 457-463, doi: 10.1097/SLA.0000000000001850.

Haliyur, R., Tong, X., Sanyoura, M., Shrestha, S., Lindner, J., Saunders, D. C., Aramandla, R., Poffenberger, G., Redick, S. D., Bottino, R., Prasad, N., Levy, S. E., Blind, R. D., Harlan, D. M., Philipson, L. H., Stein, R. W., Brissova, M. and Powers, A. C. (2019). **Human islets expressing HNF1A variant have defective β cell transcriptional regulatory networks**. The Journal of Clinical Investigation *129 (1)*, 246-251, doi: 10.1172/JCI121994.

Harries, L. W., Ellard, S., Stride, A., Morgan, N. G. and Hattersley, A. T. (2006). **Isomers of the TCF1 gene encoding hepatocyte nuclear factor-1 alpha show differential expression in the pancreas and define the relationship between mutation position and clinical phenotype in monogenic diabetes**. Human Molecular Genetics *15 (14)*, 2216-2224, doi: 10.1093/hmg/ddl147.

Hoskins, J. W., Jia, J., Flandez, M., Parikh, H., Xiao, W., Collins, I., Emmanuel, M. A., Ibrahim, A., Powell, J., Zhang, L., Malats, N., Bamlet, W. R., Petersen, G. M., Real, F. X. and Amundadottir, L. T. (2014). **Transcriptome analysis of pancreatic cancer reveals a tumour suppressor function for HNF1A**. Carcinogenesis *35 (12)*, 2670-2678, doi: 10.1093/carcin/bgu193.

Howard A. Burris III, M. J. M., John Andersen, Mark R. Green, Mace L. Rothenberg, Manuel R.

Modiano,M. Christine Cripps, Russell K. Portenoy, Anna Maria Storniolo, Peter Tarassoff, Robert Nelson, F. Andrew Dorr,C.D. Stephens, and Daniel D. Von Hoff (1997). **Improvements in survival and clinical benefit with gemcitabine as first-line therapy for patients with advanced pancreas cancer: a randomized trial**. Journal of Clinical Oncology *15(6)*, 2403-2413, doi: 10.1200/JCO.1997.15.6.2403.

Hruban, S. Z. A. Y. S. E. R. H. (2009). **Atlas of Pancreatic Cytopathology: With Histopathologic Correlations**,

Hsu, M.-H. and Johnson, E. F. (2019). **Active-site differences between substrate-free and ritonavir-bound cytochrome P450 (CYP) 3A5 reveal plasticity differences between CYP3A5 and CYP3A4**. The Journal of Biological Chemistry *294 (20)*, 8015-8022, doi: 10.1074/jbc.RA119.007928.

Huber-Ruano, I. and Pastor-Anglada, M. (2009). **Transport of Nucleoside Analogs Across the Plasma Membrane: A Clue to Understanding Drug-Induced Cytotoxicity**. Current Drug Metabolism *10 (4)*, 347-358, doi: 10.2174/138920009788499030.

Ingelman-Sundberg, M. and Lauschke, V. M. (2020). **Can CYP Inhibition Overcome Chemotherapy Resistance?** Trends in Pharmacological Sciences *41 (8)*, 503-506, doi: 10.1016/j.tips.2020.05.007.

Jiang, F., Chen, L., Yang, Y.-C., Wang, X.-m., Wang, R.-Y., Li, L., Wen, W., Chang, Y.-X., Chen, C.-Y., Tang, J., Liu, G.-M.-Y., Huang, W.-T., Xu, L. and Wang, H.-Y. (2015). **CYP3A5 Functions as a Tumour Suppressor in Hepatocellular Carcinoma by Regulating mTORC2/Akt Signaling**. Cancer Research *75 (7)*, 1470-1481, doi: 10.1158/0008-5472.CAN-14-1589.

Jones, S., Zhang, X., Parsons, D. W., Lin, J. C., Leary, R. J., Angenendt, P., Mankoo, P., Carter, H., Kamiyama, H., Jimeno, A., Hong, S. M., Fu, B., Lin, M. T., Calhoun, E. S., Kamiyama, M., Walter, K., Nikolskaya, T., Nikolsky, Y., Hartigan, J., Smith, D. R., Hidalgo, M., Leach, S. D., Klein, A. P., Jaffee, E. M., Goggins, M., Maitra, A., Iacobuzio-Donahue, C., Eshleman, J. R., Kern, S. E., Hruban, R. H., Karchin, R., Papadopoulos, N., Parmigiani, G., Vogelstein, B., Velculescu, V. E. and Kinzler, K. W. (2008). **Core signaling pathways in human pancreatic cancers revealed by global genomic analyses**. Science *321 (5897)*, 1801-1806, doi: 10.1126/science.1164368.

Kalisz, M., Bernardo, E., Beucher, A., Maestro, M. A., del Pozo, N., Millán, I., Haeberle, L., Schlensog, M., Safi, S. A., Knoefel, W. T., Grau, V., de Vas, M., Shpargel, K. B., Vaquero, E., Magnuson, T., Ortega, S., Esposito, I., Real, F. X. and Ferrer, J. (2020). **HNF1A recruits KDM6A to activate differentiated acinar cell programs that suppress pancreatic cancer**. The EMBO Journal *39 (9)*, doi: 10.15252/embj.2019102808.

Kamijo, H., Miyagaki, T., Shishido-Takahashi, N., Nakajima, R., Oka, T., Suga, H., Sugaya, M. and Sato, S. (2018). **Aberrant CD137 ligand expression induced by GATA6 overexpression**

promotes tumour progression in cutaneous T-cell lymphoma. Blood *132 (18)*, 1922-1935, doi: 10.1182/blood-2018-04-845834.

Ketola, I., Otonkoski, T., Pulkkinen, M.-A., Niemi, H., Palgi, J., Jacobsen, C. M., Wilson, D. B. and Heikinheimo, M. (2004). **Transcription factor GATA-6 is expressed in the endocrine and GATA-4 in the exocrine pancreas**. Molecular and Cellular Endocrinology *226 (1-2)*, 51-57, doi: 10.1016/j.mce.2004.06.007.

Khorana, A. A., Mangu, P. B., Berlin, J., Engebretson, A., Hong, T. S., Maitra, A., Mohile, S. G., Mumber, M., Schulick, R., Shapiro, M., Urba, S., Zeh, H. J. and Katz, M. H. G. (2017). **Potentially Curable Pancreatic Cancer: American Society of Clinical Oncology Clinical Practice Guideline Update**. Journal of Clinical Oncology: Official Journal of the American Society of Clinical Oncology *35 (20)*, 2324-2328, doi: 10.1200/JCO.2017.72.4948.

Kim, J., Kim, H., Lee, J.-c., Kim, J. W., Paik, W. H., Lee, S. H., Hwang, J.-H., Ryu, J. K. and Kim, Y.-T. (2018). **Human equilibrative nucleoside transporter 1 (hENT1) expression as a predictive biomarker for gemcitabine chemotherapy in biliary tract cancer**. PLOS ONE *13 (12)*, e0209104, doi: 10.1371/journal.pone.0209104.

Kleeff, J., Friess, H. and Büchler, M. W. (2007). **Neoadjuvant therapy for pancreatic cancer**. British Journal of Surgery *94 (3)*, 261-262, doi: 10.1002/bjs.5737.

Kleeff, J., Korc, M., Apte, M., La Vecchia, C., Johnson, C. D., Biankin, A. V., Neale, R. E., Tempero, M., Tuveson, D. A., Hruban, R. H. and Neoptolemos, J. P. (2016). **Pancreatic cancer**. Nat Rev Dis Primers *2*, 16022, doi: 10.1038/nrdp.2016.22.

Klein, A. P. (2021). **Pancreatic cancer epidemiology: understanding the role of lifestyle and inherited risk factors**. Nat Rev Gastroenterol Hepatol *18 (7)*, 493-502, doi: 10.1038/s41575-021-00457-x.

Klinkenbijl, J. H., Jeekel, J., Sahmoud, T., van Pel, R., Couvreur, M. L., Veenhof, C. H., Arnaud, J. P., Gonzalez, D. G., de Wit, L. T., Hennipman, A. and Wils, J. (1999). **Adjuvant radiotherapy and 5-fluorouracil after curative resection of cancer of the pancreas and periampullary region: phase III trial of the EORTC gastrointestinal tract cancer cooperative group**. Annals of Surgery *230 (6)*, 776-782; discussion 782-784, doi: 10.1097/00000658-199912000-00006.

Korc, M., Jeon, C. Y., Edderkaoui, M., Pandol, S. J. and Petrov, M. S. (2017). **TOBACCO AND ALCOHOL AS RISK FACTORS FOR PANCREATIC CANCER**. Best practice & research. Clinical gastroenterology *31 (5)*, 529-536, doi: 10.1016/j.bpg.2017.09.001.

Kuehl, P., Zhang, J., Lin, Y., Lamba, J., Assem, M., Schuetz, J., Watkins, P. B., Daly, A., Wrighton, S. A., Hall, S. D., Maurel, P., Relling, M., Brimer, C., Yasuda, K., Venkataramanan, R., Strom, S., Thummel, K., Boguski, M. S. and Schuetz, E. (2001). **Sequence diversity in CYP3A**

promoters and characterization of the genetic basis of polymorphic CYP3A5 expression. Nature Genetics *27 (4)*, 383-391, doi: 10.1038/86882.

Kwei, K. A., Bashyam, M. D., Kao, J., Ratheesh, R., Reddy, E. C., Kim, Y. H., Montgomery, K., Giacomini, C. P., Choi, Y.-L., Chatterjee, S., Karikari, C. A., Salari, K., Wang, P., Hernandez-Boussard, T., Swarnalata, G., Rijn, M. v. d., Maitra, A. and Pollack, J. R. (2008). **Genomic Profiling Identifies GATA6 as a Candidate Oncogene Amplified in Pancreatobiliary Cancer**. PLOS Genetics *4 (5)*, e1000081, doi: 10.1371/journal.pgen.1000081.

Labriet, A., De Mattia, E., Cecchin, E., Lévesque, É., Jonker, D., Couture, F., Buonadonna, A., D'Andrea, M., Villeneuve, L., Toffoli, G. and Guillemette, C. (2017). **Improved Progression-Free Survival in Irinotecan-Treated Metastatic Colorectal Cancer Patients Carrying the HNF1A Coding Variant p.I27L**. Frontiers in Pharmacology *8*, doi: 10.3389/fphar.2017.00712.

Langbein, L., Rogers, M. A., Winter, H., Praetzel, S. and Schweizer, J. (2001). **The Catalog of Human Hair Keratins II. Expression of The Six Type II Members in The Hair Follicle and The Combined CAatalog of Human Type I and II Keratins**. Journal of Biological Chemistry *276 (37)*, 35123-35132, doi: 10.1074/jbc.M103305200.

Langbein, L. and Schweizer, J. (2005). **Keratins of the human hair follicle**. International Review of Cytology *243*, 1-78, doi: 10.1016/S0074-7696(05)43001-6.

Lax, S. F. (2017). **Hereditary breast and ovarian cancer**. Der Pathologe *38 (3)*, 149-155, doi: 10.1007/s00292-017-0298-5.

Leahy, J. L., Bumbalo, L. M. and Chen, C. (1993). **Beta-cell hypersensitivity for glucose precedes loss of glucose-induced insulin secretion in 90% pancreatectomized rats**. Diabetologia *36 (12)*, 1238-1244, doi: 10.1007/BF00400800.

Lee, E. S. and Lee, J. M. (2014). **Imaging diagnosis of pancreatic cancer: a state-of-the-art review**. World Journal of Gastroenterology *20 (24)*, 7864-7877, doi: 10.3748/wjg.v20.i24.7864.

Leonhardt, C. S., Traub, B., Hackert, T., Klaiber, U., Strobel, O., Büchler, M. W. and Neoptolemos, J. P. (2020). **Adjuvant and neoadjuvant chemotherapy in pancreatic ductal adenocarcinoma**. Journal of Pancreatology *3 (1)*, 1-11, doi: 10.1097/jp9.0000000000000040.

Li, H. B., Wang, J. L., Jin, X. D., Zhao, L., Ye, H. L., Kuang, Y. B., Ma, Y., Jiang, X. Y. and Yu, Z. Y. (2021). **Comprehensive analysis of the transcriptional expressions and prognostic value of S100A family in pancreatic ductal adenocarcinoma**. BMC Cancer *21 (1)*, 1039, doi: 10.1186/s12885-021-08769-6.

Liao, C.-M., Mukherjee, S., Tiyaboonchai, A., Maguire, J. A., Cardenas-Diaz, F. L., French, D. L. and Gadue, P. **GATA6 suppression enhances lung specification from human pluripotent stem cells**. The Journal of Clinical Investigation *128 (7)*, 2944-2950, doi: 10.1172/JCI96539.

Lu, Y., Li, D., Liu, G., Xiao, E., Mu, S., Pan, Y., Qin, F., Zhai, Y., Duan, S., Li, D. and Yan, G. (2021). **Identification of Critical Pathways and Potential Key Genes in Poorly Differentiated Pancreatic Adenocarcinoma**. Onco Targets Ther *14*, 711-723, doi: 10.2147/OTT.S279287.

Luo, Z., Li, Y., Wang, H., Fleming, J., Li, M., Kang, Y., Zhang, R. and Li, D. (2015). **Hepatocyte Nuclear Factor 1A (HNF1A) as a Possible Tumour Suppressor in Pancreatic Cancer**. PLOS ONE *10 (3)*, e0121082, doi: 10.1371/journal.pone.0121082.

Maeda, M., Ohashi, K. and Ohashi-Kobayashi, A. (2005). **Further extension of mammalian GATA-6**. Dev Growth Differ *47 (9)*, 591-600, doi: 10.1111/j.1440-169X.2005.00837.x.

Maisonneuve, P. (2019). **Epidemiology and burden of pancreatic cancer**. La Presse Médicale *48 (3)*, e113-e123, doi: 10.1016/j.lpm.2019.02.030.

Marcé, S., Molina-Arcas, M., Villamor, N., Casado, F. J., Campo, E., Pastor-Anglada, M. and Colomer, D. **Expression of human equilibrative nucleoside transporter 1 (hENT1) and its correlation with gemcitabine uptake and cytotoxicity in mantle cell lymphoma**. 9.

Mario, C., Marilisa, F., Kryssia, I. R.-C., Pellegrino, C., Ginevra, C., Chiara, M., Alberto, B., Antonio, N., Gioacchino, L., Tiziana, M., Gian, L. d. A. and Francesco, D. M. (2018). **Epidemiology and risk factors of pancreatic cancer**. Acta Bio Medica : Atenei Parmensis *89 (Suppl 9)*, 141-146, doi: 10.23750/abm.v89i9-S.7923.

Martinelli, P., Cañamero, M., Pozo, N. d., Madriles, F., Zapata, A. and Real, F. X. (2013). **Gata6 is required for complete acinar differentiation and maintenance of the exocrine pancreas in adult mice**. Gut *62 (10)*, 1481-1488, doi: 10.1136/gutjnl-2012-303328.

Martinelli, P., Carrillo-de Santa Pau, E., Cox, T., Sainz, B., Dusetti, N., Greenhalf, W., Rinaldi, L., Costello, E., Ghaneh, P., Malats, N., Büchler, M., Pajic, M., Biankin, A. V., Iovanna, J., Neoptolemos, J. and Real, F. X. (2017). **GATA6 regulates EMT and tumour dissemination, and is a marker of response to adjuvant chemotherapy in pancreatic cancer**. Gut *66 (9)*, 1665-1676, doi: 10.1136/gutjnl-2015-311256.

Matthew H. G. Katz, Q. S., Jeffrey P. Meyers, Joseph M. Herman, Michael Choung, Brian M. Wolpin, Syed Ahmad, Robert de Wilton Marsh, Lawrence Howard Schwartz, Spencer Behr, Wendy L. Frankel, Eric Andrew Collisson, James Lewis Leenstra, Terence Marques Williams, Gina M. Vaccaro, Alan P. Venook, Jeffrey A Meyerhardt, Eileen Mary O'Reilly (2021). **Alliance A021501: Preoperative mFOLFIRINOX or mFOLFIRINOX plus hypofractionated radiation therapy (RT) for borderline resectable (BR) adenocarcinoma of the**

pancreas. . Journal of Clinical Oncology *39:3_suppl*, 377, doi: 10.1200/JCO.2021.39.3_suppl.377.

Maurer, C., Holmstrom, S. R., He, J., Laise, P., Su, T., Ahmed, A., Hibshoosh, H., Chabot, J. A., Oberstein, P. E., Sepulveda, A. R., Genkinger, J. M., Zhang, J., Iuga, A. C., Bansal, M., Califano, A. and Olive, K. P. (2019). **Experimental microdissection enables functional harmonisation of pancreatic cancer subtypes**. Gut *68 (6)*, 1034-1043, doi: 10.1136/gutjnl-2018-317706.

Mitra, R. and Goodman, O. B. (2015). **CYP3A5 regulates prostate cancer cell growth by facilitating nuclear translocation of AR**. The Prostate *75 (5)*, 527-538, doi: 10.1002/pros.22940.

Moffitt, R. A., Marayati, R., Flate, E. L., Volmar, K. E., Loeza, S. G., Hoadley, K. A., Rashid, N. U., Williams, L. A., Eaton, S. C., Chung, A. H., Smyla, J. K., Anderson, J. M., Kim, H. J., Bentrem, D. J., Talamonti, M. S., Iacobuzio-Donahue, C. A., Hollingsworth, M. A. and Yeh, J. J. (2015). **Virtual microdissection identifies distinct tumour- and stroma-specific subtypes of pancreatic ductal adenocarcinoma**. Nat Genet *47 (10)*, 1168-1178, doi: 10.1038/ng.3398.

Moilanen, A.-M., Hakkola, J., Vaarala, M. H., Kauppila, S., Hirvikoski, P., Vuoristo, J. T., Edwards, R. J. and Paavonen, T. K. (2007). **Characterization of androgen-regulated expression of CYP3A5 in human prostate**. Carcinogenesis *28 (5)*, 916-921, doi: 10.1093/carcin/bgl222.

Morris, J. P. t., Wang, S. C. and Hebrok, M. (2010). **KRAS, Hedgehog, Wnt and the twisted developmental biology of pancreatic ductal adenocarcinoma**. Nat Rev Cancer *10 (10)*, 683-695, doi: 10.1038/nrc2899.

Mosele, F., Remon, J., Mateo, J., Westphalen, C. B., Barlesi, F., Lolkema, M. P., Normanno, N., Scarpa, A., Robson, M., Meric-Bernstam, F., Wagle, N., Stenzinger, A., Bonastre, J., Bayle, A., Michiels, S., Bieche, I., Rouleau, E., Jezdic, S., Douillard, J. Y., Reis-Filho, J. S., Dienstmann, R. and Andre, F. (2020). **Recommendations for the use of next-generation sequencing (NGS) for patients with metastatic cancers: a report from the ESMO Precision Medicine Working Group**. Ann Oncol *31 (11)*, 1491-1505, doi: 10.1016/j.annonc.2020.07.014.

Muckenhuber, A., Berger, A. K., Schlitter, A. M., Steiger, K., Konukiewitz, B., Trumpp, A., Eils, R., Werner, J., Friess, H., Esposito, I., Klöppel, G., Ceyhan, G. O., Jesinghaus, M., Denkert, C., Bahra, M., Stenzinger, A., Sprick, M. R., Jäger, D., Springfeld, C. and Weichert, W. (2018). **Pancreatic Ductal Adenocarcinoma Subtyping Using the Biomarkers Hepatocyte Nuclear Factor-1A and Cytokeratin-81 Correlates with Outcome and Treatment Response**. Clinical Cancer Research *24 (2)*, 351-359, doi: 10.1158/1078-0432.CCR-17-2180.

Neoptolemos, J. P., Dunn, J. A., Stocken, D. D., Almond, J., Link, K., Beger, H., Bassi, C., Falconi, M., Pederzoli, P., Dervenis, C., Fernandez-Cruz, L., Lacaine, F., Pap, A., Spooner, D., Kerr, D. J., Friess, H. and Büchler, M. W. (2001). **Adjuvant chemoradiotherapy and chemotherapy in resectable pancreatic cancer: a randomised controlled trial**. The Lancet *358 (9293)*, 1576-1585, doi: 10.1016/s0140-6736(01)06651-x.

Neoptolemos, J. P., Kleeff, J., Michl, P., Costello, E., Greenhalf, W. and Palmer, D. H. (2018). **Therapeutic developments in pancreatic cancer: current and future perspectives**. Nature Reviews. Gastroenterology & Hepatology *15 (6)*, 333-348, doi: 10.1038/s41575-018-0005-x.

Neoptolemos, J. P., Palmer, D. H., Ghaneh, P., Psarelli, E. E., Valle, J. W., Halloran, C. M., Faluyi, O., O'Reilly, D. A., Cunningham, D., Wadsley, J., Darby, S., Meyer, T., Gillmore, R., Anthoney, A., Lind, P., Glimelius, B., Falk, S., Izbicki, J. R., Middleton, G. W., Cummins, S., Ross, P. J., Wasan, H., McDonald, A., Crosby, T., Ma, Y. T., Patel, K., Sherriff, D., Soomal, R., Borg, D., Sothi, S., Hammel, P., Hackert, T., Jackson, R., Büchler, M. W. and European Study Group for Pancreatic, C. (2017). **Comparison of adjuvant gemcitabine and capecitabine with gemcitabine monotherapy in patients with resected pancreatic cancer (ESPAC-4): a multicentre, open-label, randomised, phase 3 trial**. Lancet (London, England) *389 (10073)*, 1011-1024, doi: 10.1016/S0140-6736(16)32409-6.

Neoptolemos, J. P., Stocken, D. D., Friess, H., Bassi, C., Dunn, J. A., Hickey, H., Beger, H., Fernandez-Cruz, L., Dervenis, C., Lacaine, F., Falconi, M., Pederzoli, P., Pap, A., Spooner, D., Kerr, D. J., Büchler, M. W. and European Study Group for Pancreatic, C. (2004). **A randomized trial of chemoradiotherapy and chemotherapy after resection of pancreatic cancer**. The New England Journal of Medicine *350 (12)*, 1200-1210, doi: 10.1056/NEJMoa032295.

Neoptolemos, J. P., Stocken, D. D., Bassi, C., Ghaneh, P., Cunningham, D., Goldstein, D., Padbury, R., Moore, M. J., Gallinger, S., Mariette, C., Wente, M. N., Izbicki, J. R., Friess, H., Lerch, M. M., Dervenis, C., Oláh, A., Butturini, G., Doi, R., Lind, P. A., Smith, D., European Study Group for Pancreatic Cancer. (2010). **Adjuvant chemotherapy with fluorouracil plus folinic acid vs gemcitabine following pancreatic cancer resection: a randomized controlled trial**. JAMA *(304(10))*, 1073-1081, doi: 10.1001/jama.2010.1275.

Noll, E. M., Eisen, C., Stenzinger, A., Espinet, E., Muckenhuber, A., Klein, C., Vogel, V., Klaus, B., Nadler, W., Rösli, C., Lutz, C., Kulke, M., Engelhardt, J., Zickgraf, F. M., Espinosa, O., Schlesner, M., Jiang, X., Kopp-Schneider, A., Neuhaus, P., Bahra, M., Sinn, B. V., Eils, R., Giese, N. A., Hackert, T., Strobel, O., Werner, J., Büchler, M. W., Weichert, W., Trumpp, A. and Sprick, M. R. (2016). **CYP3A5 mediates basal and acquired therapy resistance in different subtypes of pancreatic ductal adenocarcinoma**. Nature Medicine *22 (3)*, 278-287, doi: 10.1038/nm.4038.

Nones, K., Waddell, N., Song, S., Patch, A. M., Miller, D., Johns, A., Wu, J., Kassahn, K. S., Wood, D., Bailey, P., Fink, L., Manning, S., Christ, A. N., Nourse, C., Kazakoff, S., Taylor, D., Leonard,

C., Chang, D. K., Jones, M. D., Thomas, M., Watson, C., Pinese, M., Cowley, M., Rooman, I., Pajic, M., Apgi, Butturini, G., Malpaga, A., Corbo, V., Crippa, S., Falconi, M., Zamboni, G., Castelli, P., Lawlor, R. T., Gill, A. J., Scarpa, A., Pearson, J. V., Biankin, A. V. and Grimmond, S. M. (2014). **Genome-wide DNA methylation patterns in pancreatic ductal adenocarcinoma reveal epigenetic deregulation of SLIT-ROBO, ITGA2 and MET signaling**. Int J Cancer *135 (5)*, 1110-1118, doi: 10.1002/ijc.28765.

O'Kane, G. M., Grünwald, B. T., Jang, G.-H., Masoomian, M., Picardo, S., Grant, R. C., Denroche, R. E., Zhang, A., Wang, Y., Lam, B., Krzyzanowski, P. M., Lungu, I. M., Bartlett, J. M. S., Peralta, M., Vyas, F., Khokha, R., Biagi, J., Chadwick, D., Ramotar, S., Hutchinson, S., Dodd, A., Wilson, J. M., Notta, F., Zogopoulos, G., Gallinger, S., Knox, J. J. and Fischer, S. E. (2020). **GATA6 Expression Distinguishes Classical and Basal-like Subtypes in Advanced Pancreatic Cancer**. Clinical Cancer Research *26 (18)*, 4901-4910, doi: 10.1158/1078-0432.CCR-19-3724.

Oguri, T., Achiwa, H., Muramatsu, H., Ozasa, H., Sato, S., Shimizu, S., Yamazaki, H., Eimoto, T. and Ueda, R. (2007). **The absence of human equilibrative nucleoside transporter 1 expression predicts nonresponse to gemcitabine-containing chemotherapy in non-small cell lung cancer**. Cancer Letters *256 (1)*, 112-119, doi: 10.1016/j.canlet.2007.06.012.

Párrizas, M., Maestro, M. A., Boj, S. F., Paniagua, A., Casamitjana, R., Gomis, R., Rivera, F. and Ferrer, J. (2001). **Hepatic nuclear factor 1-alpha directs nucleosomal hyperacetylation to its tissue-specific transcriptional targets**. Molecular and Cellular Biology *21 (9)*, 3234-3243, doi: 10.1128/MCB.21.9.3234-3243.2001.

Pastor-Anglada, M. and Pérez-Torras, S. (2018). **Emerging Roles of Nucleoside Transporters**. Frontiers in Pharmacology *9*, 606, doi: 10.3389/fphar.2018.00606.

Pierce, B. L. and Ahsan, H. (2011). **Genome-wide "Pleiotropy Scan" Identifies HNF1A Region as a Novel Pancreatic Cancer Susceptibility Locus**. Cancer research *71 (13)*, 4352-4358, doi: 10.1158/0008-5472.CAN-11-0124.

Pietryga, J. A. and Morgan, D. E. (2015). **Imaging preoperatively for pancreatic adenocarcinoma**. Journal of Gastrointestinal Oncology *6 (4)*, 343-357, doi: 10.3978/j.issn.2078-6891.2015.024.

Prejzner, W. (2002). **Relationship of the BCR gene breakpoint and the type of BCR/ABL transcript to clinical course, prognostic indexes and survival in patients with chronic myeloid leukemia**. Medical Science Monitor: International Medical Journal of Experimental and Clinical Research *8 (5)*, BR193-197.

Puleo, F., Nicolle, R., Blum, Y., Cros, J., Marisa, L., Demetter, P., Quertinmont, E., Svrcek, M., Elarouci, N., Iovanna, J., Franchimont, D., Verset, L., Galdon, M. G., Deviere, J., de Reynies, A., Laurent-Puig, P., Van Laethem, J. L., Bachet, J. B. and Marechal, R. (2018). **Stratification**

of Pancreatic Ductal Adenocarcinomas Based on Tumour and Microenvironment Features. Gastroenterology *155 (6)*, 1999-2013 e1993, doi: 10.1053/j.gastro.2018.08.033.

Rahib, L., Smith, B. D., Aizenberg, R., Rosenzweig, A. B., Fleshman, J. M. and Matrisian, L. M. (2014). **Projecting cancer incidence and deaths to 2030: the unexpected burden of thyroid, liver, and pancreas cancers in the United States**. Cancer Research *74 (11)*, 2913-2921, doi: 10.1158/0008-5472.CAN-14-0155.

Rawla, P., Sunkara, T. and Gaduputi, V. (2019). **Epidemiology of Pancreatic Cancer: Global Trends, Etiology and Risk Factors**. World Journal of Oncology *10 (1)*, 10-27, doi: 10.14740/wjon1166.

Risch, H. A., Lu, L., Wang, J., Zhang, W., Ni, Q., Gao, Y.-T. and Yu, H. (2013). **ABO Blood Group and Risk of Pancreatic Cancer: A Study in Shanghai and Meta-Analysis**. American Journal of Epidemiology *177 (12)*, 1326-1337, doi: 10.1093/aje/kws458.

Rizzato, C., Campa, D., Pezzilli, R., Soucek, P., Greenhalf, W., Capurso, G., Talar-Wojnarowska, R., Heller, A., Jamroziak, K., Khaw, K.-T., Key, T. J., Bambi, F., Landi, S., Mohelnikova-Duchonova, B., Vodickova, L., Büchler, M. W., Bugert, P., Vodicka, P., Neoptolemos, J. P., Werner, J., Hoheisel, J. D., Bauer, A. S., Giese, N. and Canzian, F. (2013). **ABO blood groups and pancreatic cancer risk and survival: Results from the PANcreatic Disease ReseArch (PANDoRA) consortium**. Oncology Reports *29 (4)*, 1637-1644, doi: 10.3892/or.2013.2285.

Roa-Pena, L., Leiton, C. V., Babu, S., Pan, C. H., Vanner, E. A., Akalin, A., Bandovic, J., Moffitt, R. A., Shroyer, K. R. and Escobar-Hoyos, L. F. (2019). **Keratin 17 identifies the most lethal molecular subtype of pancreatic cancer**. Sci Rep *9 (1)*, 11239, doi: 10.1038/s41598-019-47519-4.

Russo, S., Ammori, J., Eads, J. and Dorth, J. (2016). **The role of neoadjuvant therapy in pancreatic cancer: a review**. Future Oncology *12 (5)*, 669-685, doi: 10.2217/fon.15.335.

Scott, A. J. and Wilkinson, J. C. (2016). **HNF1A, KRT81, and CYP3A5: three more straws on the back of pancreatic cancer?** Translational cancer research *5 (Suppl 2)*, S253-S256, doi: 10.21037/tcr.2016.08.12.

Shen, S., Vagner, S. and Robert, C. (2020). **Persistent Cancer Cells: The Deadly Survivors**. Cell *183 (4)*, 860-874, doi: 10.1016/j.cell.2020.10.027.

Shore, S., Raraty, M. G. T., Ghaneh, P. and Neoptolemos, J. P. (2003). **Review article: chemotherapy for pancreatic cancer**. Alimentary Pharmacology & Therapeutics *18 (11-12)*, 1049-1069, doi: 10.1111/j.1365-2036.2003.01781.x.

Siegel, R. L., Miller, K. D., Fuchs, H. E. and Jemal, A. (2021). **Cancer Statistics, 2021**. CA Cancer J

Clin *71 (1)*, 7-33, doi: 10.3322/caac.21654.

Skiles, J. L., Chiang, C., Li, C. H., Martin, S., Smith, E. L., Olbara, G., Jones, D. R., Vik, T. A., Mostert, S., Abbink, F., Kaspers, G. J., Li, L., Njuguna, F., Sajdyk, T. J. and Renbarger, J. L. (2018). **CYP3A5 genotype and its impact on vincristine pharmacokinetics and development of neuropathy in Kenyan children with cancer**. Pediatric blood & cancer *65 (3)*, doi: 10.1002/pbc.26854.

Sohal DPS, M. D., Syed A. Ahmad, Namita S. Gandhi, M. Shaalan Beg, Andrea Wang-Gillam, James L. Wade, E. Gabriela Chiorean, Katherine A. Guthrie, Andrew M. Lowy, Philip A. Philip, and Howard S. Hochster. (2021). **Efficacy of Perioperative Chemotherapy for Resectable Pancreatic Adenocarcinoma: A Phase 2 Randomized Clinical Trial.** JAMA Oncol. *7(3)*, 421-427, doi: 10.1001/jamaoncol.2020.7328.

Springfeld, C., Jäger, D., Büchler, M. W., Strobel, O., Hackert, T., Palmer, D. H. and Neoptolemos, J. P. (2019). **Chemotherapy for pancreatic cancer**. La Presse Médicale *48 (3)*, e159-e174, doi: 10.1016/j.lpm.2019.02.025.

Springfeld, C. and Neoptolemos, J. P. (2022). **The role of neoadjuvant therapy for resectable pancreatic cancer remains uncertain**. Nat Rev Clin Oncol, doi: 10.1038/s41571-022-00612-6.

Sultana, A., Tudur Smith, C., Cunningham, D., Starling, N., Neoptolemos, J. P. and Ghaneh, P. (2008). **Meta-analyses of chemotherapy for locally advanced and metastatic pancreatic cancer: results of secondary end points analyses**. British Journal of Cancer *99 (1)*, 6-13, doi: 10.1038/sj.bjc.6604436.

Sundaram, M., Yao, S. Y. M., Ingram, J. C., Berry, Z. A., Abidi, F., Cass, C. E., Baldwin, S. A. and Young, J. D. (2001). **Topology of a Human Equilibrative, Nitrobenzylthioinosine (NBMPR)-sensitive Nucleoside Transporter (hENT1) Implicated in the Cellular Uptake of Adenosine and Anti-cancer Drugs**. Journal of Biological Chemistry *276 (48)*, 45270-45275, doi: 10.1074/jbc.M107169200.

Suzuki, E., Evans, T., Lowry, J., Truong, L., Bell, D. W., Testa, J. R. and Walsh, K. (1996). **The Human GATA-6 Gene: Structure, Chromosomal Location, and Regulation of Expression by Tissue-Specific and Mitogen-Responsive Signals**. Genomics *38 (3)*, 283-290, doi: 10.1006/geno.1996.0630.

Takaori, K., Bassi, C., Biankin, A., Brunner, T. B., Cataldo, I., Campbell, F., Cunningham, D., Falconi, M., Frampton, A. E., Furuse, J., Giovannini, M., Jackson, R., Nakamura, A., Nealon, W., Neoptolemos, J. P., Real, F. X., Scarpa, A., Sclafani, F., Windsor, J. A., Yamaguchi, K., Wolfgang, C. and Johnson, C. D. (2016). **International Association of Pancreatology (IAP)/European Pancreatic Club (EPC) consensus review of guidelines for the treatment of pancreatic cancer**. Pancreatology *16 (1)*, 14-27, doi:

10.1016/j.pan.2015.10.013.

Tempero, M. A., Malafa, M. P., Al-Hawary, M., Asbun, H., Bain, A., Behrman, S. W., Benson, A. B., Binder, E., Cardin, D. B., Cha, C., Chiorean, E. G., Chung, V., Czito, B., Dillhoff, M., Dotan, E., Ferrone, C. R., Hardacre, J., Hawkins, W. G., Herman, J., Ko, A. H., Komanduri, S., Koong, A., LoConte, N., Lowy, A. M., Moravek, C., Nakakura, E. K., O'Reilly, E. M., Obando, J., Reddy, S., Scaife, C., Thayer, S., Weekes, C. D., Wolff, R. A., Wolpin, B. M., Burns, J. and Darlow, S. (2017). **Pancreatic Adenocarcinoma, Version 2.2017, NCCN Clinical Practice Guidelines in Oncology**. Journal of the National Comprehensive Cancer Network *15 (8)*, 1028-1061, doi: 10.6004/jnccn.2017.0131.

Thompson, P. A., Seyedi, F., Lang, N. P., MacLeod, S. L., Wogan, G. N., Anderson, K. E., Tang, Y. M., Coles, B. and Kadlubar, F. F. (1999). **Comparison of DNA adduct levels associated with exogenous and endogenous exposures in human pancreas in relation to metabolic genotype**. Mutation Research/Fundamental and Molecular Mechanisms of Mutagenesis *424 (1)*, 263-274, doi: 10.1016/S0027-5107(99)00024-X.

Tian, F., Li, D., Chen, J., Liu, W., Cai, L., Li, J., Jiang, P., Liu, Z., Zhao, X., Guo, F., Li, X. and Wang, S. (2013). **Aberrant expression of GATA binding protein 6 correlates with poor prognosis and promotes metastasis in cholangiocarcinoma**. European Journal of Cancer (Oxford, England: 1990) *49 (7)*, 1771-1780, doi: 10.1016/j.ejca.2012.12.015.

Tiriac, H., Belleau, P., Engle, D. D., Plenker, D., Deschênes, A., Somerville, T. D. D., Froeling, F. E. M., Burkhart, R. A., Denroche, R. E., Jang, G.-H., Miyabayashi, K., Young, C. M., Patel, H., Ma, M., LaComb, J. F., Palmaira, R. L. D., Javed, A. A., Huynh, J. C., Johnson, M., Arora, K., Robine, N., Shah, M., Sanghvi, R., Goetz, A. B., Lowder, C. Y., Martello, L., Driehuis, E., LeComte, N., Askan, G., Iacobuzio-Donahue, C. A., Clevers, H., Wood, L. D., Hruban, R. H., Thompson, E., Aguirre, A. J., Wolpin, B. M., Sasson, A., Kim, J., Wu, M., Bucobo, J. C., Allen, P., Sejpal, D. V., Nealon, W., Sullivan, J. D., Winter, J. M., Gimotty, P. A., Grem, J. L., DiMaio, D. J., Buscaglia, J. M., Grandgenett, P. M., Brody, J. R., Hollingsworth, M. A., O'Kane, G. M., Notta, F., Kim, E., Crawford, J. M., Devoe, C., Ocean, A., Wolfgang, C. L., Yu, K. H., Li, E., Vakoc, C. R., Hubert, B., Fischer, S. E., Wilson, J. M., Moffitt, R., Knox, J., Krasnitz, A., Gallinger, S. and Tuveson, D. A. (2018). **Organoid Profiling Identifies Common Responders to Chemotherapy in Pancreatic Cancer**. Cancer Discovery *8 (9)*, 1112-1129, doi: 10.1158/2159-8290.CD-18-0349.

Towles, J. K., Clark, R. N., Wahlin, M. D., Uttamsingh, V., Rettie, A. E. and Jackson, K. D. (2016). **Cytochrome P450 3A4 and CYP3A5-Catalyzed Bioactivation of Lapatinib**. Drug Metabolism and Disposition *44 (10)*, 1584-1597, doi: 10.1124/dmd.116.070839.

Tramacere, I., Scotti, L., Jenab, M., Bagnardi, V., Bellocco, R., Rota, M., Corrao, G., Bravi, F., Boffetta, P. and La Vecchia, C. (2010). **Alcohol drinking and pancreatic cancer risk: a meta-analysis of the dose-risk relation**. International Journal of Cancer *126 (6)*, 1474-1486, doi: 10.1002/ijc.24936.

Tsukihara, H., Tsunekuni, K. and Takechi, T. (2016). **Folic Acid-Metabolizing Enzymes Regulate the Antitumour Effect of 5-Fluoro-2'-Deoxyuridine in Colorectal Cancer Cell Lines**. PLoS One *11 (9)*, e0163961, doi: 10.1371/journal.pone.0163961.

Versteijne, E., Suker, M., Groothuis, K., Akkermans-Vogelaar, J. M., Besselink, M. G., Bonsing, B. A., Buijsen, J., Busch, O. R., Creemers, G. M., van Dam, R. M., Eskens, F., Festen, S., de Groot, J. W. B., Groot Koerkamp, B., de Hingh, I. H., Homs, M. Y. V., van Hooft, J. E., Kerver, E. D., Luelmo, S. A. C., Neelis, K. J., Nuyttens, J., Paardekooper, G., Patijn, G. A., van der Sangen, M. J. C., de Vos-Geelen, J., Wilmink, J. W., Zwinderman, A. H., Punt, C. J., van Eijck, C. H., van Tienhoven, G. and Dutch Pancreatic Cancer, G. (2020). **Preoperative Chemoradiotherapy Versus Immediate Surgery for Resectable and Borderline Resectable Pancreatic Cancer: Results of the Dutch Randomized Phase III PREOPANC Trial**. J Clin Oncol *38 (16)*, 1763-1773, doi: 10.1200/JCO.19.02274.

Von Hoff, D. D., Ervin, T., Arena, F. P., Chiorean, E. G., Infante, J., Moore, M., Seay, T., Tjulandin, S. A., Ma, W. W., Saleh, M. N., Harris, M., Reni, M., Dowden, S., Laheru, D., Bahary, N., Ramanathan, R. K., Tabernero, J., Hidalgo, M., Goldstein, D., Van Cutsem, E., Wei, X., Iglesias, J. and Renschler, M. F. (2013). **Increased Survival in Pancreatic Cancer with nab-Paclitaxel plus Gemcitabine**. The New England journal of medicine *369 (18)*, 1691-1703, doi: 10.1056/NEJMoa1304369.

Waddell, N., Pajic, M., Patch, A. M., Chang, D. K., Kassahn, K. S., Bailey, P., Johns, A. L., Miller, D., Nones, K., Quek, K., Quinn, M. C., Robertson, A. J., Fadlullah, M. Z., Bruxner, T. J., Christ, A. N., Harliwong, I., Idrisoglu, S., Manning, S., Nourse, C., Nourbakhsh, E., Wani, S., Wilson, P. J., Markham, E., Cloonan, N., Anderson, M. J., Fink, J. L., Holmes, O., Kazakoff, S. H., Leonard, C., Newell, F., Poudel, B., Song, S., Taylor, D., Waddell, N., Wood, S., Xu, Q., Wu, J., Pinese, M., Cowley, M. J., Lee, H. C., Jones, M. D., Nagrial, A. M., Humphris, J., Chantrill, L. A., Chin, V., Steinmann, A. M., Mawson, A., Humphrey, E. S., Colvin, E. K., Chou, A., Scarlett, C. J., Pinho, A. V., Giry-Laterriere, M., Rooman, I., Samra, J. S., Kench, J. G., Pettitt, J. A., Merrett, N. D., Toon, C., Epari, K., Nguyen, N. Q., Barbour, A., Zeps, N., Jamieson, N. B., Graham, J. S., Niclou, S. P., Bjerkvig, R., Grutzmann, R., Aust, D., Hruban, R. H., Maitra, A., Iacobuzio-Donahue, C. A., Wolfgang, C. L., Morgan, R. A., Lawlor, R. T., Corbo, V., Bassi, C., Falconi, M., Zamboni, G., Tortora, G., Tempero, M. A., Australian Pancreatic Cancer Genome, I., Gill, A. J., Eshleman, J. R., Pilarsky, C., Scarpa, A., Musgrove, E. A., Pearson, J. V., Biankin, A. V. and Grimmond, S. M. (2015). **Whole genomes redefine the mutational landscape of pancreatic cancer**. Nature *518 (7540)*, 495-501, doi: 10.1038/nature14169.

Walker, E. M., Thompson, C. A., Kohlnhofer, B. M., Faber, M. L. and Battle, M. A. (2014). **Characterization of the developing small intestine in the absence of either GATA4 or GATA6**. BMC Research Notes *7*, doi: 10.1186/1756-0500-7-902.

Waring, R. H. (2020). **Cytochrome P450: genotype to phenotype**. Xenobiotica *50 (1)*, 9-18, doi: 10.1080/00498254.2019.1648911.

Wong, M. C. S., Jiang, J. Y., Liang, M., Fang, Y., Yeung, M. S. and Sung, J. J. Y. (2017). **Global temporal patterns of pancreatic cancer and association with socioeconomic development**. Sci Rep *7 (1)*, 3165, doi: 10.1038/s41598-017-02997-2.

Wrighton, S. A., Brian, W. R., Sari, M. A., Iwasaki, M., Guengerich, F. P., Raucy, J. L., Molowa, D. T. and Vandenbranden, M. (1990). **Studies on the expression and metabolic capabilities of human liver cytochrome P450IIIA5 (HLp3)**. Molecular Pharmacology *38 (2)*, 207-213.

Xu, Y.-J., Di, R.-M., Qiao, Q., Li, X.-M., Huang, R.-T., Xue, S., Liu, X.-Y., Wang, J. and Yang, Y.-Q. (2018). **GATA6 loss-of-function mutation contributes to congenital bicuspid aortic valve**. Gene *663*, 115-120, doi: 10.1016/j.gene.2018.04.018.

Yadav, D. and Lowenfels, A. B. (2013). **The Epidemiology of Pancreatitis and Pancreatic Cancer**. Gastroenterology *144 (6)*, 1252-1261, doi: 10.1053/j.gastro.2013.01.068.

Yamagata, K. (2014). **Chapter Sixteen - Roles of HNF1α and HNF4α in Pancreatic β-Cells: Lessons from a Monogenic Form of Diabetes (MODY)**. In: Vitamins & Hormones, ed. Litwack, G., Academic Press, pp. 407-423.

Yamagata, K., Oda, N., Kaisaki, P. J., Menzel, S., Furuta, H., Vaxillaire, M., Southam, L., Cox, R. D., Lathrop, G. M., Boriraj, V. V., Chen, X., Cox, N. J., Oda, Y., Yano, H., Le Beau, M. M., Yamada, S., Nishigori, H., Takeda, J., Fajans, S. S., Hattersley, A. T., Iwasaki, N., Hansen, T., Pedersen, O., Polonsky, K. S. and Bell, G. I. (1996). **Mutations in the hepatocyte nuclear factor-1alpha gene in maturity-onset diabetes of the young (MODY3)**. Nature *384 (6608)*, 455-458, doi: 10.1038/384455a0.

Yamagata, K., Yang, Q., Yamamoto, K., Iwahashi, H., Miyagawa, J., Okita, K., Yoshiuchi, I., Miyazaki, J., Noguchi, T., Nakajima, H., Namba, M., Hanafusa, T. and Matsuzawa, Y. (1998). **Mutation P291fsinsC in the transcription factor hepatocyte nuclear factor-1alpha is dominant negative**. Diabetes *47 (8)*, 1231-1235, doi: 10.2337/diab.47.8.1231.

Yao, S. Y. M., Ng, A. M. L., Cass, C. E., Baldwin, S. A. and Young, J. D. (2011). **Nucleobase Transport by Human Equilibrative Nucleoside Transporter 1 (hENT1)**. Journal of Biological Chemistry *286 (37)*, 32552-32562, doi: 10.1074/jbc.M111.236117.

Yoshifumi Sato, M. M. R., Masaki Haneda, Tomonori Tsuyama, Tomoya Mizumoto, Tatsuya Yoshizawa, Tadahiro Kitamura, Frank J Gonzalez, Ken-Ichi Yamamura, Kazuya Yamagata (2020). **HNF1α controls glucagon secretion in pancreatic α-cells through modulation of SGLT1**. Biochim Biophys Acta Mol Basis Dis *1866(11)*, 165898, doi: 10.1016/j.bbadis.2020.165898.

Yu, Y., Liang, S., Zhou, Y., Li, S., Li, Y. and Liao, W. (2019). **HNF1A/CASC2 regulates pancreatic cancer cell proliferation through PTEN/Akt signaling**. Journal of Cellular Biochemistry

120 (3), 2816-2827, doi: 10.1002/jcb.26395.

Zhang, Y. P., Zuo, X. C., Huang, Z. J., Cai, J. J., Wen, J., Duan, D. D. and Yuan, H. (2014). **CYP3A5 polymorphism, amlodipine and hypertension**. Journal of Human Hypertension *28 (3)*, 145-149, doi: 10.1038/jhh.2013.67.

Zhao, R., Watt, A. J., Battle, M. A., Li, J., Bondow, B. J. and Duncan, S. A. (2008). **Loss of both GATA4 and GATA6 blocks cardiac myocyte differentiation and results in acardia in mice**. Developmental biology *317 (2)*, 614-619, doi: 10.1016/j.ydbio.2008.03.013.

Zhao, R., Watt, A. J., Li, J., Luebke-Wheeler, J., Morrisey, E. E. and Duncan, S. A. (2005). **GATA6 Is Essential for Embryonic Development of the Liver but Dispensable for Early Heart Formation**. Molecular and Cellular Biology *25 (7)*, 2622-2631, doi: 10.1128/MCB.25.7.2622-2631.2005.

Zheng, G.-F., Wei, D., Zhao, H., Zhou, N., Yang, Y.-Q. and Liu, X.-Y. (2012). **A novel GATA6 mutation associated with congenital ventricular septal defect**. International Journal of Molecular Medicine *29 (6)*, 1065-1071, doi: 10.3892/ijmm.2012.930.

Supplementary Material

Supplementary Table 1. Cell count of GATA6 by immunofluorescence (IF).

GATA6	Adjuvant therapy (n=79)								Neoadjuvant therapy (n=72)								Normal pancreas (n=9)
	GEM (n=59)	%	FFX (n=9)	%	COMB (n=7)	%	NA (n=4)	%	GEM (n=29)	%	FFX (n=32)	%	COMB (n=3)	%	NA (n=8)	%	
Total cells	12309043	76	2024437	12	1169435	7	747286	5	3851711	45	2807216	33	270710	3	1668544	19	2514501
$CK19^+$ cells	2832467	73	582221	15	281806	7	188263	5	1252400	48	643344	25	91638	4	595423	23	343129
GATA6 $nuclear^+$ cells	3083998	73	578789	14	333998	8	231746	5	2072963	46	1334843	30	128105	3	983630	22	1797400
GATA6 $nuclear^+$ in CK19 cells	1657413	70	370412	16	194549	8	134867	6	1167382	50	571116	24	58423	3	538664	23	325019
GATA6 $cytosol^+$ cells	4625648	71	1066489	16	487605	8	302265	5	2568444	46	1696270	30	184381	3	1179156	21	1828865
GATA6 $cytosol^+$ in $CK19^+$ cells	2306431	70	542766	17	251291	8	175786	5	1316888	51	648348	25	39451	2	586759	23	340636
$GATA6^+$ cells	6131947	73	1243913	15	617339	7	392633	5	2958023	46	1999660	31	206479	3	1305395	20	2366148
$GATA6^+$ in $CK19^+$ cells	2455800	71	561138	16	268614	8	182169	5	1285994	49	645313	25	85284	3	591063	23	342988

Supplementary Table 2. Cell count of CYP3A5 by immunofluorescence (IF).

CYP3A5	Adjuvant therapy (n=79)								Neoadjuvant therapy (n=72)								Normal pancreas (n=9)
	GEM (n=59)	%	FFX (n=9)	%	COMB (n=7)	%	NA (n=4)	%	GEM (n=29)	%	FFX (n=32)	%	COMB (n=3)	%	NA (n=8)	%	
Total cells	8655636	76	1205372	11	913967	8	575928	5	4114300	47	3238216	37	101644	1	1255844	14	589033
$CK19^+$ cells	1185655	84	82369	6	75817	5	70769	5	147194	38	157609	41	6324	2	74568	19	886
$CYP3A5^+$ cells	339919	97	1369	0.4	10304	3	390	0.1	123316	52	103902	44	673	0.3	9423	4	23
$CYP3A5^+$ in $CK19^+$ cells	188567	97	747	0.4	4081	2	132	0.1	15441	37	23404	56	542	1	2335	6	0

Supplementary Table 3. Cell count of HNF1A by immunofluorescence (IF).

HNF1A	Adjuvant therapy (n=79)								Neoadjuvant therapy (n=72)								Normal pancreas (n=9)
	GEM (n=59)	%	FFX (n=9)	%	COMB (n=7)	%	NA (n=4)	%	GEM (n=29)	%	FFX (n=32)	%	COMB (n=3)	%	NA (n=8)	%	
Total cells	11811388	76	1778899	12	1109466	7	761200	5	4920811	41	4681743	40	315322	3	1966317	16	1831710
CK19$^+$ cells	3489880	77	589949	13	232143	5	212222	5	1335863	52	720743	29	46406	2	438808	17	251707
HNF1A nuclear$^+$ cells	828912	72	301795	26	11845	1	7077	0.6	552219	51	426224	39	36714	3	73201	7	32675
HNF1A nuclear$^+$ in CK19 cells	383421	68	173077	31	3668	1	5854	1	222690	50	171830	39	11445	3	35765	8	3924
HNF1A cytosol$^+$ cells	1900018	73	617754	24	72587	3	23825	1	1453132	49	1203944	41	75320	3	204105	7	195246
HNF1A cytosol$^+$ in CK19$^+$ cells	896553	73	284482	23	31647	3	13937	1	560743	55	360743	35	19932	2	79170	8	30416
HNF1A$^+$ cells	2399944	74	713108	22	108448	3	33928	1	1874410	49	1527879	41	106320	3	265958	7	299872
HNF1A$^+$ in CK19$^+$ cells	1111091	74	313612	21	50993	3	19194	1	720900	56	432695	34	26786	2	100784	8	45630

Supplementary Table 4. Cell count of KRT81 by immunofluorescence (IF).

KRT81	Adjuvant therapy (n=79)								Neoadjuvant therapy (n=72)								Normal pancreas (n=9)
	GEM (n=59)	%	FFX (n=9)	%	COMB (n=7)	%	NA (n=4)	%	GEM (n=29)	%	FFX (n=32)	%	COMB (n=3)	%	NA (n=8)	%	
Total cells	10207499	74	1535502	11	1205809	9	784336	6	5033356	44	4198321	36	292765	3	2030976	18	1867751
CK19$^+$ cells	3096781	76	494991	12	269959	7	201879	5	1340162	52	619285	24	45475	2	560609	22	135687
KRT81$^+$ cells	281746	69	81466	20	7609	2	40134	10	265766	67	99208	25	5901	1.5	24192	6	2355
KRT81$^+$ in CK19$^+$ cells	232627	69	60328	18	6031	2	38548	11	177982	73	43595	18	4196	2	17465	7	340

Supplementary Table 5. Cell count of hENT1 by immunofluorescence (IF).

hENT1	Adjuvant therapy (n=79)								Neoadjuvant therapy (n=72)								Normal pancreas (n=9)
	GEM (n=59)	%	FFX (n=9)	%	COMB (n=7)	%	NA (n=4)	%	GEM (n=29)	%	FFX (n=32)	%	COMB (n=3)	%	NA (n=8)	%	
Total cells	10932480	79	1270122	9	997592	7	628915	5	3302997	45	2446582	33	293835	4	1372724	19	1379592
CK19$^+$ cells	2820980	80	334912	9	217834	6	154328	4	1037428	49	540066	25	73786	3	486890	23	89880
hENT1$^+$ cells	870865	71	219605	18	112132	9	31167	3	444697	43	240928	23	25990	3	319528	31	28404
hENT1$^+$ in CK19$^+$ cells	493772	71	121642	17	58197	8	24815	4	340379	42	165183	20	20581	3	285502	35	1507

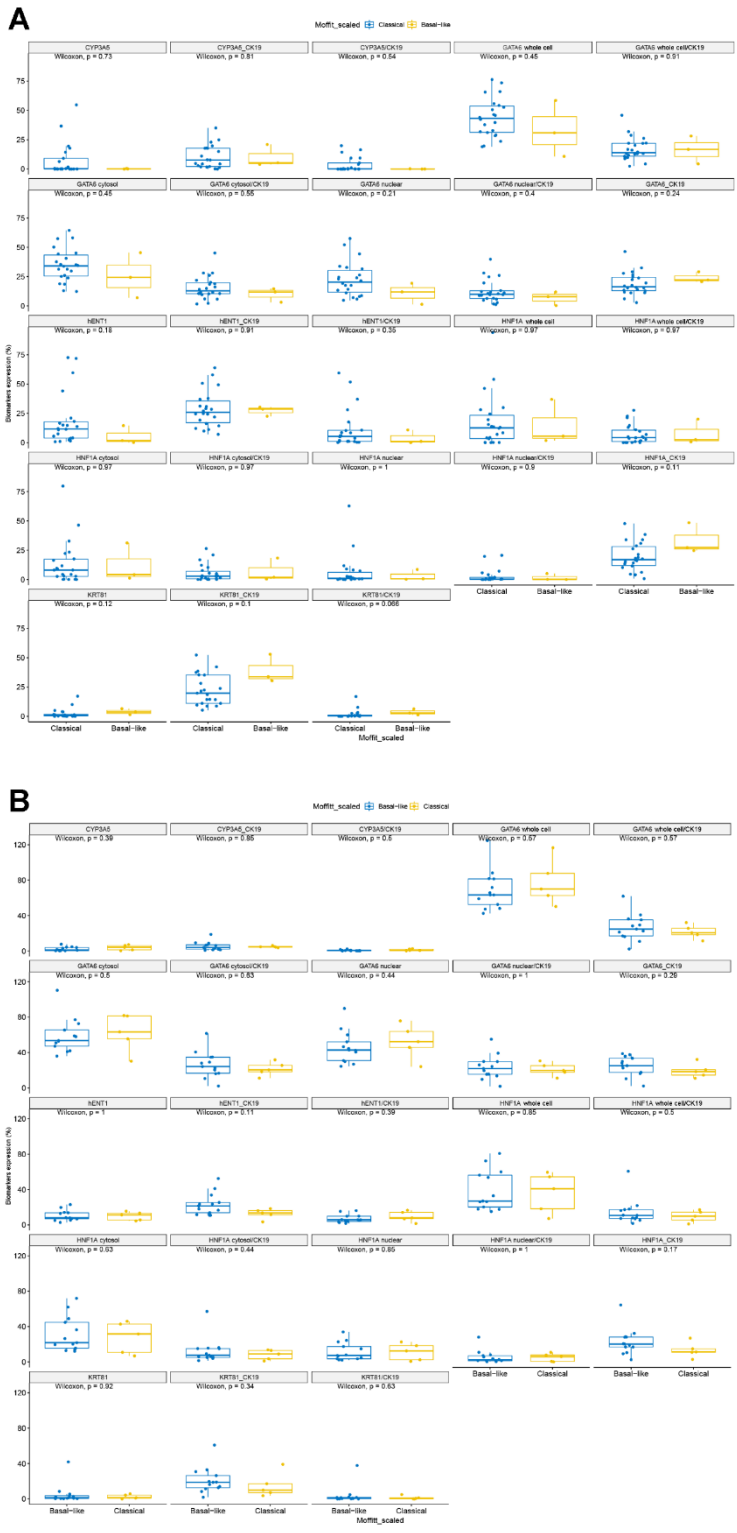

Supplementary Fig 1. Protein expression of the biomarkers according to Moffitt classification in chemo-naïve patients (**A**) and in post-treatment patients (**B**).

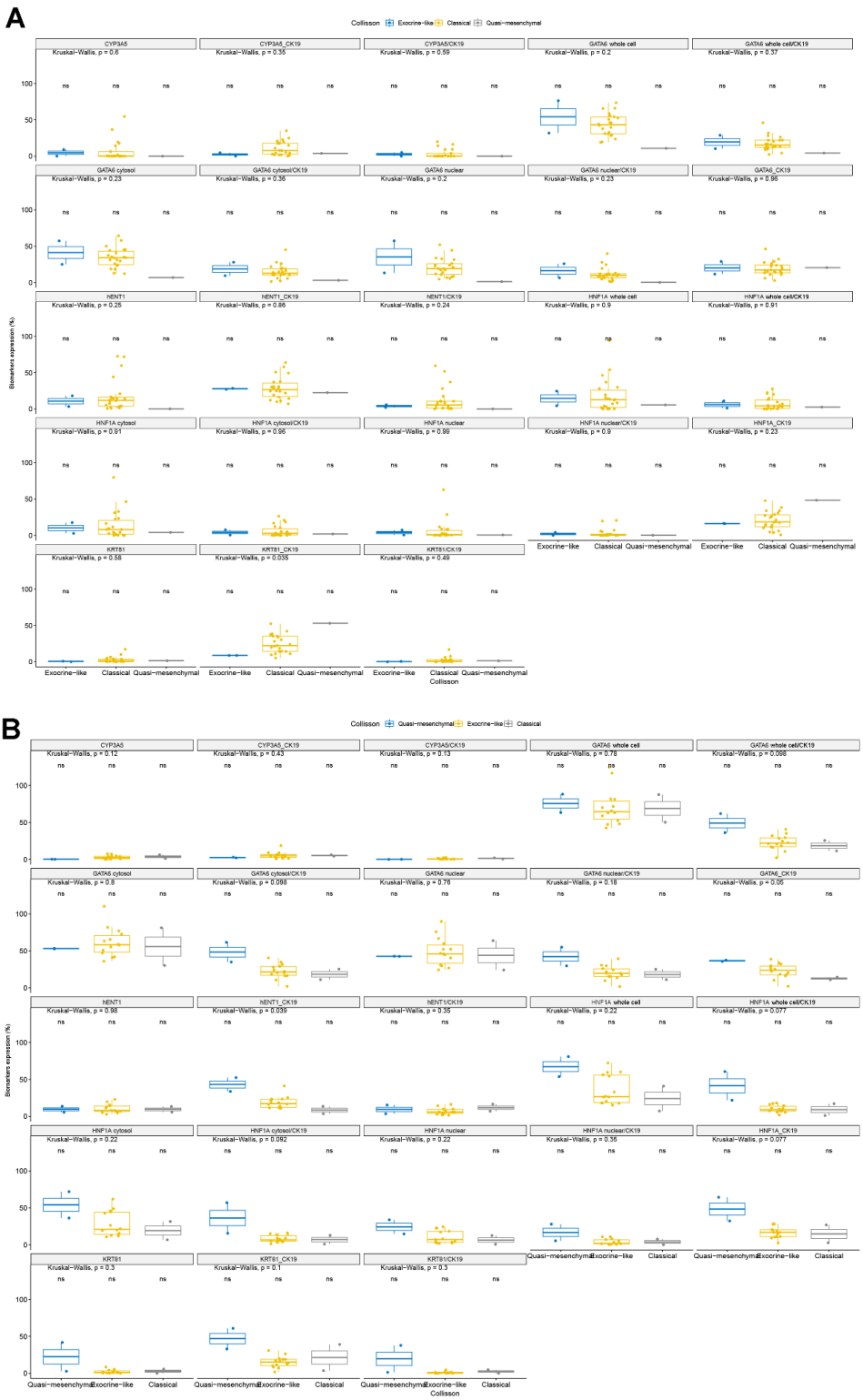

Supplementary Fig 2. Protein expression of the biomarkers according to Collisson classification in chemo-naïve patients (**A**) and in post-treatment patients (**B**).

Supplementary Fig 3. Protein expression of the biomarkers according to Notta classification in chemo-naïve patients (**A**) and in post-treatment patients (**B**).

Chemo-naive group

A

Survival proportions: Survival of Adj-HNF1A nuclear

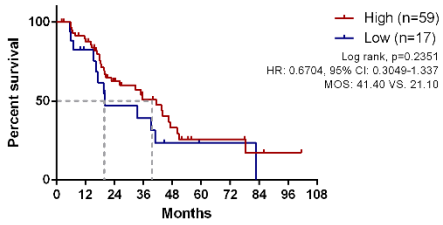

D

Survival proportions: Survival of Adj-HNF1A nuclear/CK19

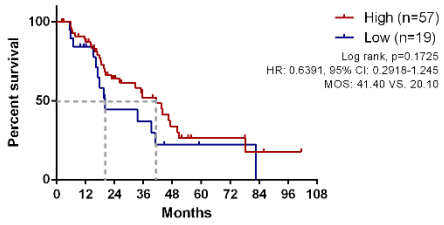

B

Survival proportions: Survival of Adj-HNF1A cytosol

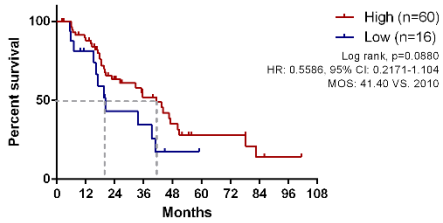

E

Survival proportions: Survival of Adj-HNF1A cytosol/CK19

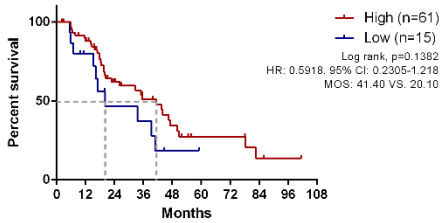

C

Survival proportions: Survival of Adj-HNF1A whole cell

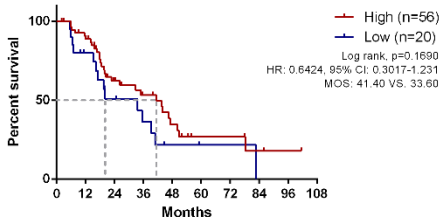

F

Survival proportions: Survival of Adj-HNF1A whole cell/CK19

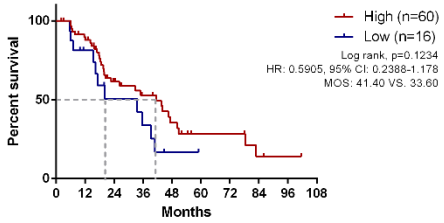

Post-chemotherapy group

G

Survival proportions: Survival of Neo-HNF1A nuclear

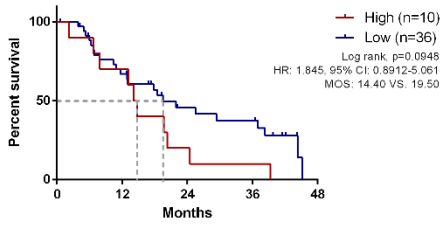

J

Survival proportions: Survival of Neo-HNF1A nuclear/CK19

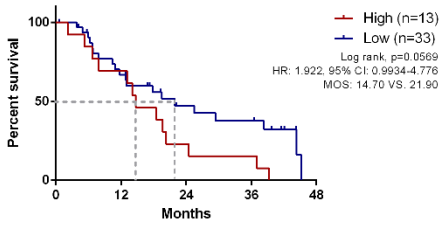

H

Survival proportions: Survival of Neo-HNF1A cytosol

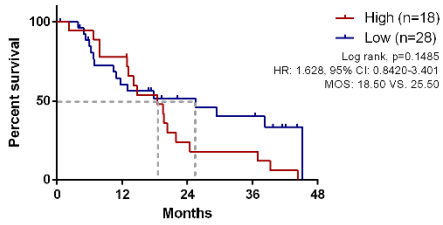

K

Survival proportions: Survival of Neo-HNF1A cytosol/CK19

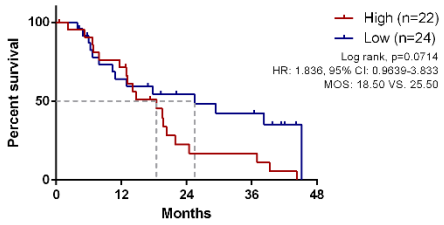

I

Survival proportions: Survival of Neo-HNF1A whole cell

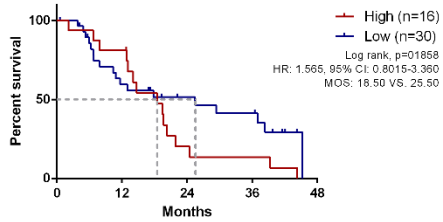

L

Survival proportions: Survival of Neo-HNF1A whole cell/CK19

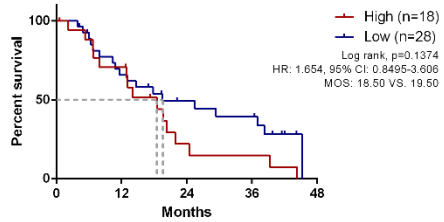

Supplementary Fig 4. (A-F) Kaplan-Meier curve showed the overall survival of chemo-naïve patients according to HNF1A nuclear, cytosol, whole cell expression (A-C) and HNF1A expression in CK19+ cells (D-F), respectively. (G-L) Overall survival of patients after neoadjuvant therapy according to HNF1A nuclear, cytosol, whole cell expression (G-I) and HNF1A expression in $CK19^{+}$ cells (J-L), respectively (Log-rank test, $p < 0.05$).

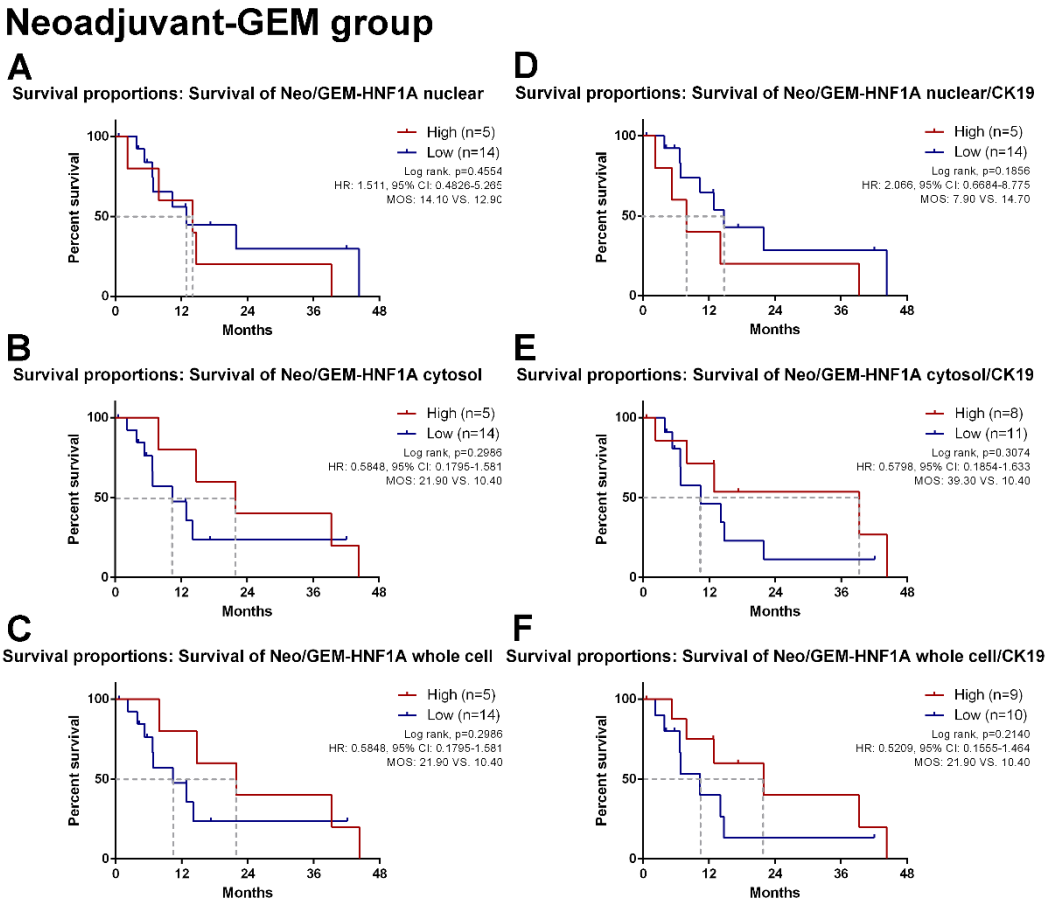

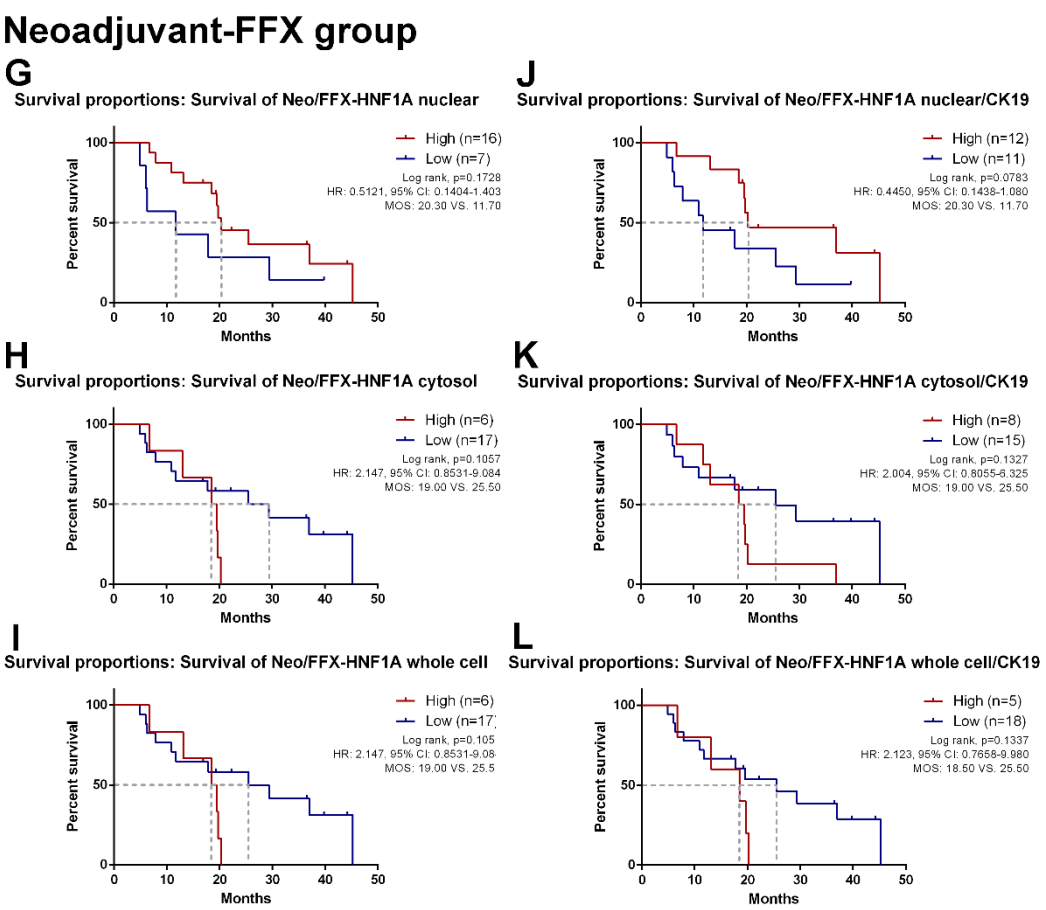

Supplementary Fig 5. (A-F) Kaplan-Meier curve showed the overall survival of patients with gemcitabine-based neoadjuvant treatment according to HNF1A nuclear, cytosol, whole cell expression (A-C) and HNF1A expression in $CK19^{+}$ cells (D-F), respectively. (G-L) Overall survival of patients with FFX neoadjuvant treatment according to HNF1A nuclear, cytosol, whole cell expression (G-I) and HNF1A expression in $CK19^{+}$ cells (J-L), respectively (Log-rank test, $p < 0.05$).

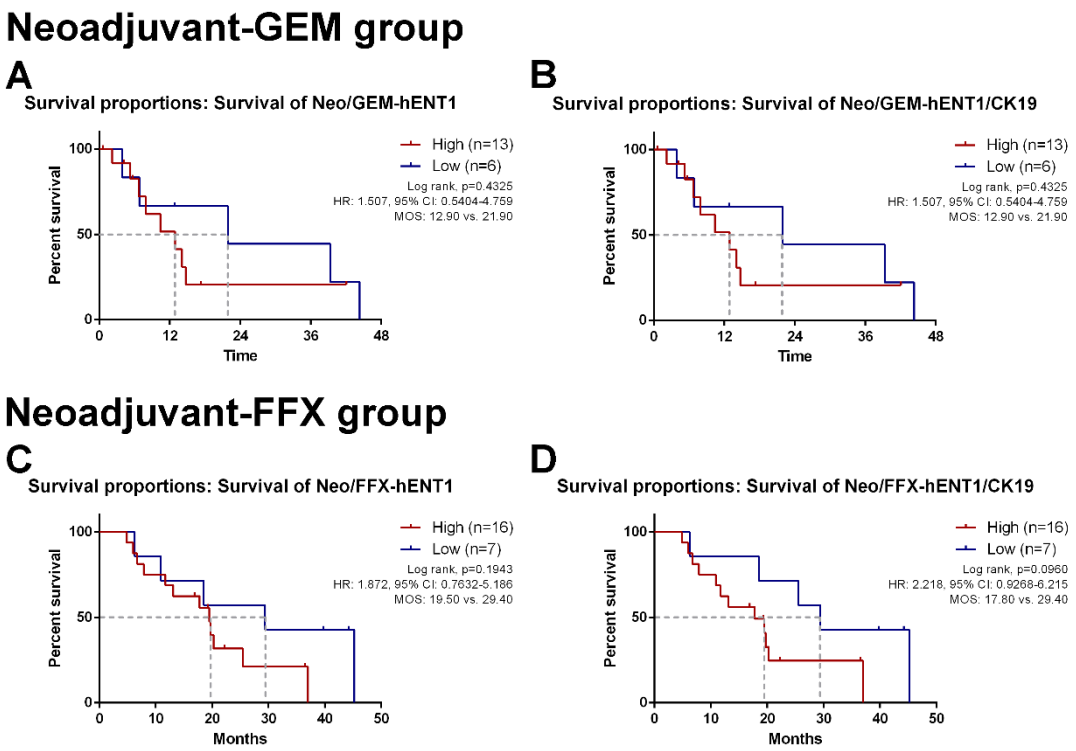

Supplementary Fig 6. Kaplan-Meier curve showed the overall survival of patients with GEM neoadjuvant therapy according to hENT1 expression (A) and its expression in $CK19^+$ cells (B), and patients with FFX neoadjuvant therapy according to hENT1 expression (C) and its expression in $CK19^+$ cells (D) (Log-rank test, $p < 0.05$).

Curriculum vitae

Personal information

Name:	Zhou
First name:	Xu
Gender:	Female
Date of Birth:	05/05/1992
Place of Birth:	Baotou, China
Nationality:	Chinese
Email-address:	dmuzhouxu@gmail.com

Education (From High School)

Sep. 2008 - Jul. 2010	Nr. 9 High School of Baotou, Inner Mongolia, China
Sep. 2010 - Jun. 2015	Central South University, Changsha, China
	• Bachelor Degree of Clinical Medicine, June 2015
Sep. 2015 - Jun. 2017	Dalian Medical University, Dalian, China
	• Master Degree of Surgery, June 2017
Sep. 2018 – Present	Section of Surgery Research, University Clinic Heidelberg, Heidelberg, Germany

Work Experience

June. 2011 - Jun. 2015	Internship in Clinical Laboratory Department of Hunan Cancer Hospital, the Affiliated Cancer Hospital of Xaingya School of Medicine, Central South University

Publications

Zhou X, Hu K, Bailey P, Springfeld C, Kurilov R, Brors B, Gress T, Wei K, Peccerella T, Büchler M. W., Hackert T, Neoptolemos J. P. (2021). Clinical impact of molecular subtyping of pancreatic cancer. Front Cell Dev Biol, 5;9:743908. doi: 10.3389/fcell.2021.743908.

Wen S, Liu T, Zhang H, **Zhou X**, JinH, Sun M, Yun Z, Luo H, Ni Z, Zhao R, Fan B (2021). Whole-exome sequencing reveals new potential mutations genes for primary mucosa-associated lymphoid tissue lymphoma arising from the kidney. Front Oncol, 10:609839. doi: 10.3389/fonc.2020.609839.

Li X, Na H, Xu L, Zhang X, Feng Z, **Zhou X**, Cui J, Zhang J, Lin F, Yang S, Yue F, Mousa H, Zuo Y (2019). DC-SIGN mediates gastric cancer progression by regulating the JAK2/STAT3 signalling pathway and affecting LncRNA RP11-181G12.2 expression. Biomed Pharmacother, 121:109644. doi: 10.1016/j.biopha.2019.109644.

Zhang Y, Zhang Q, Zhang M, Yuan M, Wang Z, Zhang J, Zhou X, Zhang Y, Lin F, Na H, Ren S, Zuo Y (2017). DC-SIGNR by influencing the lncRNA HNRNPKP2 upregulates the expression of CXCR4 in gastric cancer liver metastasis. Mol Cancer, 13;16(1):78. doi: 10.1186/s12943-017-0639-2.

Acknowledgements

Here I give my sincere gratitude to all the professors, and dear work colleagues involved in this project. I would also convey my thanks to my family and friends who unreservedly support me in all aspects.

Firstly, I have to give the deepest gratitude to my supervisors: Prof. Dr. med. John P. Neoptolemos, PD. Dr. Franco Fortunato and Dr. Peter Bailey, who have given me a lot of scientific guidance and pertinent suggestions to promote the project, and have helped me a lot during my doctoral study period. Prof. Dr. med. John P. Neoptolemos, the leader of this project, firstly offered me the chance to study in University of Heidelberg, patiently introduced me the whole idea and the design of the project, guided me through the whole process of this study, and made sure that the research was carried on efficiently towards the main objective. With his and Dr Bailey's help, I successfully published a review article during my doctoral study. PD. Dr. Franco Fortunato, my "Doctorvater", directly provided me detailed help in the lab from PDAC sample recruiting, data analyzing and dissertation writing. The basic experimental techniques that I have learnt here are all due to his patient and careful teaching and guidance. Dr. Peter Bailey, an authoritative expert of PDAC molecular classification, kindly explained the current research status of PDAC to me, generously offering his professional help in sequencing data analysis, and shared his experience in the study.

Secondly, I would like to thank Prof. Markus W. Büchler, Prof. Thilo Hackert, and Prof. Ingrid Herr from the Section Surgical Research department for affording me this opportunity to study and obtaining training at the University of Heidelberg. Thanks also

to Prof. Dr. Dr. Christoph Springfeld from National Centre for Tumour Diseases Heidelberg (NCT), who is responsible for patient follow-up collection, sample quality control and submission; PD Dr. med. Nathalia A. Giese and Dr. Klaus Felix from European Pancreatic Centre (EPZ), who kindly provided samples from tissue biobank; PD Dr. med. Frank Bergmann and PD Dr. Stephanie Rössler from the Institute of Pathology, who undertook considerable work on pathological validation of the PDAC tissue, kindly instructed me on the LCM procedure, and shared a lot of their experience with me.

I am also grateful to Ellen Watson, Sonja Bauer, Karin Ruf, Wolfgang Groß, Michael Schäfer, and my dear lab colleagues Jingyu An, Teresa Peccerella, Kai Hu, Roma Kurilov, Zhenhua Huang, Zhen Xu and Leizhou Xia, for their kind help in my scientific research and daily life. We are a good team.

Finally, there is special thanks to my parents, Jianlin Zhou and Shuzhen Kang and close friends Xiaomeng Li and Zinan Guo who have provided me with constant support and encouragement.

This work is dedicated to all patients with pancreatic cancer and their families in the hope that we can help more and more patients to live longer and ultimately for cure.

EIDESSTATTLICHE VERSICHERUNG

1. Bei der eingereichten Dissertation zu dem Thema “ Tumour biomarkers that identify molecular subtypes and best responders to chemotherapy in patients with pancreatic ductal adenocarcinoma”, handelt es sich um meine eigenständig erbrachte Leistung.

2. Ich habe nur die angegebenen Quellen und Hilfsmittel benutzt und mich keiner unzulässigen Hilfe Dritter bedient. Insbesondere habe ich wörtlich oder sinngemäß aus anderen Werken übernommene Inhalte als solche kenntlich gemacht.

3. Die Arbeit oder Teile davon habe ich bislang nicht an einer Hochschule des In oder Auslands als Bestandteil einer Prüfungs- oder Qualifikationsleistung vorgelegt.

4. Die Richtigkeit der vorstehenden Erklärungen bestätige ich.

5. Die Bedeutung der eidesstattlichen Versicherung und die strafrechtlichen Folgen einer unrichtigen oder unvollständigen eidesstattlichen Versicherung sind mir bekannt. Ich versichere an Eides Statt, dass ich nach bestem Wissen die reine Wahrheit erklärt und nichts verschwiegen habe.

Ort und Datum Unterschrift